US Army Corps of Engineers

TECHNICAL REPORT HL-88-18

SEDIMENT TRANSPORT IN HYPERCONCENTRATED FLOWS IN SAND-BED STREAMS OF VOLCANIC ORIGIN

by

Bobby J. Brown

Hydraulics Laboratory

DEPARTMENT OF THE ARMY
Waterways Experiment Station, Corps of Engineers
PO Box 631, Vicksburg, Mississippi 39180-0631

August 1988

Final Report

Approved For Public Release; Distribution Unlimited

Prepared for DEPARTMENT OF THE ARMY
US Army Corps of Engineers
Washington, DC 20314-1000

HYDRAULICS LABORATORY

Unclassified
SECURITY CLASSIFICATION OF THIS PAGE

REPORT DOCUMENTATION PAGE

Form Approved OMB No. 0704-0188

1a. REPORT SECURITY CLASSIFICATION Unclassified	1b. RESTRICTIVE MARKINGS
2a. SECURITY CLASSIFICATION AUTHORITY	3. DISTRIBUTION/AVAILABILITY OF REPORT Approved for public release; distribution unlimited.
2b. DECLASSIFICATION/DOWNGRADING SCHEDULE	
4. PERFORMING ORGANIZATION REPORT NUMBER(S) Technical Report HL-88-18	5. MONITORING ORGANIZATION REPORT NUMBER(S)
6a. NAME OF PERFORMING ORGANIZATION USAEWES Hydraulics Laboratory 6b. OFFICE SYMBOL (If applicable) CEWES-HS-H	7a. NAME OF MONITORING ORGANIZATION
6c. ADDRESS (City, State, and ZIP Code) PO Box 631 Vicksburg, MS 39180-0631	7b. ADDRESS (City, State, and ZIP Code)
8a. NAME OF FUNDING/SPONSORING ORGANIZATION US Army Corps of Engineers 8b. OFFICE SYMBOL (If applicable)	9. PROCUREMENT INSTRUMENT IDENTIFICATION NUMBER
8c. ADDRESS (City, State, and ZIP Code) Washington, DC 20314-1000	10. SOURCE OF FUNDING NUMBERS See reverse PROGRAM ELEMENT NO. / PROJECT NO. / TASK NO. / WORK UNIT ACCESSION NO.

11. TITLE (Include Security Classification)

Sediment Transport in Hyperconcentrated Flows in Sand-Bed Streams of Volcanic Origin

12. PERSONAL AUTHOR(S)

Brown, Bobby J.

13a. TYPE OF REPORT	13b. TIME COVERED	14. DATE OF REPORT (Year, Month, Day)	15. PAGE COUNT
Final Report	FROM ____ TO ____	August 1988	184

16. SUPPLEMENTARY NOTATION Available from National Technical Information Service, 5285 Port Royal Road, Springfield, VA 22161. Originally submitted in partial fulfillment of the requirements for the degree of Doctor of Philosophy in Civil Engineering to (Continued)

17. COSATI CODES			18. SUBJECT TERMS (Continue on reverse if necessary and identify by block number)
FIELD	GROUP	SUB-GROUP	Hyperconcentrated Flow; Sediment Discharge; Volcanic Ash; Rheological Properties; Sediment Transport; Sediment Concentration; Streams.

19. ABSTRACT (Continue on reverse if necessary and identify by block number)

This study advances the understanding of sediment transport of bed material discharged in sand bed channels through application of recently developed theoretical concepts related to the effects of high concentration of suspended sediment on rheological properties of the water-sediment mixture. The study demonstrates the utility of developing empirical adjustment coefficients for fine material concentration ($d_{50} < 0.0625$ mm) that can be used in the Colby method for predicting total bed material discharge from gaging and sediment sampling data commonly available to the engineer. The prototype data set used in the study was collected and reported by the US Geological Survey at four gaging and sediment sampling stations along a 27-mile reach of the Cowlitz and Toutle rivers, Washington, during 1 October 1981-30 September 1982. The data set included stream gaging measurements, bed material samples, and depth-integrated suspended sediment measurements. (Continued)

20. DISTRIBUTION/AVAILABILITY OF ABSTRACT ☒ UNCLASSIFIED/UNLIMITED ☐ SAME AS RPT. ☐ DTIC USERS	21. ABSTRACT SECURITY CLASSIFICATION Unclassified
22a. NAME OF RESPONSIBLE INDIVIDUAL	22b. TELEPHONE (Include Area Code) / 22c. OFFICE SYMBOL

10. WORK UNIT ACCESSION NO. (Continued).

Funding provided by Civil Works Investigation Work Unit No. 31158, sponsored by the Headquarters, US Army Corps of Engineers.

16. SUPPLEMENTARY NOTATION (Continued).

Colorado State University, Fort Collins CO.

19. ABSTRACT (Continued).

The modified Einstein method was used to estimate the total bed material discharge, and the fluid properties were varied according to recently developed methodologies that take into account the increase in viscosity and density due to suspended sediment concentration. A sensitivity analysis of the effect of viscosity on the estimated bed material discharge by the modified Einstein method and a comparison of the unmeasured sediment discharge to results obtained by other investigators showed that this method provides a reasonably accurate estimate of the total bed material discharge for turbulent hyperconcentrated flows up to total suspended sediment concentrations of approximately 40 percent by weight.

A comparison between total bed material discharge calculated by Colby's method and the prototype data set illustrated that Colby's adjustment coefficient for fine sediment concentration was inadequate for the Cowlitz and Toutle rivers. Colby's method consistently underpredicted the bed material discharge. The assumption was made that Colby's adjustment coefficients for median bed material size and temperature were applicable, and a new set of adjustment coefficients for fine sediment concentration has been developed that should be applicable to streams of similar geometry and flow conditions in the Mount St. Helens area and perhaps in the Cascade Mountain Range. The utility of developing a similar set of curves for any stream from data commonly available to the engineer has been demonstrated.

PREFACE

The study described herein was performed at the US Army Engineer Waterways Experiment Station (WES) during the period 1983-1987 for the Headquarters, US Army Corps of Engineers (USACE), as part of the Civil Works Research and Development Program. Funds were allocated under the Flood-Control Hydraulics Program, Civil Works Investigation Work Unit No. 31158, "Collection, Analysis, and Dissemination of Hydraulic Design Criteria," under USACE Program Monitor Mr. Tom Munsey.

This study was accomplished under the direction of Messrs. H. B. Simmons, former Chief of the Hydraulics Laboratory, WES; F. A. Herrmann, Jr., Chief of the Hydraulics Laboratory; M. B. Boyd, Chief of the Hydraulic Analysis Division; and G. A. Pickering, Chief of the Hydraulic Structures Division. This report was written by Dr. B. J. Brown, Chief of the Hydraulic Analysis Branch, and edited by Mrs. Marsha Gay, Information Technology Laboratory, WES.

This report was also submitted to the Academic Faculty of Colorado State University, Fort Collins, CO, in partial fulfillment of the requirements for the degree of Doctor of Philosophy in Civil Engineering.

COL Dwayne G. Lee, EN, is the Commander and Director of WES. Dr. Robert W. Whalin is the Technical Director.

TABLE OF CONTENTS

TABLE OF CONTENTS (Continued)

TABLE OF CONTENTS (Continued)

TABLE OF CONTENTS (Continued)

CONVERSION FACTORS, NON-SI TO SI (METRIC) UNITS OF MEASUREMENT

Non-SI units of measurement used in this report can be converted to SI (metric) units as follows:

Multiply	By	To Obtain
cubic feet	0.02831685	cubic metres
cubic yards	0.7645549	cubic metres
feet	0.3048	metres
miles (US statute)	1.609347	kilometres
pounds (mass)	0.4535924	kilograms
pounds (mass) per cubic foot	16.01846	kilograms per cubic metre
square feet	0.09290304	square metres
tons (2,000 pounds, mass)	907.1847	kilograms

SEDIMENT TRANSPORT IN HYPERCONCENTRATED FLOWS IN SAND-BED STREAMS OF VOLCANIC ORIGIN

CHAPTER 1

INTRODUCTION

1.1 PROBLEM STATEMENT

The occurrence of extremely high suspended sediment concentrations is rather common in streams throughout the world. Streams which have water-sediment mixtures described as "too thin to plow and too thick to drink" are especially prevalent in mountainous and semiarid regions where there is an abundance of smaller particle size material available for transport. A clear flowing stream which has little or no suspended sediment can easily be converted into a stream that transports more solids than water by a catastrophic disturbance in the watershed. During the eruption of Mount St. Helens on May 18, 1980, a debris avalanche deposited some 3 billion cubic yards* of rock, ice, and other material in the upper 17 miles of the North Fork Toutle River valley. Mudflows triggered by the eruption carried large volumes of sediment from the debris avalanche into the Toutle-Cowlitz-Columbia River system (Figure 1.1).

The US Army Corps of Engineers (CE) had the arduous task of determining the sediment yield from the Toutle River watershed, sediment deposition in the Cowlitz River, and the sediment delivery to the Columbia River. In their work to numerically model the movement of water and sediment through the highly disturbed river system, Brown and Thomas (1982) adopted the Colby (1964) method with some modifications because it was the only existing method for predicting total bed

---

* A table of factors for converting non-SI units of measurement to SI (metric) units of measurement is found on page vi.

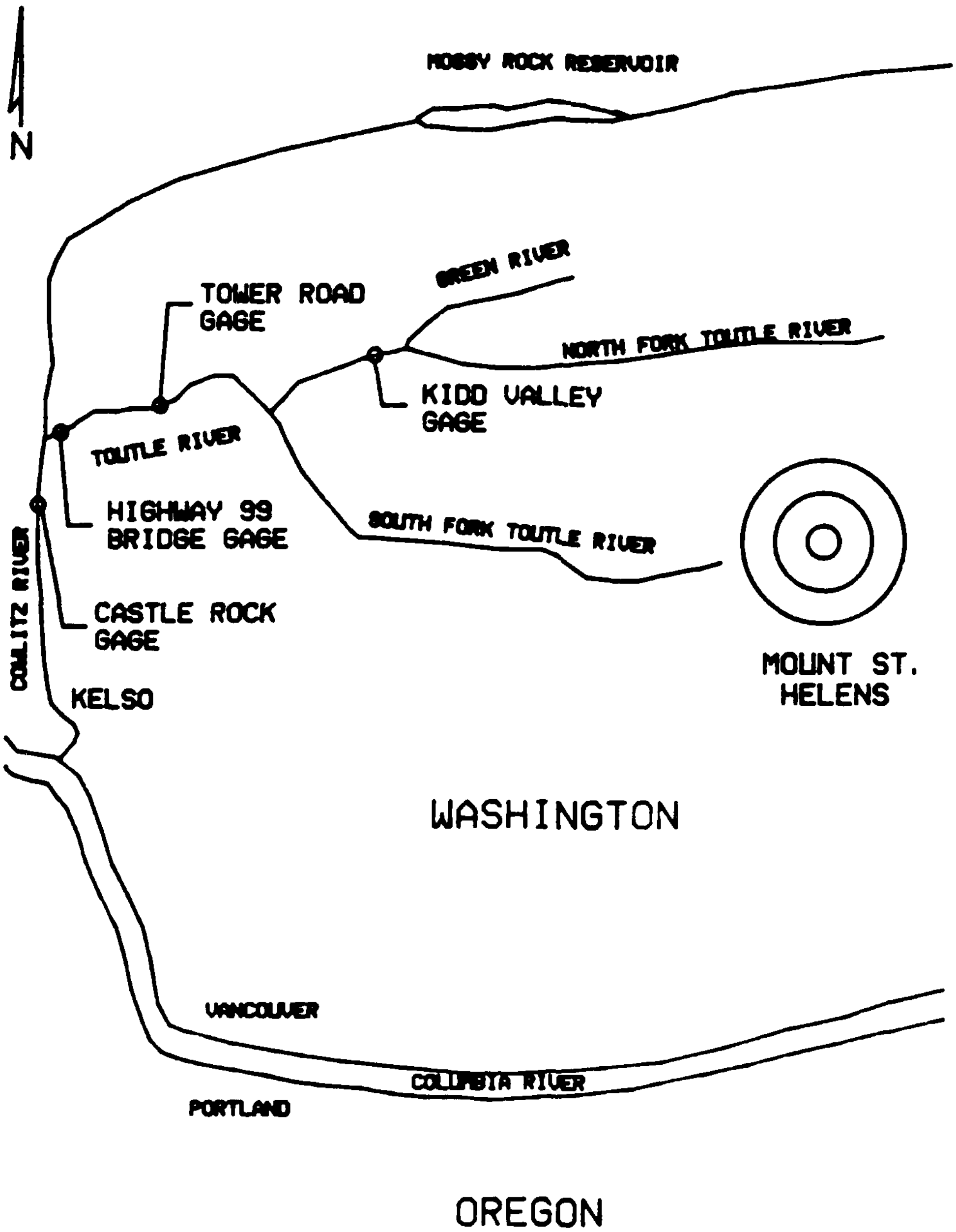

Figure 1.1. Location map

material discharge in hyperconcentrated sediment flow. The modification to the Colby method involved extrapolation of Colby's graphical procedure to flow velocities and concentration of fines beyond upper limits that were already questionable because of the very limited data that Colby had to work with in developing the curves.

Since the eruption of Mount St. Helens, significant research has been directed at understanding the mechanics of hyperconcentrated flow. Theoretical analyses and laboratory experiments have been conducted by universities and Government agencies in an attempt to develop the theory of the effects of hyperconcentrations of sediment on fluid and flow characteristics and transport of bed material in alluvial channels. Although much insight has been gained from these investigations, there is still a need to verify with prototype data theories and procedures set forth in these studies. Furthermore, there is a critical need to develop or adapt an existing sediment transport function that will be applicable over the wide range of sediment concentrations that occur in nature and that requires as input, sediment and hydraulic parameters that are normally collected and reported by such agencies as the US Geological Survey (USGS).

The impact of high concentrations of suspended fine sediment (particle diameter < 0.0625 mm) upon the transport of sand-sized sediment can best be illustrated with data from Mount St. Helens. Figure 1.2 is a plot of measured suspended bed material discharge versus streamflow discharge for water year (WY) 1982 (October 1, 1981-September 30, 1982) at the Toutle River-Highway 99 Bridge gaging and sediment measuring site operated by USGS (Figure 1.1). These data can be grouped into three distinct and unusual water-sediment flow

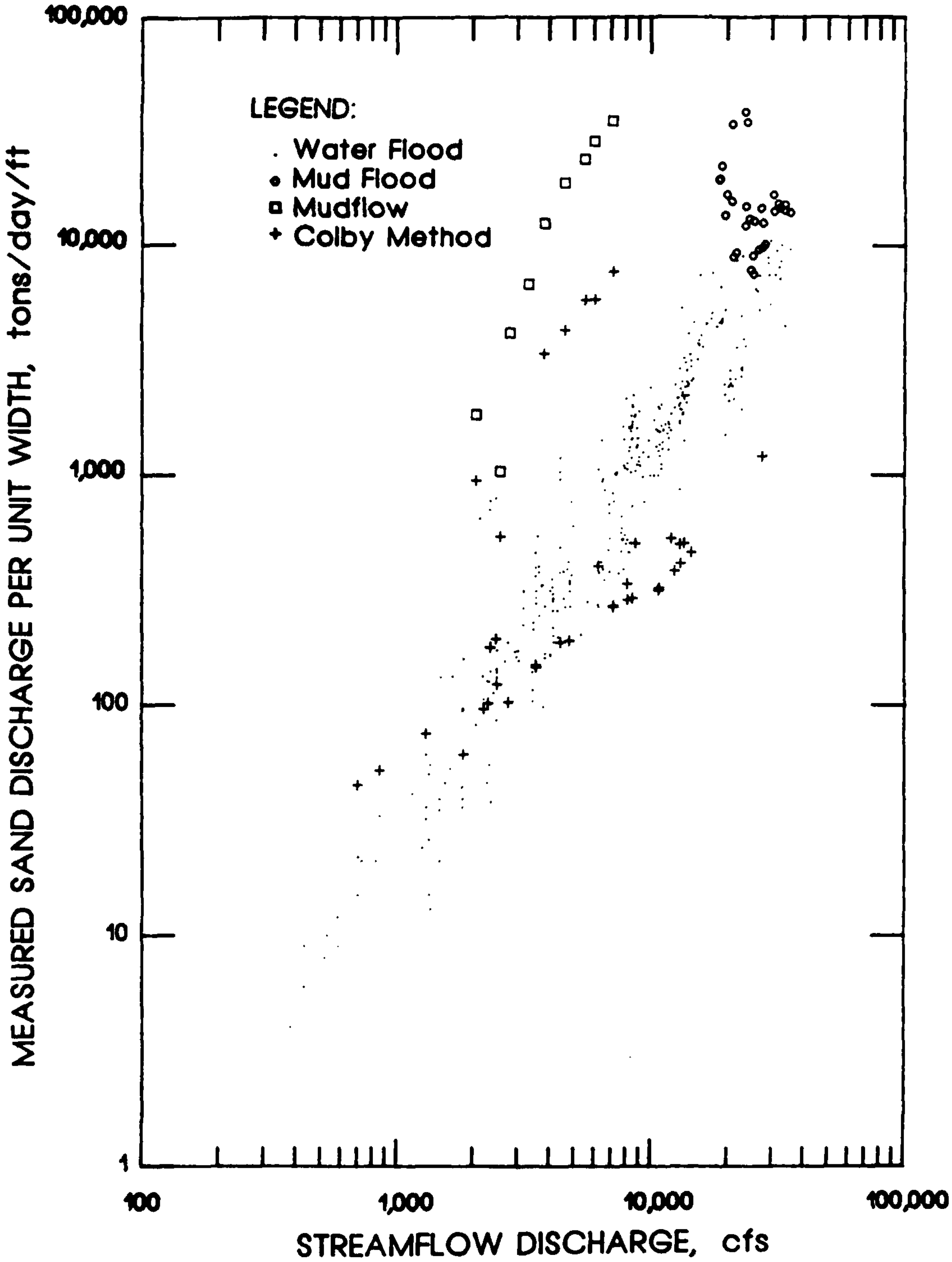

Figure 1.2. Measured sand discharge Toutle River-Highway 99 gage, WY 1982

phenomena. Using the definition of mass wasting promulgated by the National Research Council Committee on Methodologies for Predicting Mudflows (National Research Council 1982), as shown in Figure 1.3, the data from WY 1982 indicate that the Toutle River at this gaging station experienced three of the four flow processes--water flood, mud flood, and mudflow.

Most of the data in Figure 1.2 fall into the water flood category, but the concentration of fine sediment is unusually high because of the abundant sediment source from the debris avalanche. The data representing the mud flood reflect an anomaly that occurred in February 1982. Apparently, a locally intense rainstorm fell on the debris avalanche, causing the concentration of fine sediment to increase to 5-10 times that of the water flood concentrations (100,000 ppm by weight). The sand discharge increased one order of magnitude for essentially the same flow depth and velocity (see Figure 1.2). The third group of data represents the sand discharge for a mudflow that occurred on March 20, 1982, as a result of an eruption of the volcano. The eruption melted the snow pack in the crater causing a large volume of water to spill over the crater rim and down the mountain. The measured concentrations of fine sediment were about 30 times (300,000 ppm by weight) those of water flood measurements, and the measured suspended sand discharge was greater by two orders of magnitude (see Figure 1.2).

Figure 1.2 also illustrates the inadequacy of a widely used method for predicting total bed material discharge in sand-bed streams with extremely high concentrations of suspended sediment. Colby's method (1964), to the author's knowledge, is the only predictive method where the effect of high concentrations of fine sediment on bed material

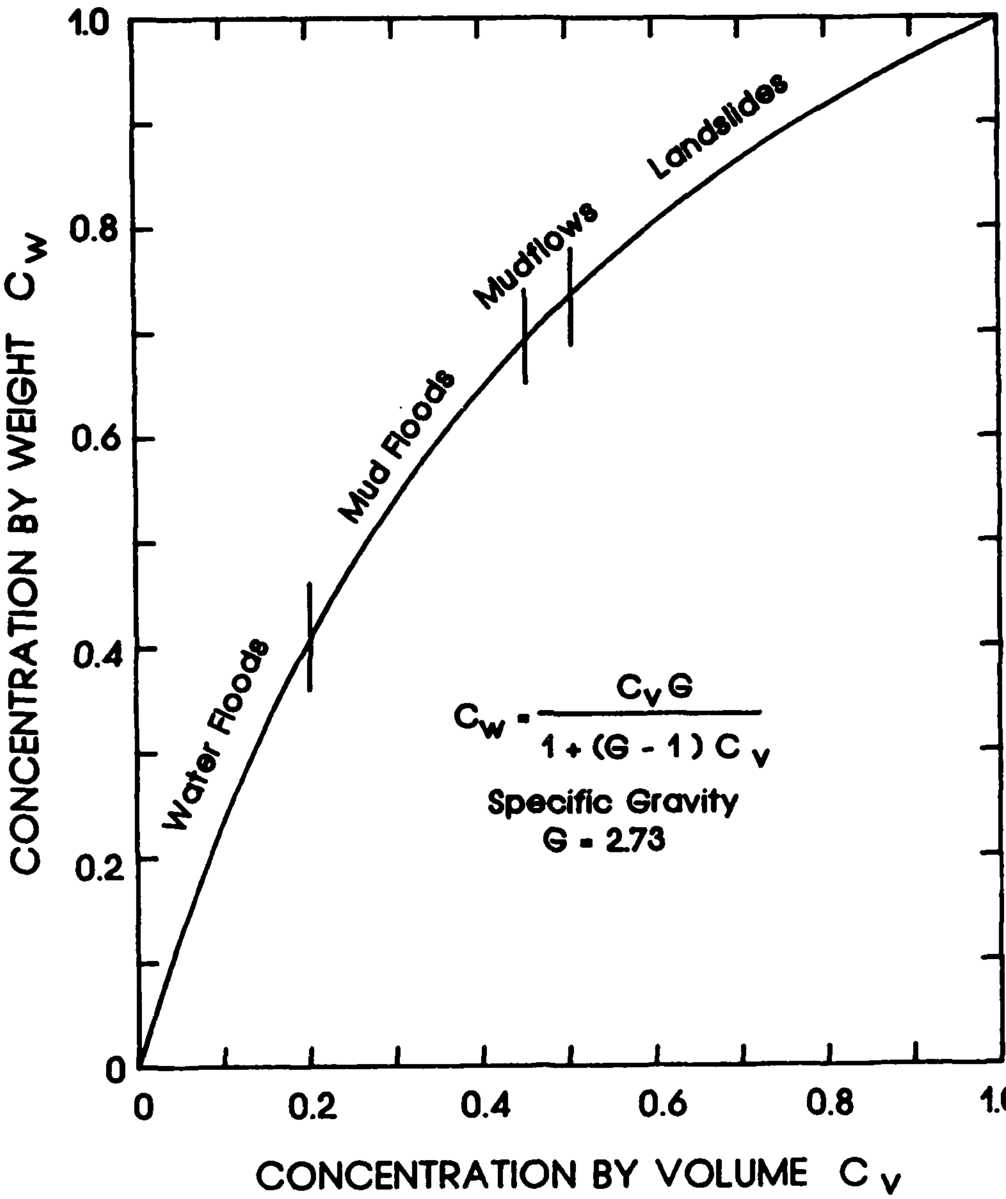

Figure 1.3. Hyperconcentrated sediment flow classification (after National Research Council 1982)

discharge is taken into account. The upper limits of both concentration of fine sediment and flow velocity are exceeded in the Toutle River at this gaging station, and the method underpredicts the sand discharge at the streamflows that correspond to higher fine sediment concentrations. However, Colby clearly states that the adjustment coefficients for high concentration of fine sediment that he developed were only crude estimates and they are unlikely to apply to streams other than the Rio Puerco, New Mexico, for which they were defined. Colby's method (1964) is widely used in the United States because it has proven to be a reasonably accurate predictor of total bed discharge in sand bed streams for moderate flow depths (<10 ft), low to moderate flow velocities (<10 fps), and low concentrations of fine sediment (<10,000 ppm).

1.2 STUDY DESCRIPTION

The Mount St. Helens data afford the opportunity to compare field data to recent theoretical and laboratory studies of the effects of suspended fine sediment upon fluid and flow characteristics and upon bed material discharge. The study will focus on analyzing gaging, suspended sediment, and bed material data, obtained by the USGS at four gaging stations along a 27-mile reach of the Cowlitz-Toutle River system (Figure 1.1) during WY 1982 (October 1, 1981-September 30, 1982).

The WY 1982 data set was selected because of several unique characteristics. As previously discussed, three of the four flow processes according to the National Research Council (1982) classification scheme occurred during this year, and the USGS had mobilized its forces so that data collection efforts were at their peak. The original mudflow deposited thousands of cubic yards of sand along the entire length of the river system, providing essentially an infinite sediment supply, and the stream's sediment transport capability was at its capacity as manifested by the continuous aggradation at every gaging station throughout the year (see Section 3.3). The eruption occurred late in WY 1981; thus the first substantial flushing storm events did not occur until WY 1982, and massive cleanup efforts in the Toutle River did not get into full operation until after the rainy season of WY 1982.

The Mount St. Helens data have the deficiencies found in most field data sets and lack the detail of laboratory data, particularly with regard to vertical point sediment and vertical velocity profile measurements. Furthermore, measurements of the rheological properties of the water-sediment mixture are lacking, and these deficiencies will limit the direct comparison of some of the recently developed theory with these prototype data.

1.3 STUDY OBJECTIVES

The objectives of the study are as follows:

1. In conjunction with other researchers, study the effects of high concentrations of fine suspended sediment on rheological properties of the water-sediment mixture such as density and viscosity.
2. Study the effects of high concentrations of suspended sediment on particle fall velocity and flow characteristics such as flow regime and flow resistance.
3. Test the validity of using existing sediment transport formulas, and where they exist, show their limits of application in heavy sediment-laden flow.

4. If possible, suggest modifications that will enable determination of the bed material discharge over the wide range of suspended sediment concentrations that occur in nature.

CHAPTER 2

THEORETICAL DEVELOPMENT

2.1 INTRODUCTION

Colby (1964) states that the two practical objectives of sedimentation studies are to determine the effects of major factors on sediment discharge in streams and to develop methods of computing the sediment discharge. Prior to the eruption of Mount St. Helens in 1980, most researchers had concentrated their efforts relative to these objectives in the ordinary transport range which does not exceed several percentages by weight. There existed no complete explanation of hyperconcentrated sediment flow, which, contrary to popular belief, is a common occurrence. However, Mount St. Helens, with its destructive consequences and abundant data source, renewed interest in this important phenomenon; and since 1980, analytical and laboratory studies have been conducted that have contributed to a better understanding of the effects of the major factors on hyperconcentrated sediment discharge. The purpose of this dissertation is to summarize the results of these studies on the effects of hyperconcentrations of sediment on fluid and flow characteristics and bed material discharge and develop practical methods of computing sediment discharge for hyperconcentrated sediment flows.

To accomplish this purpose, it becomes necessary to understand research fields related to the phenomena to include classification of sediment-laden flow; the rheology of water-sediment mixtures; the vertical velocity distribution of sediment-laden flow in open channels; the fall velocity of sand-sized particles in combined water-sediment flow; flow resistance; and the existing theories and formulas concerning bed material discharge.

2.2 CLASSIFICATION SCHEMES OF HIGH CONCENTRATION FLOWS

In reviewing the literature on fluvial processes with high concentrations of suspended sediment, it quickly becomes apparent that there are numerous explanations and descriptions of mass-movement phenomena, and the definitions and concepts are not always clearly presented. Woo (1985) and Bradley (1986) present excellent summaries of the most common classification schemes found in the literature. Bradley's summary is given in Figure 2.1 to illustrate the disagreement concerning terms and definitions. In addition to the schemes discussed by Bradley and Woo, the author reviewed literature from the Soviet Union. The results are included in Figure 2.1, and discussed in the following paragraph.

Classification of massive subaerial sediment flows into "turbulent" and "structural" mudflows seems to be generally accepted in the Soviet Union (Gagoshidze 1969). Structural mudflow is defined as a dense mud and rock mass (80-90 percent solids by weight) consisting of rock fragments, stones, gravel, plant remains, and enveloping mud which is cohesive and structured. The water in the mud mass (10-20 percent by weight) is bound and does not perform a transforming function. The specific weight of the mixture is approximately 120-145 pcf. The initiation of movement for this type flow is caused by avalanches, earthquakes, volcanic eruptions, and landslides in the area of mud-forming centers; breaches of jams of mudflow masses from mudflow centers; and masses from under glaciers. Turbulent mudflow (also called mud floods in Soviet literature) is defined as a water and sediment mass that is fluid, turbulent, and noncohesive. The water in turbulent mudflows is enriched with colloidal suspension, and the mixture contains a large

SOURCE	Concentration Percent by Weight (100% by Weight = 1,000,000 ppm: 23, 40, 52, 63, 72, 80, 87, 93, 97, 100 — Concentration Percent by Volume (Specific Gravity = 2.65): 10, 20, 30, 40, 50, 60, 70, 80, 90, 100
Beverage and Culbertson (1964)	High; Ex-treme; Hyperconcentrated; Mudflow
Costa (1984)	Water Flood; Hyperconcentrated; Debris Flow
O'Brien and Julien (1985) Using National Research Council (1982)	Water Flood; Mud Flood; Mudflow; Landslide
Takahashi (1981)	Fluid Flow; Debris or Grain Flow; Fall, Landslide, Creep, Sturzstrom, Pyroclastic Flow
Chinese Investigators (Fan and Dou, 1980)	← Sediment Laden; ← Hyperconcentrated Flow →; ← Debris or Mudflow →
Pierson and Costa (1984)	STREAMFLOW Normal; Hyperconcentrated; SLURRY FLOW (Debris Torrent), Debris & Mudflow, Solifluction; GRANULAR FLOW Sturzstrom, Debris Avalanche, Earthflow, Soil Creep
Soviet Investigators (Gagoshidze 1969) (Vinogradov 1969)	Flash Flood; Turbulent Mudflow; Structural Mudflow

Figure 2.1. Classification of hyperconcentrated flows (after Bradley 1986)

amount of suspended sediment (20-30 percent by weight) containing sand, gravel, cobbles, and even large boulders. The specific weight of the mixture is approximately 70-80 pcf. The main reasons for initiation of motion of turbulent mudflows are rainfall; warm rainfall on a heavy snowpack; breach of mountain lakes, dams, and jams of mudflow masses; and scouring of mudflow deposits. Turbulent mudflows are common in mountain streams with mudflow deposits. Gagoshidze (1969) also includes in this category of flows flash floods which contain turbid water, but a relative low concentration of sediment (3-4 percent by weight) and a specific weight of the mixture of approximately 64-66 pcf.

The literature on hyperconcentrated flow, as summarized previously, illustrates that differentiation between various classifications is not as clear-cut as the schemes may indicate because sampled mudflows have resulted in reported concentrations by weight that range from 20 to 90 percent solid (Costa and Jarrett 1981). Bradley (1986) in laboratory flume tests observed laminar mudflows with concentrations of bentonite of only 10 percent by weight. Perhaps of more concern than whether a flow is classified as a "water flood," "mud flood," or "mudflow" is whether measurements of sediment characteristics and hydraulic data commonly collected and available to the engineer are adequate with presently known theory to predict the fluid and flow characteristics, and with reasonable accuracy and confidence, to estimate the bed material discharge of a stream regardless of the sediment type and concentration.

2.3 RHEOLOGICAL PROPERTIES OF WATER-SEDIMENT MIXTURES

2.3.1 Density

The bulk density or bulk unit weight of a water-sediment mixture is the sum of the densities or unit weights of all contained solids and interstitial water and depends in large measure upon concentration values. Densities have been reported from 87 pcf (Okuda et al. 1977) to 158 pcf (Curry 1966). These are equivalent to a volume concentration of solid material from about 25 percent to 70 or 80 percent, respectively. Thus, during an extremely highly concentrated flow, more solids than water can be moved and water actually can be a very small percentage of the total flow.

Woo (1985) discusses in detail the theoretical development of equations for determining the density or specific weight of water-sediment mixtures, and it is summarized for the reader's convenience. The specific weight γ_m* is obtained by

$$\gamma_m = \sum_i C_{vi} \gamma_i \tag{2.1}$$

in which C_{vi} and γ_i are the volume fraction and specific weight of the ith phase, respectively. Thus, when the suspension is composed of fine sediment (silt and clay), sand particles, and water, the specific weight is expressed as

$$\gamma_m = \gamma_c C_{vf} + \gamma_s C_{vs} + \gamma_w (1 - C_{vf} - C_{vs}) \tag{2.2}$$

where

γ_c = specific weight of fine sediment

C_{vf} = concentration of fines by volume

---

* For convenience, symbols and unusual abbreviations are listed and defined in the Notation, Appendix D.

γ_s = specific weight of sand particles

C_{vs} = concentration of volume by sand

γ_w = specific weight of pure water

When γ_c is expressed as $\gamma_c = a\gamma_s$, where a is a constant, the specific weight of the mixture is expressed as

$$\gamma_m = \gamma_s(aC_{vf} + C_{vs}) + \gamma_w(1 - C_{vf} - C_{vs}) \qquad (2.3)$$

When the fine sediment is composed of clays and silts, the value of a can be practically assumed to be unity (Woo 1985). Then,

$$\gamma_m = \gamma_w + (\gamma_s - \gamma_w)C_v \qquad (2.4)$$

in which C_v is the volumetric concentration of suspended sediment. The concentration of suspended sediment by weight C_s is expressed in terms of C_v as

$$C_s = \frac{\gamma_s}{\gamma_s - \gamma_w + \frac{\gamma_w}{C_v}} \qquad (2.5)$$

Therefore, the specific weight of the water-sedimemt mixture in terms of C_s rather than C_v is expressed as

$$\gamma_m = \frac{\gamma_s\gamma_w}{\gamma_s - (\gamma_s - \gamma_w)C_s} \qquad (2.6)$$

The specific weight of the water-sediment mixture as determined by Equation 2.6 is an apparent specific weight when using average sediment concentration over depth from depth-integrated concentrations of suspended sediment.

Figure 2.2 shows the conversion from C_v to C_s and from C_s to the apparent specific weight γ_m of the water-sediment mixture for average concentration over depth. The specific gravity of the sediment particles used in the conversion was 2.73 since this was the value

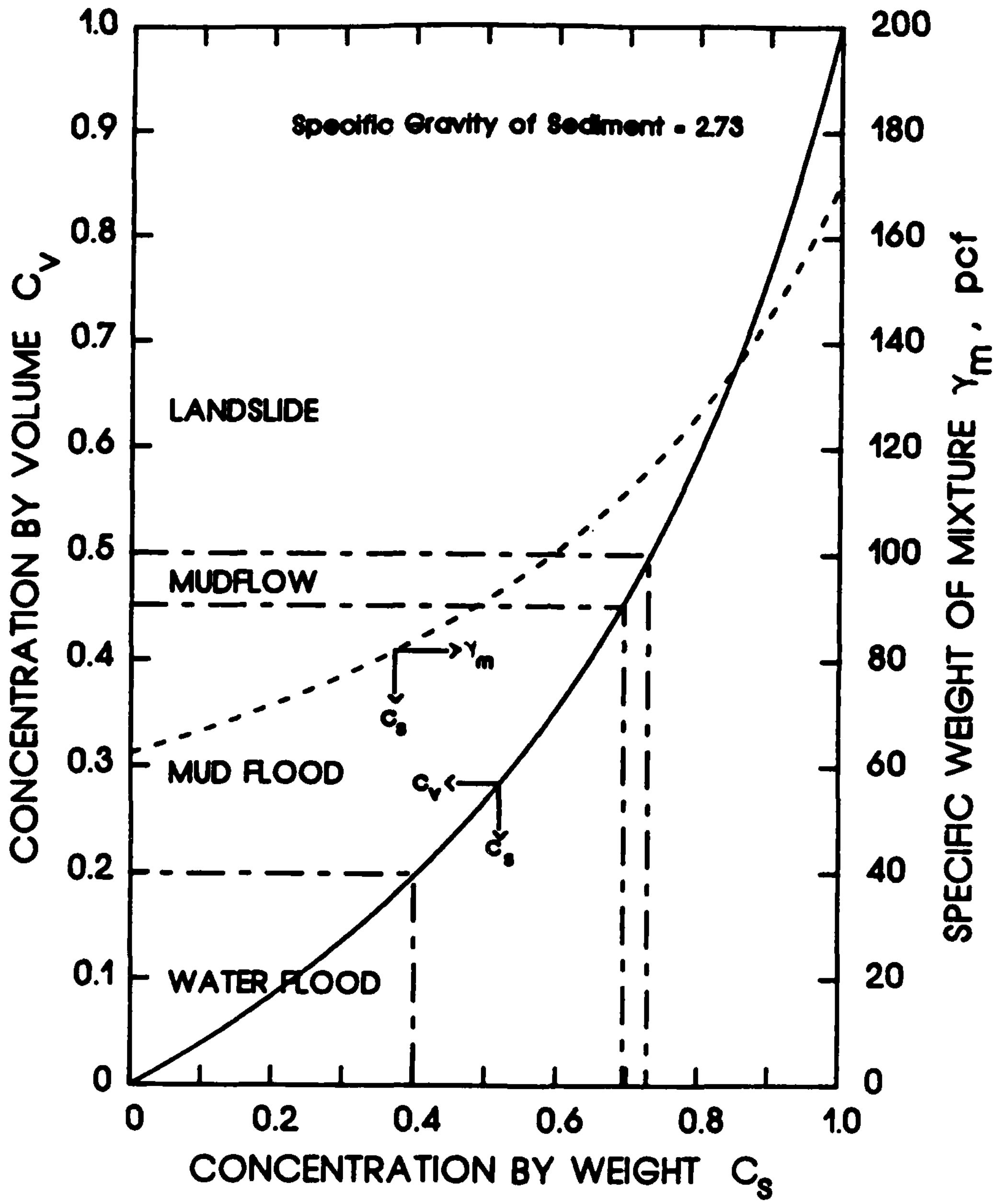

Figure 2.2. Concentration and density properties of hyperconcentrated flow

determined for the Mount St. Helens sediment (see paragraph 4.1.2). Also shown for reference on Figure 2.2 are the four classes of flow suggested by the National Research Council (1982) and the concentration range for each class as determined from experiments by O'Brien and Julien (1985) involving material from Colorado mudflow deposits. These are the four classes of flow that will be referred to in this study.

Woo (1985) has shown that when the density or unit weight of the suspension with sand particles in a water-fine sediment mixture is considered, the unit weight is expressed as

$$\gamma_m = \gamma_f + (\gamma_s - \gamma_f)C_{vs} \tag{2.7}$$

where γ_f is the apparent specific weight of the water-fine sediment mixture. When the concentration of fine sediment is uniform over depth, the apparent unit weight of the water-fine sediment mixture is given by

$$\gamma_f = \gamma_w + (\gamma_c - \gamma_w)C_{vf'} \tag{2.8}$$

where $C_{vf'} = C_{vf}/(1 - C_{vs})$ by approximating $a = 1$. Thus, as Woo has pointed out, the unit weight of water-sediment mixtures changes with depth even if the fine sediment has a uniform concentration when the concentration of sand particles is nonuniform. $C_{vf'}$ in Equation 2.8 is expressed in terms of C_{wf} and C_{ws} as

$$C_{vf'} = \frac{C_{wf}}{SG(1 - C_{ws} - C_{wf}) + C_{wf}} \tag{2.9}$$

where

C_{wf} = concentration of fines by weight

SG = specific gravity

C_{ws} = concentration of sand by weight

Woo further states that the influence of sand particles along the depth is rather small and γ_f can be calculated from Equation 2.8 with C_{vf} rather than C_{vf}, without significant error.

The term fine sediment is used in this study to represent clay- and silt-sized particles (d < 0.0625 mm) that normally are distributed uniformly over depth for a given flow condition in a channel. Woo (1985) analyzed Nordin's (1963) data on the Rio Puerco for concentration distribution of different sized particles in hyperconcentrated flow and reported that 0.0625 mm appeared to be the most adequate criterion for separating sediment material into a fine and a coarser part. He reported that the concentration of the total sediment material smaller than 0.0625 mm was about uniform with depth and particles larger than 0.0625 mm were not distributed uniformly with depth. Furthermore, any methodologies developed in this study should be able to make maximum use of field data since the vast majority of size distribution data on suspended sediment concentration reported by water and sediment data collection agencies report only the "sand break" or that fraction of sediment particles smaller than 0.0625 mm.

2.3.2 Viscosity

The viscosity of water-sediment mixture is increased by the presence of fine sediment (Simons, Richardson, and Haushild 1963), and it may be further increased by the concentration of coarse sediment (O'Brien and Julien 1985). A number of investigators have attempted to relate relative viscosity, defined as the ratio of the viscosity of the suspension to the viscosity of the suspending medium, to sediment concentration and temperature.

Woo (1985) discusses many of the existing theoretical and experimental equations for the relative viscosity such as Einstein (1906), Ward (1955), Oliver and Ward (1959), Roscoe (1953), Bagnold (1954, 1956), and Thomas (1965). These are shown in Figure 2.3. Woo (1985) recognized that the equations represented in Figure 2.3 do not satisfy the criterion for predicting the relative viscosity of suspensions which are unstable (a stable suspension is defined as one where the solid particles are neither downward- nor upward-settling), nonuniform, and composed of nonspherical solid particles of different sizes. However, he recommended use of Thomas' (1965) equation for estimating the apparent viscosity of sand-water mixtures which behave as a Newtonian fluid. Thomas' equation is in the form

$$\frac{\mu_m}{\mu_o} = 1 + 2.5C_v + 10.05C_v^2 + 0.00273 \exp (16.6C_v) \qquad (2.10)$$

in which μ_m is the viscosity of mixture, and μ_o is the Newtonian viscosity of the suspending medium. Woo (1985) states that fine sediment-water mixtures behave as Bingham fluids and both the yield stress and the plastic viscosity should be measured directly because no general method exists for predicting these parameters. He further states that in hyperconcentrated flows these parameters should be determined from the fine sediment-water mixture, neglecting the contribution of concentration of sands. Then the plastic viscosity of the overall water-sediment mixture is approximately estimated using Equation 2.10 by substituting the plastic viscosity of fine sediment-water mixture into the equation for μ_o .

Simons, Richardson, and Haushild (1963) showed an increase in fluid viscosity over the viscosity of water for bentonite and kaolinite clays.

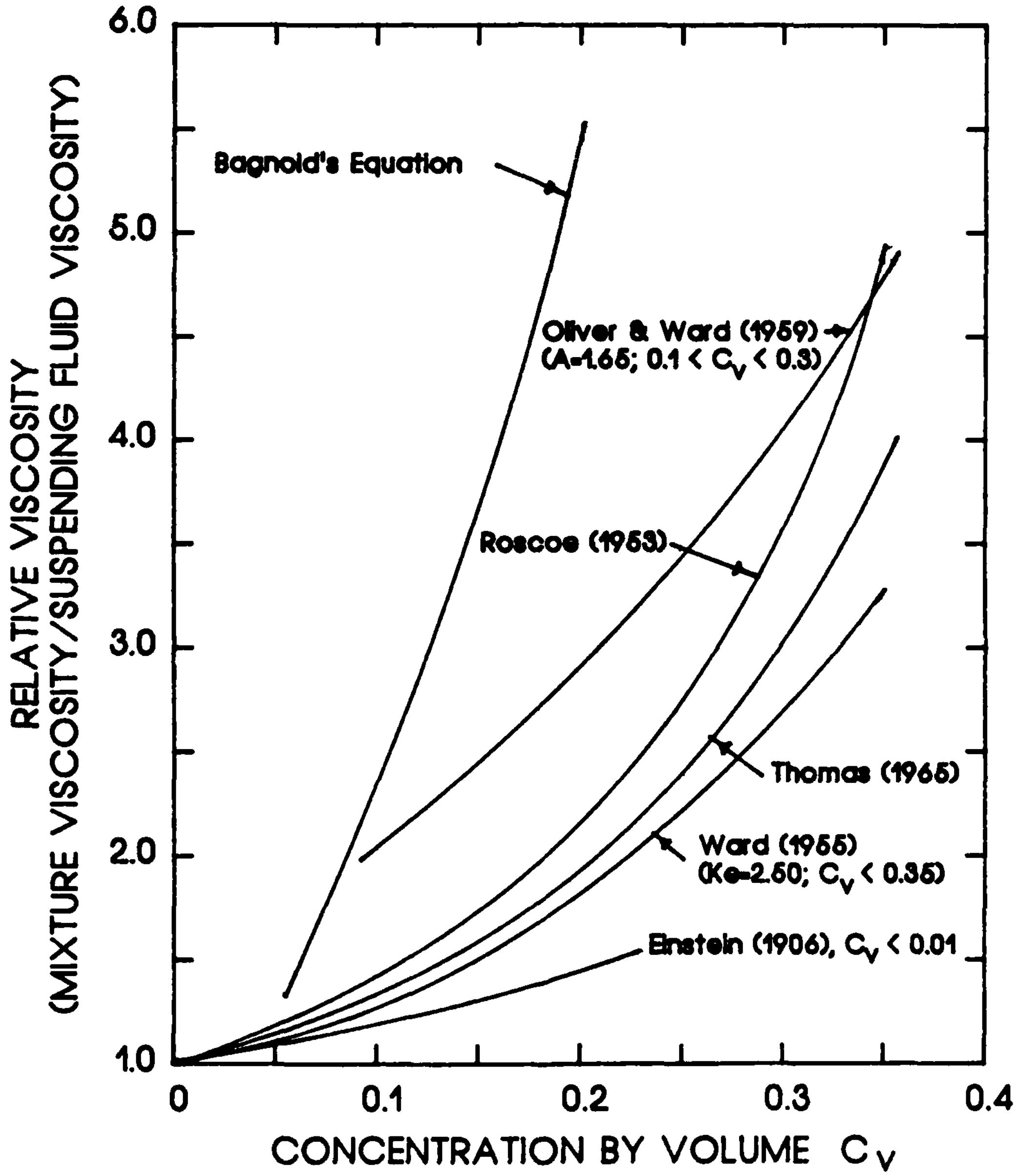

Figure 2.3. Comparison of relative viscosities of water-sediment mixtures by empirical equations (after Woo 1985)

Bradley (1986) conducted viscosity tests on bentonite clay suspensions and showed differences in fluid viscosity of pure water and bentonite suspensions of approximately 10 percent by weight to be as great as three or four orders of magnitude (Figure 2.4). Simons, Richardson, and Haushild (1963) make the point that the apparent viscosity of aqueous dispersions appears to be primarily a function of the concentration of fine material because their tests indicated that the viscosity did not change due to the settling out of the coarser particles.

Viscometric measurements were made by Mills (1983) using a coaxial cylinder viscometer on slurries composed of the fine fraction of mudflow material from Mount St. Helens. The results, shown in Figure 2.5, indicate the validity of assuming a Bingham model for the basic slurry. Mills (1983) also made viscometric measurements on kaolin clay slurries to examine the effects of temperature on the values of the Bingham constants of plastic viscosity and yield stress. The effects of temperature on these parameters are shown in Figures 2.6 and 2.7.

In Figure 2.6, note that the experimental curve of temperature dependence of pure water obtained by Mills is well represented by the empirical equation of Andrade (1930) for estimating the viscosity of liquid μ for a given temperature. It is in the form

$$\mu(\text{lb-sec/ft}^2) \times 10^6 = A \exp\,(B/T) \qquad (2.11)$$

in which T is the temperature in absolute degrees (degrees Kelvin), the constant A equals 0.0116, and the constant B equals 2,204.0 for pure water over a normal temperature range.

Mills (1983) concluded from the data in Figure 2.7 that the temperature dependence of yield stress seems to be influenced by material characteristics, thus making it difficult to prescribe a unique

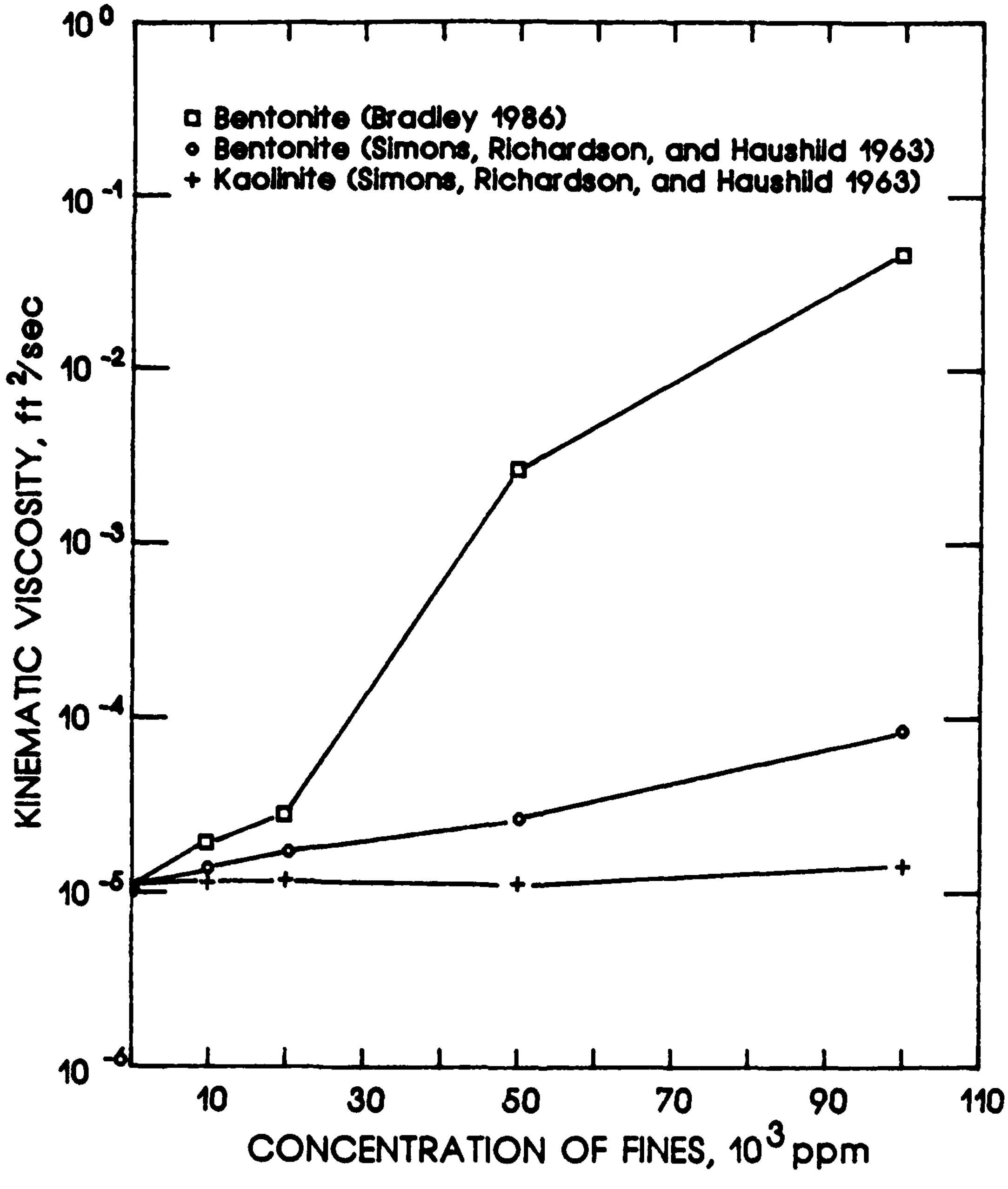

Figure 2.4. Viscosity versus concentration of fines relation for bentonite and kaolinite suspensions (after Bradley 1986)

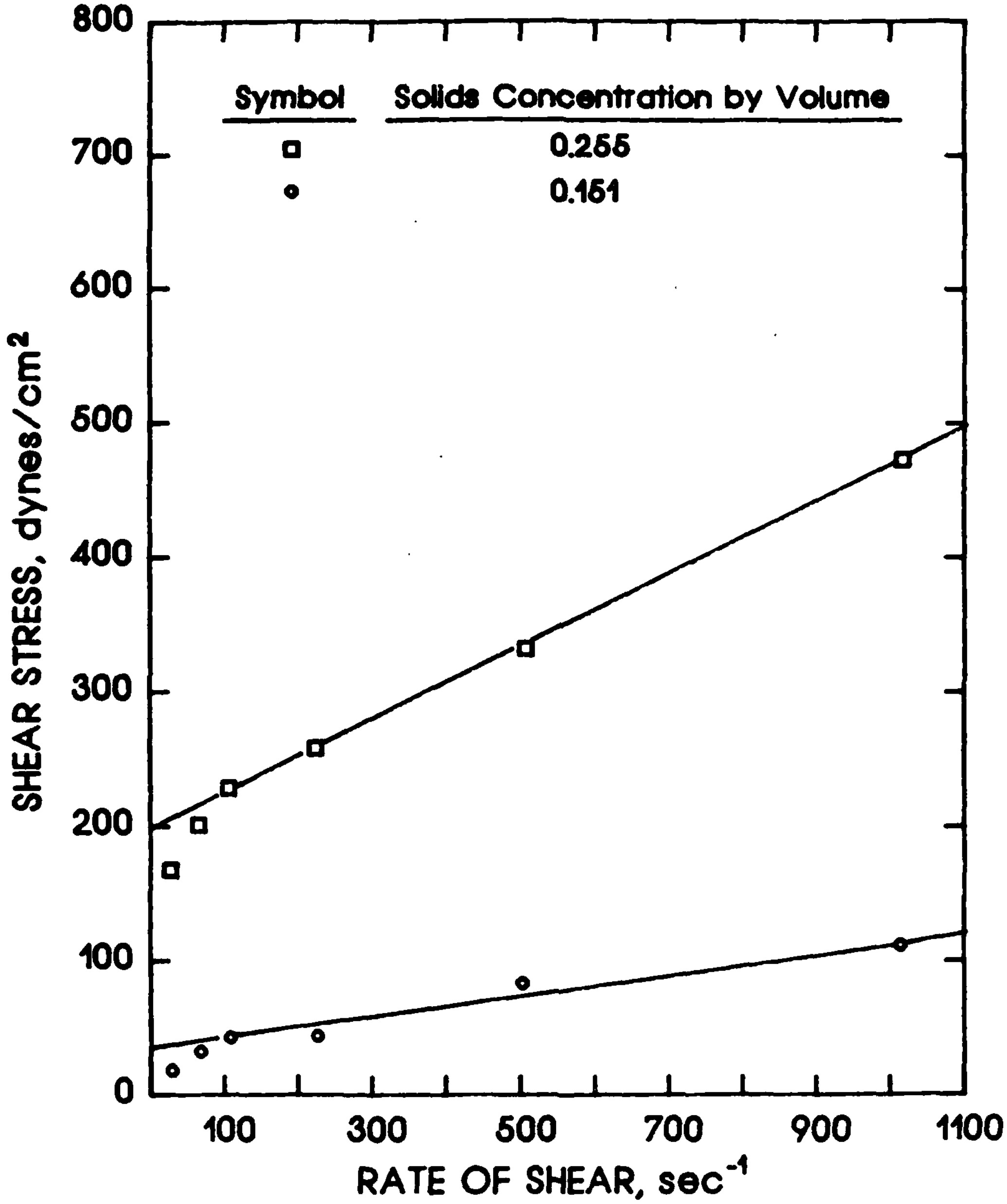

Figure 2.5. Shear stress versus shear rate for Mount St. Helens mudflow material (after Mills 1983)

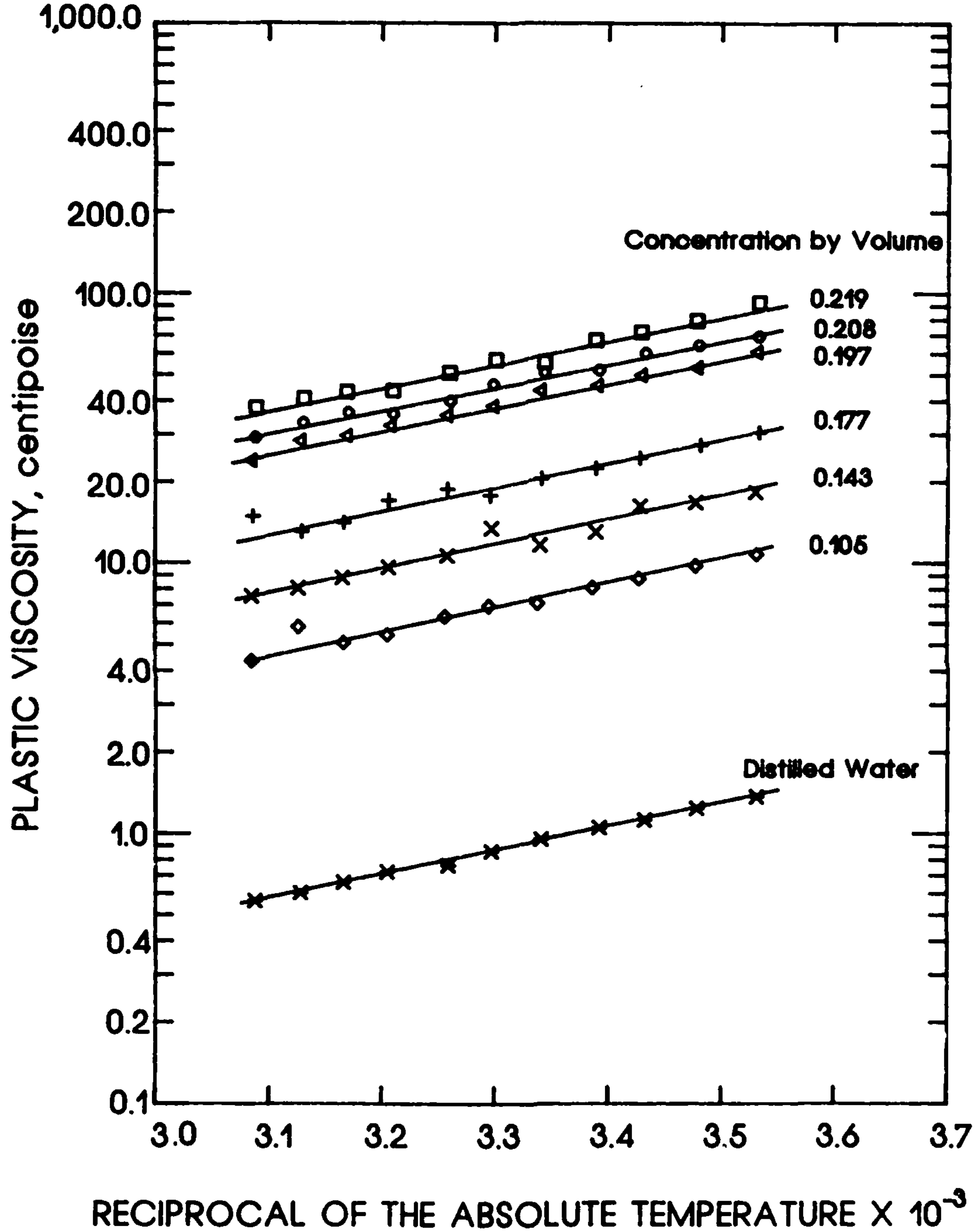

Figure 2.6. Relationship between temperature and the plastic viscosity for kaolinite suspensions (after Mills 1983)

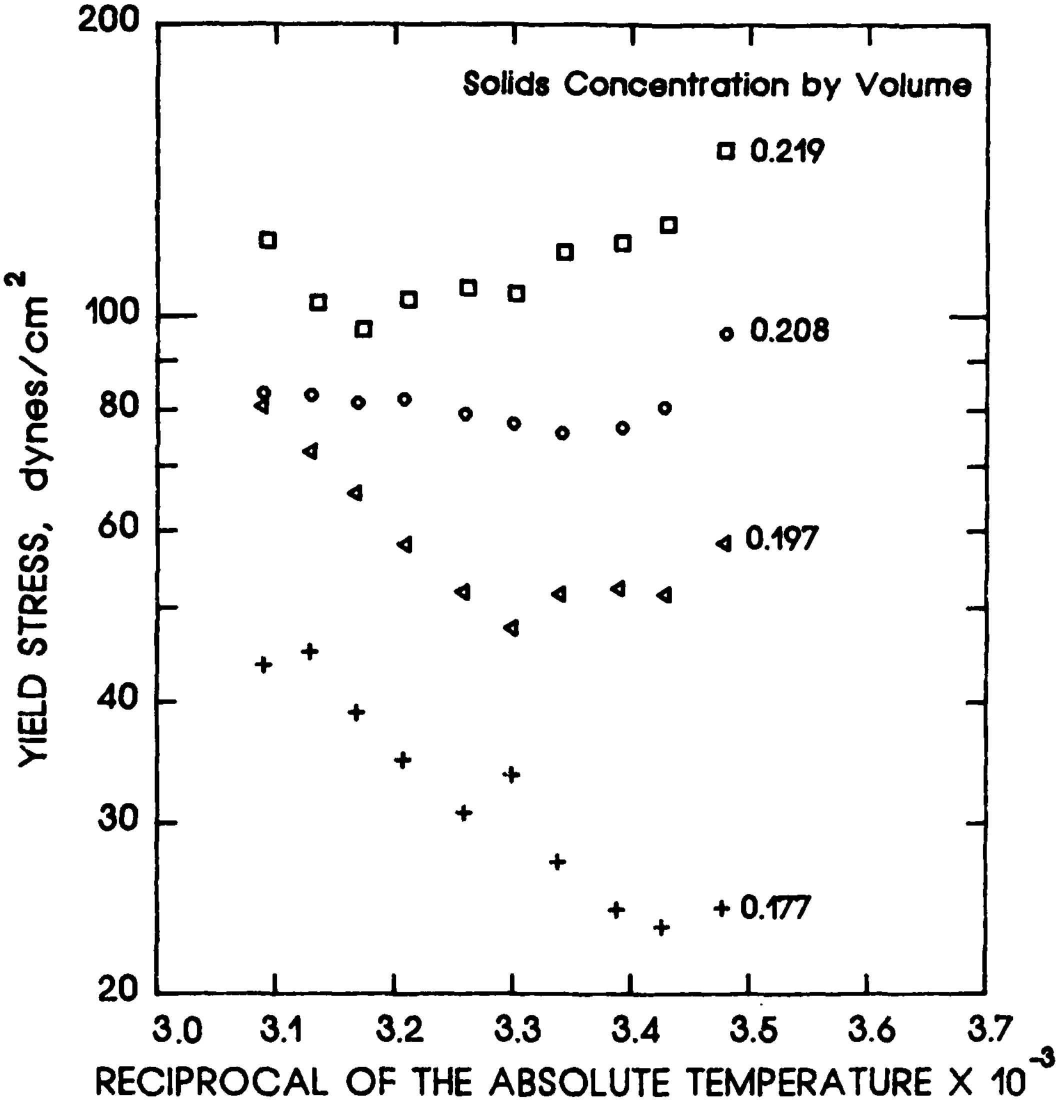

Figure 2.7. Relationship between temperature and the yield stress for kaolinite suspension (after Mills 1983)

relationship for predictive purposes. He recommended further research to obtain meaningful relationships between temperature effects, material characteristics, and yield stress; and that until such research is completed, it be kept in mind that significant error may be involved as a result of temperature effects on yield stress.

O'Brien and Julien (1985) conducted experiments to measure shear stress as a function of shear rate for various mixtures of clay and silt and for mudflow deposit samples extracted from undisturbed deposits in Colorado. The rheological measurements were performed in a specially designed concentric cylinder viscometer, and the tests were conducted at much lower shear rates than previous investigations. Temperature variation was controlled by inserting the whole apparatus into a large water bath. They make the point that most of the available water-sediment mixture viscometer data have been collected on dilute slurries of bentonite and kaolin clays at very high shear rates well in excess of 100 sec^{-1} (see Figure 2.5) and these data require careful interpretation because shear rates for hyperconcentrated sediment flow in the field are on the order of 5 to 50 sec^{-1}. To illustrate the point, they cite the data of Johnson (1970) and Yano and Daido (1965), which show the shear rate to be of a magnitude of 10 sec^{-1} or less for open channel mudflows of concentrations up to 35 percent by weight. They further state that rates of shear in excess of 50 sec^{-1} are uncommon in open channel mudflows, and thus these data have led to very high estimates of yield stress and corresponding low estimates of viscosity. Figure 2.8 shows the results of one of O'Brien and Julien's tests at the much lower shear rate. The viscosity is shown to vary with the shear rates. At low shear rates the measured viscosity is much greater, and correspondingly,

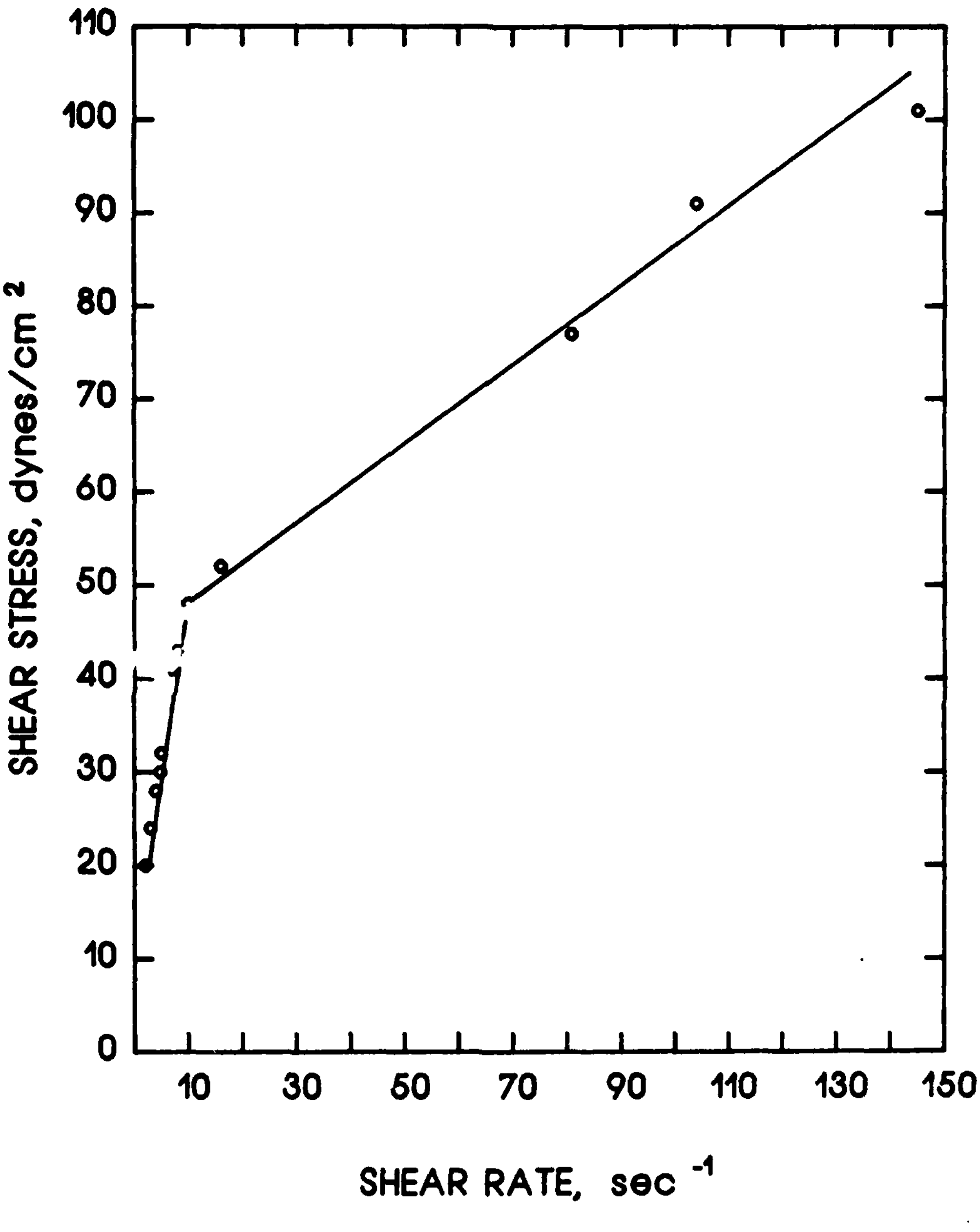

Figure 2.8. Shear stress versus shear rate. Aspen soils concentration by volume 34 percent (after O'Brien and Julien 1985)

the yield stress is much less than those measurements taken at high shear rates in other studies.

O'Brien and Julien (1985) also conducted a series of tests shown in Figure 2.9 which consisted of adding sand to various clay or mudflow mixtures. Initially the viscosity decreased with increasing sand concentration, then increased dramatically. The decrease in viscosity occurred with an increase in concentration by volume up to about 10 or 20 percent by weight. They hypothesized that the sand assists in the dispersion and destruction of the clay floccules, with less energy required to break the bonding, and results in a slight reduction in the viscosity and that particle collision for concentrations greater than 20 percent by volume may explain the significant increase in viscosity.

O'Brien and Julien concluded from these tests that the Bingham model is an appropriate rheological model for flow deformation of hyperconcentrated sediment flows when examined at low shear rates. In these flows there does exist a yield stress, albeit smaller than previously thought, thus indicating that some bonding between flocculated structures must be broken to initiate motion. They also concluded that the use of the Bingham model parameters to evaluate the fluid matrix properties of viscosity and yield stress results in a well-defined exponential relationship with sediment concentration, the effects of temperature, and other variables being held constant. The addition of sand to the fluid matrix had little effect on the matrix properties at volumetric concentrations less than 25 percent.

A theoretical but more complicated procedure for estimating the rheological parameters of solid dispersions in a Bingham fluid has been developed by Naik (1983) supported by the experimental work of Mills

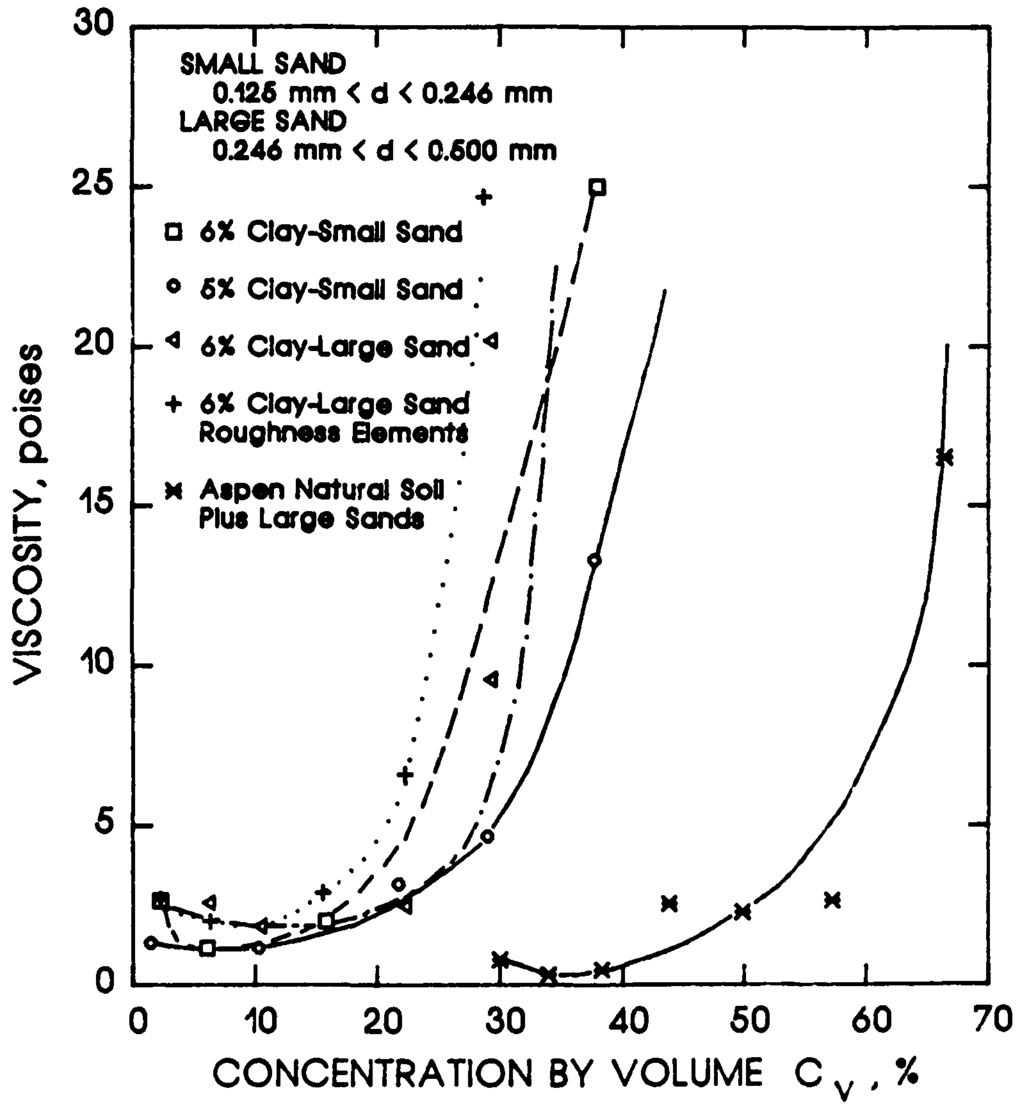

Figure 2.9. Viscosity versus concentration by volume of sand-clay mixtures (after O'Brien and Julien 1985)

(1983). Naik's analysis is based on Ackermann and Shen's (1979) approach for a Newtonian dispersion of uniform spherical particles. The Bingham parameters of the uniform spherical particle dispersion are functions of the volume fraction of solids and the Bingham parameters of the suspending fluid.

In developing the procedure, Naik (1983) assumes the mud mass to be a homogeneous dispersion of solid particles greater than 10 microns in size in a basic fluid. The basic fluid is defined as a mixture of water and clay and fine silts less than 10 microns in size. Thus, a pyramid structure is assumed involving larger and larger particles resulting in a pseudohomogeneous mass.

The work of Thomas (1961) was adopted by Naik (1983) to calculate the Bingham yield stress and plastic viscosity of the basic slurry. Since the results of Thomas were obtained from experiments with particle sizes up to 13 microns, an upper limit of 10 microns for the fine particles in the basic slurry was arbitrarily set by Naik.

Thomas' (1961) equation for yield stress τ_b and plastic viscosity η are in the form

$$\tau_b = K_1 \phi^3 \qquad (2.12)$$

$$\eta = \mu \exp (K_2 \phi) \qquad (2.13)$$

where

ϕ = the solid volume fraction

μ = the viscosity of the suspending medium

K_1, K_2 = constants, given by the following empirical equations:

$$K_1 = 210 \frac{\psi_1}{d^3} \qquad (2.14)$$

$$K_2 = 2.5 + \frac{14}{d\psi_2} \tag{2.15}$$

where d is the particle size in microns and K_1 is given in pounds per square foot. The shape factors ψ_1 and ψ_2 are given by the following equations:

$$\psi_1 = \exp\left\{0.7\left[\left(\frac{S_p}{S_o}\right) - 1\right]\right\} \tag{2.16}$$

$$\psi_2 = \left(\frac{S_p}{S_o}\right)^{1/2} \tag{2.17}$$

where S_p is the surface area per unit volume of the actual particle and S_o is the surface area per unit volume of a sphere of equivalent dimension.

One difficulty in using this procedure is estimating the ratio S_p/S_o, for it is practically impossible to predict, and a reasonable value for this ratio has to be assumed. Naik (1983) presents a table of values for the ratio in his dissertation for particles of different shapes based on values of sphericity provided by Govier and Aziz (1972). The particle geometric shapes given in Naik's table are sphere, octahedron, cube, prism, cylinder, and disk. The ratio for a sphere is unity.

Mills (1983), using the limiting value of viscosity at high rates of shear, the corresponding extrapolated values of yield stress for the slurries of fine material from Mount St. Helens (Figure 2.5), and Equations 2.12 and 2.13, calculated the value of S_p/S_o for this material as 2.0. This value corresponds to a prism shape of dimensions $a \times a \times 2a$ in Naik's (1983) table. Furthermore, Higgins et al. (1983) (this report is a summary of Naik's and Mills' work) suggest that a value of

S_p/S_o equal to 2.0 may be used by practicing engineers for mudflows in the vicinity of Mount St. Helens, and in the absence of data, the same value may be used in other areas of the Cascade Mountain Range, United States.

Once the Bingham parameters of the basic slurry are obtained, the next step is to determine the relevant rheological parameters of the suspension of solids in the basic slurry. The analytical work of Naik (1983) on the dispersion of uniform spherical particles in a Bingham fluid indicates that the resulting mixture will exhibit Bingham characteristics. The Bingham parameters of the uniform spherical particle dispersion are functions of the volume fraction of solids and the Bingham parameters of the suspending fluid (Higgins et al. 1983).

According to Naik (1983), the relative Bingham yield stress τ_r and the relative plastic viscosity η_r of the dispersion of spherical solid particles in Bingham fluids are

$$\tau_r = \frac{\tau_{bD}}{\tau_b} = \frac{C_1 T_1}{C_2} + T_2 \tag{2.18}$$

$$\eta_r = \frac{\eta_D}{\eta} = C_1 T_1 + T_2 \tag{2.19}$$

where τ_{bD} = Bingham yield stress of the dispersion

τ_b = Bingham yield stress of the basic fluid

η_D = plastic viscosity of the dispersion

The quantities C_1 , C_2 , T_1 , and T_2 are given by

$$C_1 = \left(\frac{1}{\beta^2 - 1}\right)\left[1 + \frac{2}{\left(\beta^2 - 1\right)^{1/2}} \tan^{-1}\left(\frac{\beta + 1}{\beta - 1}\right)\right]^{1/2} \tag{2.20}$$

$$C_2 = \left[\frac{2\beta^2}{\left(\beta^2 - 1\right)^{1/2}} \tan^{-1}\left(\frac{\beta + 1}{\beta - 1}\right)\right] - \frac{\pi}{2}\beta \tag{2.21}$$

$$T_1 = \frac{\pi}{4} - \frac{\pi}{6\beta} \tag{2.22}$$

$$T_2 = 1 - \frac{\pi}{4\beta^2} \tag{2.23}$$

$$\beta = \left(\frac{\phi_m}{\phi}\right)^{1/3} \tag{2.24}$$

where ϕ_m is the maximum possible volume fraction.

Mills (1983) verified Equations 2.18 and 2.19 through viscometric measurements using dispersions of spherical glass beads in a basic fluid of kaolin clay slurry. Mills conducted further experiments with dispersion of crushed quartz sand, and also coarse solid particles sieved out of mudflow material collected from Mount St. Helens. Results indicated that particle shape has a strong influence on the values of relative Bingham yield stress and relative plastic viscosity at a given reduced volume fraction and that these two equations were not accurate enough for predictive purposes.

Mills (1983) recommended that until further research is conducted to determine the effects of particle shape, that correction factors be applied to the theoretical equations. He developed the correction factors for relative yield stress C_T and for relative plastic viscosity C_E from the experimental data for the quartz sand of the form

$$C_T = \left[1 + 0.75\left(\frac{\frac{\phi}{\phi_m}}{1 - \frac{\phi}{\phi_m}}\right)^{1.14}\right]^2 \tag{2.25}$$

$$C_E = \left[1 + 0.4\left(\frac{\frac{\phi}{\phi_m}}{1 - \frac{\phi}{\phi_m}}\right)^{0.60}\right]^2 \qquad (2.26)$$

Multiplying τ_r from Equation 2.18 by C_T results in the τ_r values corresponding to the experimental values of Mills, and similarly, the product of Equation 2.19 and C_E gives the values of η_r .

A graphical method for determining the maximum possible volume fraction ϕ_m is given by Naik (1983) and Mills (1983). Size distribution data on the mudflow material is plotted on Rosin's probability paper, and a straight line is fitted to the data. The slope of the line is determined, and the porosity is obtained from Figure 2.10 with the proper choice of a curve. Rodine and Johnson's curve (1976) is a theoretical curve for a tetrahedral packing of spherical particles. Its use for engineering practice is questionable because the particles in mudflow material are highly irregular (Higgins et al. 1983). Mills (1983) conducted experiments on Mount St. Helens mudflow material and developed a relationship between porosity and slope for a certain range of porosity in his experiments. The relationship is plotted in Figure 2.10, and it is recommended by Naik until further research is conducted. The maximum volume fraction is computed as one minus the porosity.

The effects of wide size distribution of a dispersion, which is generally the case for mudflow material, require special consideration when applying theoretical and experimental results developed for either uniform size particles or particles with a narrow distribution range (Higgins et al. 1983). In Naik's (1983) procedure, the multiplicative principle of Moshev (1979) and Ackermann and Shen (1979) is adopted to

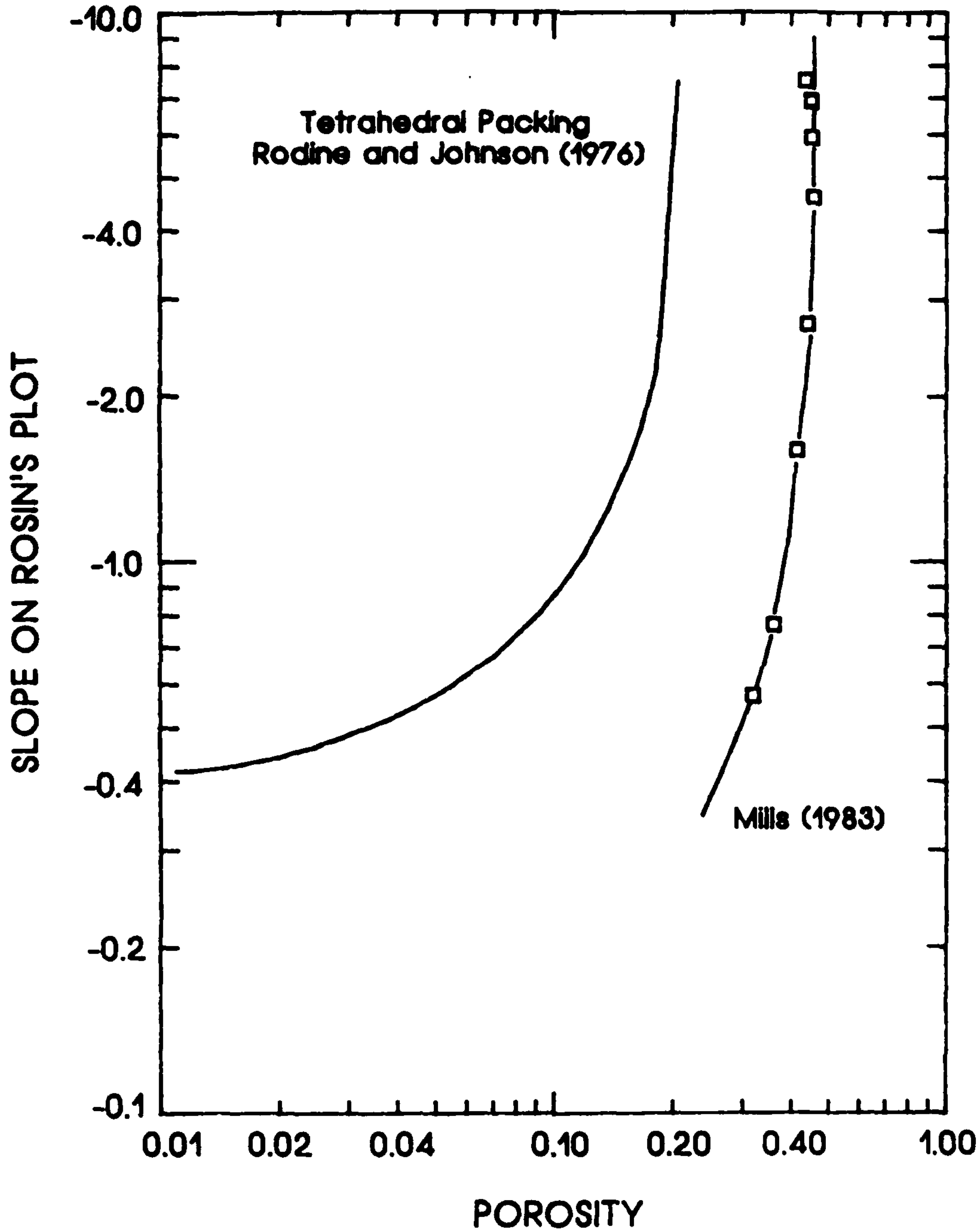

Figure 2.10. Porosity as a function of the grain-size distribution (after Mills 1983)

calculate the relative viscosity of the dispersion which is composed of particles of several discrete sizes.

According to the multiplicative principle, the relative viscosity of the dispersion can be expressed as

$$\mu_D = \mu_o \times \mu_{r1} \times \mu_{r2} \times \mu_{r3} \times \cdots \tag{2.27}$$

where

μ_D = viscosity of dispersion

$\mu_{r1}, \mu_{r2}, \mu_{r3}$ = relative viscosities of discrete sizes d_1, d_2, d_3, respectively

In applying the equation, the particle sizes d_1, d_2, d_3, ... d_n, must vary by a factor of 10. Naik (1983) extended the principle to mudflow material by considering several discrete size ranges of narrow distribution, instead of discrete sizes. He divided the solid component of sizes greater than 10 microns into discrete size ranges of 10-100 microns, 100-1,000 microns, 1-10 mm, and 10-100 mm. It is assumed that the fraction of solids greater than 100 mm is less than 1 percent of the total solid component. The mean sizes for each range are 50 microns, 500 microns, 5 mm, and 50 mm, which vary by a factor of 10. Particles less than size 10 microns are part of the basic slurry, and a mean diameter of 5 microns is used to calculate the Bingham parameters of the slurry.

Naik (1983) used the empirical equation given by Chu (1980) to calculate the volume of bound water. Bound water is defined as the layer of water which adheres to the particles and does not play a role in the computations of the effective concentration of the basic slurry. The volume fraction of the solids in the basic slurry is increased to an extent as a result of bound water being removed by particles greater than 10 microns when dispersed in the basic slurry. Chu's empirical equation is in the form

$$R_{bw} = k_b \sum_{1}^{n} \left(\frac{\delta_i}{d_i}\right)^{1/2} \Delta P_i \qquad (2.28)$$

where

R_{bw} = the ratio of the volume bound water to that of the sediment particles

k_b = an empirical constant equal to 4.4

δ_i = the bound water film thickness usually taken as 1 micron

ΔP_i = the volume of fraction of particles of diameter d_i

Naik's procedure is outlined step-by-step, and it has been incorporated into a computer program, both of which are included as Appendices D and E, respectively, of his dissertation.

The problem of accurately determining the maximum possible volume concentrations of solids in a dispersion led Woo (1985) to use Thomas' equation (Equation 2.10), although Woo makes the statement that the validity of his simplified method should be checked with experiments in accordance with Naik's (1983) procedure. However, O'Brien and Julien's (1985) study indicates that the coefficients and/or constants used in Naik's procedure, which were developed from limiting viscosity measurements on mudflow material at high shear rates, may need reinterpretation.

2.4 FALL VELOCITY OF SAND PARTICLES IN HYPERCONCENTRATIONS

2.4.1 Introduction

One of the major effects of the increased density and viscosity of water-fine sediment mixture in hyperconcentrated sediment flow is to decrease the fall velocity of the sand particles in suspension. The fall velocity of sand particles decreases as the concentration of fine sediment increases because of increased yield stress and plastic viscosity of the suspending fluid. It decreases further as the concentration of sand particles increases because of the hydrodynamic effect of fluid particles and the interparticle collisions. Woo (1985) made a comprehensive comparative analysis of theoretical and experimental studies on the fall velocity of sand particles in both Newtonian and Bingham fluids, and his observations and conclusions are relevant to this study.

2.4.2 Fall Velocity of Sand Particles in Newtonian Fluids

Figure 2.11 shows graphically the results of Woo's (1985) comparative analysis of available equations for predicting fall velocity of sand particles in water. Most of the equations were developed from experiments conducted to show the relationship between the drag coefficient C_D and the particle Reynolds number Re_p^* (see Equation 2.30) of spherical particles falling through a calm Newtonian fluid. Included in his review were the works of Gibbs, Matthews, and Link (1971), Rubey (1933), Watson (1969), Swanson (1967), Albertson (1953), and Inter-Agency Committee (1957). Although Gibbs, Matthews, and Link's (1971) equation appeared to be superior to the other equations for predicting the fall velocity of spherical particles in calm water, Woo suggested Rubey's equation for predicting the settling velocity of natural sand particles when data of particle shape are not available. Woo states several facts to reinforce his suggestion for using Rubey's equation in spite of its underestimation of fall velocity (see Figure 2.11). First,

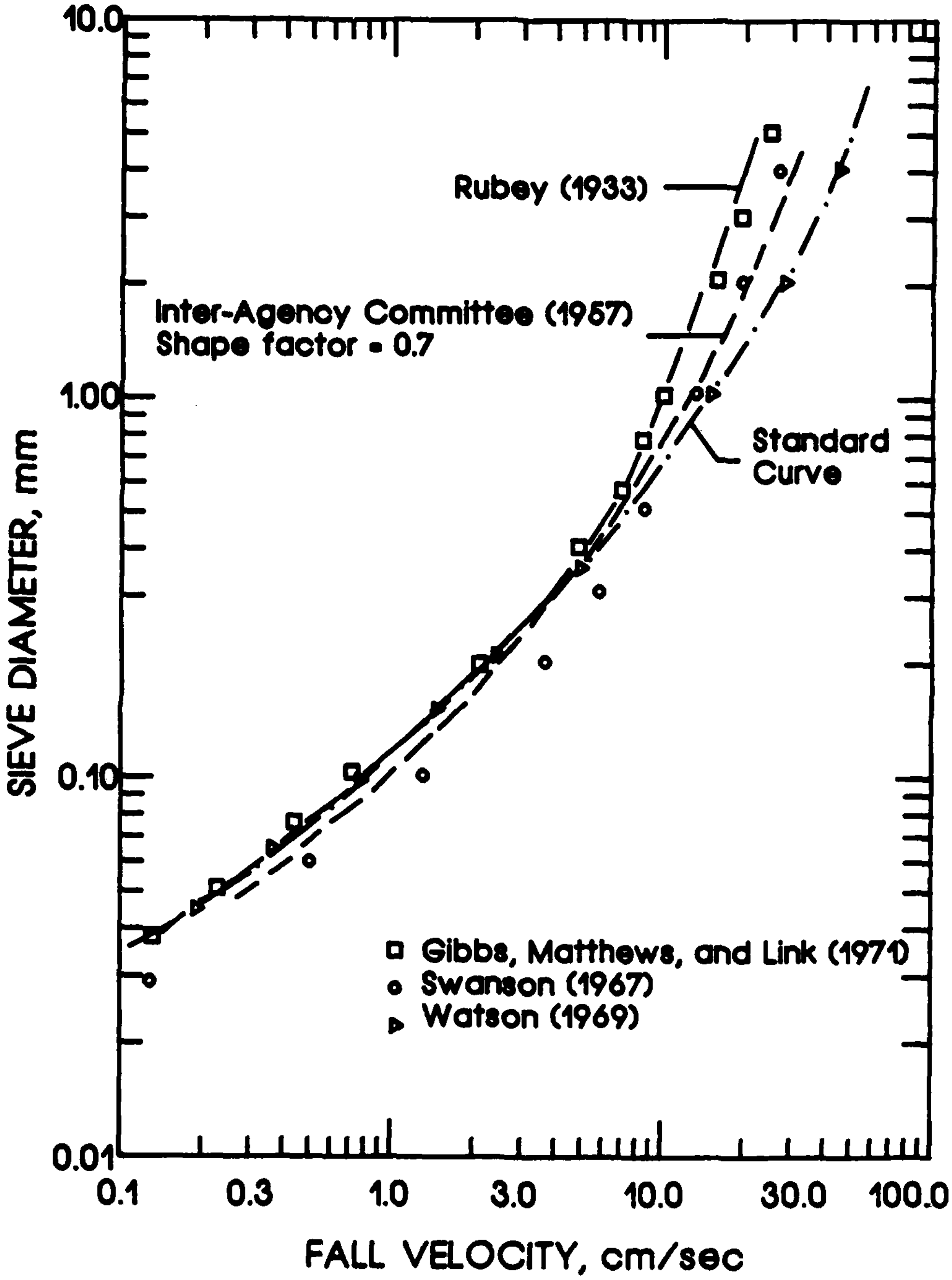

Figure 2.11. Fall velocity of quartz particles in water (specific gravity 2.65, temperature 20° C) (after Woo 1985)

the discrepancies are not so large until the diameter of particles is larger than 0.5 mm. Secondly, natural sands are not spherical. Thirdly, the effects of hindered settling and turbulence in streams have been known to reduce, more or less, the fall velocity of particles.

Rubey's (1933) equation has been frequently used in the mechanics of sediment transport (Einstein 1950). The explicit formula was developed by the simple combination of Stokes' (1851) law and Newton's impact law and is expressed as

$$W_s = \frac{\sqrt{\frac{2}{3} g \left(\frac{\gamma_s}{\gamma} - 1\right) d^3 + 36\nu^2} - 6\nu}{d} \qquad (2.29)$$

where

W_s = particle fall velocity

g = acceleration of gravity

γ = specific weight of fluid

d = particle size

ν = fluid kinematic viscosity

2.4.3 Fall Velocity of Sand Particles in Clay Suspensions

There are few studies concerned with the terminal fall velocity of a spherical or nearly spherical particle in a Bingham fluid. Woo (1985) discusses five methods he found in the literature, and after a thorough evaluation of the five, concludes that a completely satisfactory method does not exist for predicting the drag force in a Bingham fluid. The five methods evaluated by Woo were Simons, Richardson, and Haushild (1963), du Plessis and Ansley (1967), Ansley and Smith (1967), Valentik and Whitmore (1965), and Pazwash (1970). The data from the five studies resulted in 219 data points, and Woo made his evaluation of each method using all the data. The uncertainty with the methods that Woo expressed appeared to be due primarily to the inaccuracy of experimental data rather than the inadequacy of their equations. In conclusion, Woo recommended the method of Ansley and Smith (1967) because it appeared to predict the fall velocity slightly better than the other methods and is analogous to the Newtonian relation between C_D versus Re_p^* by using the effective viscosity μ_e of a Bingham fluid. The drag coefficient by Ansley and Smith can be expressed by

$$C_D = f(Re_p^*) \tag{2.30}$$

in which Re_p^* is the particle Reynolds number in the form

$$Re_p^* = \frac{\rho_f W_s d}{\mu_e} \tag{2.31}$$

where

ρ_f = the density of water-fine sediment mixture

W_s = the particle fall velocity in the water-fine sediment mixture

The value of μ_e is given by

$$\mu_e = \eta + \frac{K\tau_y d}{W_s} \tag{2.32}$$

where

η = the plastic viscosity of Bingham fluid

K = a constant with a recommended value $K = 7\pi/24$ by Ansley and Smith

τ_y = the yield stress of Bingham fluid

In situations where data are not available on the yield stress and plastic viscosity of the water-fine sediment mixture, the method of Simons, Richardson, and Haushild (1963) may be used as a rule of thumb for predicting the fall velocity of sand particles in turbulent water-fine sediment mixtures (Woo 1985).

Simons, Richardson, and Haushild (1963) measured settling velocities of sand particles in aqueous dispersions of kaolin and bentonite clays. The measured velocities were compared with calculated velocities by using the measured apparent viscosity of the water-fine sediment mixture, a particle shape factor of 0.7, and the median fall diameter (converted to a nominal diameter) of the sand particles. The C_D versus Re_p^* relationship for naturally worn sand particles that is presented in Figure 1 of Inter-Agency Committee (1957) was used for the computations. In spite of the uncertainty, that the change in fluid properties due to the clay particles can be correctly assessed by making allowances for the change in only the apparent viscosity (Howard 1962), the results of comparison by Simons, Richardson, and Haushild are remarkably good, especially for the case of kaolin suspensions.

2.4.4 Effect of Concentration of Sand on Fall Velocity

Even without fine sediment, the fall velocity of the coarser particles in a sediment-laden flow is expected to be different from that of a single particle in a flow of clear water because of the mutual interaction between particles and of a hydrodynamic interference between particles and the suspending medium. The process of reduced fall velocity of falling cohesionless particles is referred to as a hindered settling. Woo (1985), after a review of the work of McNown and Lin (1952), Richardson and Zaki (1954), and Maude and Whitmore (1958), concluded that the fall velocity of sand-sized particles in hyperconcentrated flow may be predicted reasonably well within the state of the art by combining the effect of fine particles on the fall velocity of a single sand particle and the effect of concentration on the fall velocity of sand particles themselves. Woo recommended the equation of Maude and Whitmore (1958) for estimating the effect of the sand-size concentration on the fall velocity.

The Maude and Whitmore equation (1958) is in the form

$$\frac{W_s}{W_o} = (1 - C_v)^{\alpha} \tag{2.33}$$

in which W_o is the settling rate of a single particle in the same suspending medium and α is a function of particle Reynolds number, particle shape, and size distribution. Woo suggested that α may be set at 3.5 as a rule of thumb for sand particles.

In summary, by Woo's methodology (1985), the fall velocity of a single sand particle with a certain shape factor may be estimated from existing Newtonian C_D versus Re_p^* relationships using the effective viscosity by Equation 2.32 and the apparent density or specific weight of the water-fine sediment mixture from a simplified form of Equation 2.8 of the form

$$\frac{\gamma_s - \gamma_f}{\gamma_f} = \left(\frac{\gamma_s}{\gamma_w} - 1\right)\left(1 - C_{wf}\right) \tag{2.34}$$

The yield stress and plastic viscosity are obtained by direct measurements. Then, the final fall velocity of sand particles in hyperconcentrated flow may be estimated by Equation 2.33 with α set at 3.5. The value of C_v in Equation 2.33 must be evaluated only from the concentration of sand-sized particles.

2.5 VELOCITY AND CONCENTRATION DISTRIBUTIONS

2.5.1 Introduction

The total sediment discharge is obtained by integration of the product of the sediment concentration and the flow velocity over depth; thus, proper descriptions of both the vertical velocity and vertical sediment concentration profiles are important. In turbulent flows with dilute concentrations and limited stratification of sediment, the Karman-Prandtl logarithmic velocity profile from the law of the wall (Rouse 1946) and the Rouse equation (1937) for the suspended sediment profile have generally proven adequate for most practical applications. The logarithmic velocity distribution is expressed by

$$\frac{u}{u_*} = \frac{2.3}{\kappa} \log \left(\frac{Ay}{k_s}\right) \tag{2.35}$$

where

u = velocity at a distance y from the bottom

u_* = shear velocity = $(gdS_e)^{1/2}$ where d is the flow depth and S_e is the slope of the energy grade line

κ = von Karman constant

A = parameter related to flow regimes

k_s = characteristic roughness height

The Rouse equation (1937) is

$$\frac{C_y}{C_a} = \left[\left(\frac{d - y}{y}\right)\left(\frac{a}{d - a}\right)\right]^z \tag{2.36}$$

$$z = \frac{W_s}{\beta \kappa u_*} \tag{2.37}$$

where

C_y = concentration of a grain size at a distance y above the bed

C_a = concentration of a particle size at a reference level a above the bed

d = flow depth

z = theoretical exponent of the distribution equation

W_s = fall velocity of the given particle size

Both the logarithmic velocity profile and Rouse equation have been applied to flows where stratified, suspended sediments have a large effect on the flow. This was done by empirically adjusting the von Karman constant κ and the exponent z of the suspended sediment distribution equation. The logarithmic velocity profile is a reasonable approximation for concentrations up to fairly high values. However, the limitations of the logarithmic velocity profile cannot be defined in terms of concentration alone because the average velocity influences the uniformity of the suspended sediment profile which in turn influences the velocity profile (Bradley 1986).

2.5.2 Turbulent Velocity Profiles

Both Woo (1985) and Bradley (1986) present a thorough review and discussion of a number of velocity profile equations that have been developed for turbulent flow in channels. Woo classified these equations by their development into three categories: equations that are based on the logarithmic law, equations that involve the wake flow region above the turbulent boundary layer, and equations that are based purely on empiricism such as the power-law equation. Woo further states that no equation has been introduced for the velocity profile in hyperconcentrated flow except those by Naik (1983) for a Bingham fluid flow, which are rather complicated.

Woo's (1985) criteria for adopting an equation for the velocity profile was that it must describe the time-averaged velocity distribution reasonably well especially near the bed, and it must be mathematically as simple and convenient as possible. In his judgment the power-law best met this criteria; and he chose it along with the log-law equation for comparison with data by Einstein and Chien (1955), Nordin (1963), and Nordin and Dempster (1963). The data by Einstein and Chien include high concentrations of sand particles near the flume bed, and the data by Nordin (1963) and Nordin and Dempster (1963) include high concentrations of both fine sediment and sand particles in the Rio Puerco and Rio Grande, New Mexico.

Woo (1985) reported that both equations fit reasonably well the data for flows with high concentrations of sediment. However, the power-law equation appeared to fit both flume and field data better near the bottom. The power-law equation presented by Woo is in the form

$$\frac{u}{u_{max}} = n_1 \left(\frac{y}{d}\right)^{n_2} \qquad (2.38)$$

where

u_{max} = maximum velocity assumed to be located at the free surface

$n_1 = n_2 + 1$

y = depth of point velocity

$n_2 = u_*/\kappa\bar{u}$ where $\bar{u}$ is the mean velocity

Bradley (1986) likewise reported that either the log-law or the power-law appeared to be reasonable assumptions for data collected in his flume study. A point of controversy, discussed at length in the literature and summarized by Bradley, is whether von Karman's κ varies with sediment concentration. Bradley determined κ values from vertical velocity profile in three runs of his flume study and showed that κ varied from 0.34 to 0.41, and that the data did plot as straight lines on a semilog graph which supports the log-law assumption. Furthermore, the power-law approximations which fit his observed data quite well were based on κ equivalent to 0.4. Hence Bradley concluded that once a flow is determined to be a turbulent sediment-laden flow or hyperconcentrated flow, a log-law or power-law model velocity profile will adequately describe the flow and that the power-law is preferred due to its simplicity. However, even in its simplicity, Woo (1985) suggests that it is necessary to evaluate the values of n_1 and n_2 to make use of the power-law equation in hyperconcentrated flow. Because there is no general method for predicting these values except as defined in Equation 2.38, Woo suggested direct measurements in streams to evaluate the parameters.

2.5.3 Laminar Velocity Profiles

Laminar flow of a Bingham fluid in pipes has been treated by many investigators, and a comprehensive summary of the theory is available in Govier and Aziz (1972). Treatment of the free-surface laminar flow of a Bingham fluid is not as extensive as that of the flow in pipes. A few of the more useful contributions to the laminar flow in Bingham fluids in open channels have been made by Howard (1963), Yano and Daido (1965), Kozicki and Tiu (1967), Johnson and Hampton (1969), Johnson (1970), Qian et al. (1980), Zhang et al. (1980), and Naik (1983). However, the resulting equations are complicated, and in most cases the solutions involve numerical techniques and the use of a computer.

Bradley (1986) proposes a parabolic second-degree curve that has been used in pipe flow and laminar overland sheet flow. The vertical velocity distribution equation is expressed by

$$u = \frac{2u_{max}y}{d} - \frac{u_{max}y^2}{d^2} \qquad (2.39)$$

Bradley applied Equation 2.39 to the two laminar flume runs that he observed in his study, and the predicted profiles fit the observed data reasonably well although some deviation at the bed was noted. Based on this very limited comparison, Bradley suggested that the parabolic velocity distribution equation could be used to describe laminar hyperconcentrated flow.

2.6 FLOW RESISTANCE IN HYPERCONCENTRATED SEDIMENT FLOWS

2.6.1. Introduction

The resistance to flow in open channels for Newtonian fluids has been well developed for sediment concentration in the lower range. Resistance to flow is conceptually divided into particle resistance and form resistance. Large suspended sediment concentration is a factor normally not considered when estimating either type of flow resistance. Furthermore, hyperconcentrated sediment flows can be laminar, transitional, or turbulent, and subcritical or supercritical. Transition from laminar to turbulent can be predicted theoretically for a Bingham fluid (Naik 1983).

Nordin (1963) states that hyperconcentrations of suspended sediment can significantly affect both the particle and form resistance. He explains that bed forms may vary with wash load concentration and significantly affect total roughness. Gravel beds can be smoothed and covered with sand and silt by hyperconcentrated flows and gravel may be entrained by the denser flows. In addition, subsequent water flows of lower concentration can scour fine material from debris deposits to form boulder, gravel, or sand beds.

2.6.2 Laminar Flow Resistance

Naik (1983) derived the resistance law for laminar flow of a Bingham fluid in rectangular, open channels of different aspect ratios from an expression for mean velocity V given by Kozicki and Tiu (1967) using the shape factors a and b.

$$\frac{2V}{R} = \left(\frac{\tau_w}{\eta}\right)\left\{\frac{1}{a+b} - \frac{\tau_b}{b\tau_w} + \left[\frac{a}{b(a+b)}\right]\left(\frac{\tau_b}{\tau_w}\right)^{\frac{b}{a}+1}\right\} \tag{2.40}$$

where

R = the hydraulic radius

τ_w = the boundary shear stress

a and b = shape factors given in Table 2.1

The resistance law is given by

$$\frac{1}{fR_b} = \frac{1}{16(a+b)} - \frac{H_e}{8bR_n^2} + \left[\frac{a}{b(a+b)}\right]2^{\left(\frac{b}{a}-3\right)}\left(\frac{H_e}{R_n^2}\right)^{\frac{b}{a}+1} \tag{2.41}$$

where

f = friction factor defined by $f = \tau_w/(\rho V^2/2)$

R_b = Bingham Reynolds number defined by $R_b = \rho V(4d)/\eta$ where ρ is density

H_e = Hedstrom number

R_n = quantity defined by $R_n = R_b f^{1/2}$

Table 2.1

Shape Factors a and b for Rectangular Channels

Width/Depth	a	b
2.0	0.2123	0.6759
4.0	0.2439	0.7276
6.0	0.2867	0.7817
8.0	0.3231	0.8182
10.0	0.3472	0.8446
12.0	0.3673	0.8639
14.0	0.3828	0.8787
16.0	0.3951	0.8911
18.0	0.4050	0.9010
20.0	0.4132	0.9097
100.0	0.4806	0.9795
Inf.	0.5000	1.0000

Naik verified Equation 2.41 with his experiments in a flume using kaolin clay slurry as the Bingham fluid.

Bradley (1986) presents relationships developed by Chen (1986) which are based on the theoretical development for Newtonian laminar pipe flow and given by

$$f = \frac{C}{N_R} \tag{2.42}$$

where N_R is the Reynolds number defined by $N_R = \rho V(4d)/\mu$, and C is a coefficient that equals 24 for Newtonian fluids and for a non-Newtonian Bingham fluid. C is given as

$$C = \left[\frac{8}{\left(\frac{y_o}{d}\right)^2}\right]\left[\frac{2}{1 - \left(\frac{y_o}{3d}\right)}\right] \quad (2.43)$$

where y_o is the vertical distance from the bed corresponding to the yield stress s which is defined by

$$s = \rho g S_o (d - y_o) \quad (2.44)$$

Bradley proposed that Equation 2.43 could be used to determine C and f with an observed flow depth and yield stress from viscometer data.

2.6.3 Laminar-Turbulent Transition

Naik (1983) also developed a theory of laminar-turbulent transition for wide open-channel flow of a Bingham fluid using an approach similar to that of Hanks (1963a,b). According to this theory, the transition to turbulent flow is predicted by the following equation:

$$\frac{\alpha_c}{(1 - \alpha_c)^3} = \frac{H_e}{48{,}000} \quad (2.45)$$

where α_c is the critical value of the ratio α of the Bingham yield stress, i.e.,

$$\alpha_c = \left(\frac{\tau_b}{\tau_w}\right)_c \quad (2.46)$$

The critical Bingham Reynolds number R_{bc} is given by

$$R_{bc} = \left(\frac{H_e}{12\alpha_c}\right)\left(1 - 1.5\alpha_c + 0.5\alpha_c^3\right) \quad (2.47)$$

This equation suggests that for increasing Hedstrom number, the transition to turbulent flow in an open channel for a Bingham fluid occurs at an increasingly larger Bingham Reynolds number.

Naik (1983) also verified Equations 2.45 and 2.46 with experimental flume data using kaolin clay slurry as the Bingham fluid. The data used in the verification were for flow conditions which alternated between bursts of laminar and turbulent flows, and Naik considered them close to the critical flow condition.

Bradley (1986) used Equations 2.42 and 2.43 (an approach similar to that of Hanks and Pratt (1967)) to develop a family of curves of the $f - N_R - (y_o/d)$ relationship for a Bingham fluid which he applied to his experimental flume data. The procedure consisted of computing the value of f and y_o/d for each run and then obtaining the critical Reynolds number from the $f - N_R - (y_o/d)$ graph. This value was then compared with the observed Reynolds number and the flow regime determined. Bradley showed that two of his test runs were laminar and all other runs were turbulent. He states that two other runs may have been transitional; however, because the analysis does not allow for gradual transition, they were assumed turbulent and adequate results were obtained. Bradley concluded that the criterion corresponded well with his qualitative observations and the measured longitudinal velocity profiles.

2.6.4 Turbulent Flow Resistance

A theory of turbulent flow of a Bingham fluid in smooth and rough open channels has been developed by Naik (1983) following the approach of Hanks and Dadia (1971) and using the mixing length concept of Prandtl. The resulting equations for smooth channels are complicated, and solutions in closed form cannot be obtained. Thus, numerical techniques using the computer must be employed. In developing a theory for rough boundaries, Naik neglected the laminar shear stress contribution due to plastic viscosity, but that due to the Bingham yield stress was considered. Shear stress in the flow was assumed to be equal to the bed shear stress which resulted in a logarithmic vertical velocity distribution given by

$$\frac{v}{u_*} = \frac{(1 - \alpha)^{1/2}}{\kappa} \ln \frac{30y}{k_s} \tag{2.48}$$

where v is the flow velocity at a distance y above the bed and κ was assumed by Naik equal to 0.4. Following the approach of Keulegan (1938), Naik (1983) obtained the following equations for the average flow velocity V and the flow resistance of a Bingham fluid in a rough channel:

$$V = 2.5u_*(1 - \alpha)^{1/2}\left[A_o + \ln\left(\frac{R}{k_s}\right)\right] \tag{2.49}$$

$$\frac{1}{\sqrt{f}} = 2.5\left[1 - \left(\frac{2H_e}{fR_b^2}\right)\right]^{1/2}\left[A_o + \ln\left(\frac{R}{k_s}\right)\right] \tag{2.50}$$

$$A_o = \ln\left\{\left(\frac{30d}{R}\right) \exp\left[-1 - \left(\frac{\psi d^2}{4A}\right)\right]\right\} \tag{2.51}$$

where A is the cross-section area and ψ is the cross-section shape factor equal to $A_s + 2$ for a rectangular channel in which A_s is the aspect ratio equal to width/depth.

Naik (1983) attempted to verify this theory of turbulent flow in smooth and rough boundaries with his experimental flume data. Friction factors computed using the theory for smooth turbulent flow compared well with experimental values as did vertical velocity profiles. In order to verify the theory of rough turbulent flow, he compared theoretically computed average velocities (Equation 2.49) with the experimental average velocities, and the agreement was good in the range of experimental conditions covered. However, Naik (1983) concluded that more elaborate experimental studies are necessary covering a broader range of relative roughness. He used strips of wire screen for the roughness element, and k_s was assumed equal to the actual thickness of the screen, which was 0.01 ft.

Bradley (1986) states that particle resistance can be estimated for suspended sediment concentrations smaller than 20 percent by volume where the flows are turbulent by using the Karman-Prandtl resistance equation for smooth and rough boundaries (Rouse 1946). It can also be determined using the empirical Manning or Chezy equations for rough boundaries. These relationships are applicable so long as the log-law velocity profile assumption is reasonable (Bradley 1986). Also, the National Research Council (1982) asserts that channel resistance (due to particle roughness) for turbulent hyperconcentrated flow (or mud floods) can be predicted using the same methods as for clear water floods.

2.6.5 Form Resistance

As Bradley (1986) stated, the evaluation of form resistance for clear water is in itself complicated and requires use of different relationships for different bed forms. Bed form predictors have been developed by Simons and Richardson (1966), Athaullah (1968), Vanoni (1981), and Kennedy (1963). None of the methods considers sediment concentration or related fluid property changes at higher concentrations. Simons, Richardson, and Haushild (1963) reported that suspended sediment concentration must be considered at higher concentrations because bed forms tend toward upper regime with increasing concentration for approximately constant hydraulic and temperature conditions. Smaller concentrations or those near the low end of the hyperconcentrated range have been observed to contribute to, or cause, upper regime conditions (plane bed or antidunes) in flumes (Guy, Simons, and Richardson 1966), in the

Rio Puerco in New Mexico (Nordin 1963), and at Mount St. Helens (Bradley and Graham 1983).

Bradley and Graham (1983) also observed a change from dune bed to plane bed at high concentrations of fine sediment in the Cowlitz River downstream of Mount St. Helens that resulted in substantial reduction in the resistance coefficient and subsequent reduction in flow depth. Nordin (1963), on the other hand, observed that increasing the fine sediment concentration caused a stabilization of bed form if the fine material was a reactive clay. He observed clay-cemented sand dunes in the Rio Puerco. As Bradley stated, the physical processes are complex and greatly complicate bed form and form resistance prediction.

2.7 SEDIMENT TRANSPORT IN HYPER-CONCENTRATED SEDIMENT FLOW

2.7.1 Introduction

Bradley (1986) states in his study,

> The Einstein type of transport equation may be used for high fine material loads by varying the fluid properties....At this time no data set exists which can be used to assess changes in fluid properties and check the validity of the Einstein method for hyperconcentrated flows. Another type of approach to estimate transport rates at higher fine material concentration is an empirical one developed by Colby (1964). This method corrects for bed material discharge due to the presence of fine sediment in suspension by giving a correction factor to be applied based on the concentration and depth of flow....The Colby bed material function may be extended to hyperconcentrated flows but new data in this flow range is also required.

Bradley's observation was based partly on the results of his flume study and partly on his review of Woo's (1985) results.

Woo (1985) analyzed six existing transport equations and, with the data of Einstein and Chien (1955), demonstrated the utility of using the Einstein (1950) type transport function for predicting the bed material discharge in hyperconcentrated sediment flows. His study indicated that the Einstein approach may be useful in estimating the sediment discharge in heavy sediment-laden flow by empirically relating the exponent of the concentration distribution z or the fall velocity to the concentration of fine sediment. Woo compared the Einstein equation with the flume data which included concentrations of sand as high as 25 percent by volume, but did not incorporate fine sediment. He concluded that the bed load discharge computed in the Einstein formula was less than measured data even when increased fluid density and viscosities were considered. He further concluded that a correct estimate of fall velocity in hyperconcentrated flows would improve the comparison. Woo also compared the empirical Colby (1964) procedure with the same flume data and concluded that this method also underpredicts the observed data. Bradley (1986) observed that these flume data were predominately sand transport, and Woo's comparison is not directly applicable for high concentrations of fine sediment. Bradley further asserted that the Colby method, although quite simple, may be useful if sufficient prototype and laboratory investigations are conducted for fine sediment concentrations in the 10 to 20 percent by volume range and perhaps greater.

2.7.2 Methods for Prediction of Bed Material Discharge

2.7.2.1 Introduction. The nonexistent prototype data discussed in the previous paragraph that Bradley (1986) referred to do now exist, and are the basis of analysis for this study. These and other data will be analyzed to check the validity of using the Einstein type approach to compute total bed material discharge from measured suspended sediment in heavy sediment-laden flow. These results will then be used to check the correction factors for fine material concentration of the Colby (1964) procedure.

2.7.2.2 Modified Einstein Procedure. Perhaps the most widely used procedure for computing total sediment discharge by extrapolating and interpreting data for a single cross section has been developed by Colby and Hembree (1955), and is known as the modified Einstein procedure. Colby and Hembree modified the Einstein procedure to compute total sediment discharge at a cross section from readily measurable field data like that obtained and reported by the USGS.

The measured suspended sediment discharge is calculated by the product of the average concentration by weight, the measured streamflow, and a conversion factor to obtain the measured suspended discharge in tons per day (Section 4.3). However, as Colby (1957) explains, the measured suspended sediment discharge is computed from all the flow through the cross section but from less than the true average suspended sediment concentration because depth-integrating samplers do not normally collect water-sediment mixture to within 3 to 5 in. of the streambed, and suspended sediment concentrations are highest near the bed.

The difference between the total sediment discharge of a stream and the measured sediment discharge is termed by Colby (1957) as the unmeasured sediment discharge. The unmeasured sediment discharge consists of bed load discharge (the discharge of sediment that moves along in essentially continuous contact with the bed of the stream) and part of the suspended sediment that is discharged below the lowest point of travel of the sampler nozzle in the vertical.

The modified procedure uses measurements of bed material particle sizes, suspended sediment concentrations and particle size distribution from depth-integrated samples, streamflow, and water temperature. Major advantages of this modified procedure include applicability to a single section rather than a reach of channel; use of measured velocity instead of water-surface slope; use of depth-integrated samples; and apparently fair accuracy for computing both total sediment discharge and approximate size distribution of the sediment. Because of these advantages, the modified procedure was used in this study.

A detailed description of the modified Einstein procedure is given by Colby and Hembree (1955), and outlines of the computational procedure are given by Simons and Sentürk (1977), and Simons, Li, and Associates (1982). However, for the convenience to the reader and to subsequent discussion in this study, the procedure as outlined by Simons, Li, and Associates (1982) is discussed in the following paragraphs.

Data requirements are stream discharge Q , mean velocity V , cross-sectional area A , stream width B , mean value of the depths at verticals where suspended sediment samples were taken d_v , measured suspended sediment concentration C'_s , size distribution of the measured suspended sediment i_s , size distribution of the bed material at the cross section i_b , and water temperature T .

The first step is to calculate the suspended sediment discharge of the various size fractions per unit width q'_s in the sampled zone of the cross section. If q'_{si} is used to denote the sediment discharge through the unit width of the sampled zone, then

$$q'_s = \sum_i q'_{si} = C'_s \gamma \frac{Q'}{B} \tag{2.52}$$

where Q' is the stream discharge in the sampled zone. The relation between Q' and Q is given by

$$\frac{Q'}{Q} = \frac{\int_{a'}^{d_v} u dy}{\int_0^{d_v} u dy} \tag{2.53}$$

The term a' is the distance from the streambed to the sampler inlet tube. In this study a' was assumed equal to 0.3 ft. If the point velocity is defined as

$$u = 5.75\ u_* \log \frac{30.2xy}{d_{65}} \tag{2.54}$$

where u_* = shear velocity = $\sqrt{gS_eR'}$ where R' is the hydraulic radius, then

$$\frac{Q'}{Q} = (1 - E') - 2.3\ \frac{E' \log E'}{P_m - 1} \tag{2.55}$$

where $E' = a'/d_v$, and

$$P_m \cong 2.3 \log \frac{30.2xd}{d_{65}} \tag{2.56}$$

where d = flow depth = A/B , and x is indirectly a function of the shear velocity, so the equation must be solved by trial. From Equations 2.52 and 2.55,

$$q'_{si} = i_s \gamma C'_s q\ (1 - E') - 2.3\ \frac{E' \log E'}{P_m - 1} \tag{2.57}$$

where q is the unit stream discharge.

A major difference between the Einstein and the modified Einstein procedure is in the computation of the shear velocity with respect to the sediment particles. In the modified procedure the shear velocity $\sqrt{32.2(SR)_m}$, is computed from a slight modification of Equation 9 (Einstein 1950). The modified equation is

$$\bar{u} = 5.75 \sqrt{32.3(SR)_m} \log \frac{12.27\ dx}{d_{65}} \tag{2.58}$$

or

$$u_m = \frac{\bar{u}}{5.75 \log \dfrac{12.27\ dx}{d_{65}}} \tag{2.59}$$

where $\bar{u}$ is the average velocity for the cross section and is taken from streamflow measurements, and $(SR)_m$ is the quantity that is obtained by solving Equation 2.58 for SR for a known value of $\bar{u}$. Note that the flow depth d is under the log sign rather than R' as given by Einstein. As stated previously, x must be solved by trial with the aid of Figure 4 (Einstein 1950) as follows.

A trial value of x is assumed and the shear velocity is computed from Equation 2.59. The thickness of the laminar sublayer δ is given by

$$\delta = \frac{11.6\nu}{u_m} \tag{2.60}$$

where u_m is the shear velocity. Therefore k_s/δ is determined, where $k_s = d_{65}$, and x is determined from Figure 4 (Einstein 1950). If the assumed x is different from the computed x, then the process is repeated using the computed x until there is no difference. Once x is determined, the suspended sediment discharge q'_{si} of the various size fraction per unit width is computed from Equations 2.56 and 2.57.

The bed load for the various size fraction per unit width $i_{Bw}q_{Bw}$ is computed next. The intensity of shear on the particles ψ_m is calculated from the following equations:

$$\psi_m = \frac{\left(\dfrac{\gamma_s}{\gamma} - 1\right) d_{35}}{(SR)_m} \tag{2.61}$$

$$\psi_m = \frac{0.4\left(\frac{\gamma_s}{\gamma} - 1\right) d_i}{(SR)_m} \tag{2.62}$$

where d_i is the geometric mean particle size and $(SR)_m$ is obtained from Equation 2.58. The larger ψ_m value is used to find Einstein's transport rate function ϕ_* from Einstein's $\psi_* - \phi_*$ curve, where ψ_* is the shear intensity factor, which is Figure 7.6 in Simons, Li, and Associates (1982). Then from the definition of ϕ_* ,

$$i_{Bw} q_{Bw} = \frac{1}{2}\, \phi_* i_b \gamma_s \sqrt{\frac{\gamma_s}{\gamma} - 1}\, \sqrt{g d_i^3} \tag{2.63}$$

The term ϕ_* is arbitrarily divided by a factor of 2 to fit the observed river data more closely (Colby and Hembree 1955).

The next step is to compute the suspended load exponent z_i' by trial and error for each size fraction. The equation derived by Colby and Hembree (1955) is of the form

$$\frac{Q_{si}'}{i_{Bw} Q_{bw}} = \frac{Bq_{si}'}{B(i_{Bw} q_{Bw})} = \frac{I_1}{J_1} \left(P_m J_1' + J_2'\right) \tag{2.64}$$

The values of I_1 , I_2 , J_1 , and J_2 are functions of z_i' and are obtained from Figures 7.8, 7.9, 7.12, and 7.13, respectively, in Simons, Li, and Associates (1982).

In Equation 2.64 the quantity $(Q_{si}'/i_{Bw} Q_{bw})$ for each size fraction is known. The value of z_i' can be found by trial and error such that Equation 2.64 is balanced. In this way one can solve the z_i' value for each size fraction where there is material in both the bed and suspended load. Colby and Hembree (1955) discovered that the value of z_i' could be related to the fall velocity of the sediment by

$$\frac{z_i'}{z_1'} = \left(\frac{w_i}{w_1}\right)^{0.7} \tag{2.65}$$

where z_1' is obtained by solving Equation 2.65 for the dominant grain size, and w_i is the fall velocity of a sediment grain of size d_i computed by Rubey's (1933) equation (Equation 2.29). Colby and Hembree (1955) used the size range from 0.125 to 0.250 mm as their reference size fraction.

A change in the modified Einstein procedure to compute z_i' was made by Lara (1966). He found that the z_i' determined by Equation 2.66 was not always representative. Further studies and analysis of collected data showed that the computed z_i' values should be computed for those size ranges having significant quantities in both the suspended and bed loads. These z_i' values, computed by trial and error from Equation 2.65, are plotted on logarithmic paper as a function of fall velocity W_s. When at least three points are plotted, a line of best fit for the relation

$$z_i' = aW_s^b \tag{2.66}$$

is computed by the method of least squares. From this relationship, the z_i' values for the other size ranges are determined.

Lara's procedure was used in this study because in most cases there was a significant quantity of material in both the bed material and the measured suspended sediment discharge for the three size ranges of 0.125-0.250 mm, 0.250-0.50 mm, and 0.50-1.00 mm.

The total sediment discharge through the cross section Q_{Ti} for a size fraction was computed from

$$Q_{Ti} = Q_{si}' \frac{P_m J_1 + J_2}{P_m J_1' + J_2'} \tag{2.67}$$

for the range of fine particle sizes (<0.25 mm), and the relation

$$Q_{Ti} = i_{Bw} Q_{bw} (P_m I_1 + I_2 + 1) \tag{2.68}$$

was used to determine the total transport of coarse particles sizes (>0.25 mm). The units of Q_{Ti} are dry weight per unit time.

2.7.2.3 Colby's Method. Colby (1964), after investigating the effects of mean flow velocity, shear velocity computed from mean velocity, stream power of flow, flow depth, viscosity, water temperature, and concentration of fine sediment on the bed material discharge, developed a graphical method for estimating the total bed material discharge in sand-bed streams at the higher fine sediment concentrations. The method is based on empirical relationships of bed material discharge per unit width to flow velocity and flow depth. The bed material discharges determined from these relationships are then corrected for water temperature different from 60° F and/or high concentration of fine suspended sediment. A further correction is made if the median bed material particle size is different from 0.20-0.30 mm. This amounts to correcting the bed material discharge for changes in fluid viscosity due to temperature and high concentration of fine sediment. If other factors remain constant, an increase in viscosity as a result of a decrease in water temperature causes an increase in bed material discharge because the change in viscosity causes a decrease in the fall velocity of the sediment particles. In much the same way, a high concentration of fine sediment may increase the apparent viscosity of the water-sediment mixture and thus decrease the fall velocity of the sediment particles.

The graphical analysis by Colby (1964) is largely based on judgment, and several iterations of plotting and replotting were necessary before a reasonably consistent set of curves was obtained. On parts of a graph for which data were insufficient, somewhat contradictory, or entirely lacking, rough estimates were made by comparison among graphs or by consideration of the general concept of sediment transportation. It should be understood that all curves for the 100-ft depth, most curves of the 10-ft depth, and part of the curves of 1.0-ft and 0.1-ft depth are not based entirely on data but were developed in this fashion. However, Colby's method is widely used by practitioners in the United States because it has proven to be a reasonably accurate predictor of total bed material discharge in sand-bed streams for flow depths below 10 ft, for flow velocities below 10 fps, and for low concentrations of fine suspended sediment.

The effect of water temperature on bed material discharge was also approximated by Colby and Scott (1965) with trial and error multiple correlation. A complete expression of the water temperature was not possible because of inadequate data, so Colby developed an oversimplified relationship which he suggested as a practical measure of the effect of water temperature on the discharge of sands in sand-bed streams. Colby stated that even if a complete definition of the temperature effect were possible, it would be very complicated, and its application for many flows might not appreciably improve the accuracy of computed bed material discharge.

The adjustment coefficients developed by Colby (1964) for high concentrations of fine sediment were obtained from data from the Rio Puerco near Bernardo, New Mexico, whose sediment concentrations are very high, and flume data of Simons, Richardson, and Haushild (1963). The adjustment coefficient can assume a value of over 100, and it covers a range of fine sediment concentration up to 8.7 percent by volume and mean flow velocities up to 10 fps. Colby states that the adjustment coefficients curves are only a guess at the relative effect of concentration of fine sediment for different median sizes of bed sediment and are unlikely to apply as well to other streams as to the Rio Puerco for which they were defined.

It is also interesting to note that most of the field data on total bed material discharge used to develop this method were computed from measured field data using the modified Einstein method as developed by Colby and Hembree (1955).

CHAPTER 3

DATA PRESENTATION

3.1 INTRODUCTION

Following the eruption of Mount St. Helens, a long-term program of study was initiated by several Federal agencies to provide direction for future flood damages reduction and restoration activities in the Toutle-Cowlitz-Columbia River system. To assist in this study, the USGS initiated a program of stream gaging and sediment measuring activities throughout the system. Figure 1.1 is a schematic of the region showing the location of the four USGS gaging stations pertinent to this study. The quantity of water, quantity of suspended sediment, and the bed material composition were closely monitored during the following year at the four gaging stations, thus providing a reasonably good data set to gain insight into sediment transport mechanics of heavy-laden sediment flow in sand-bed channels. The data used in this study were obtained from the USGS Water Data Storage and Retrieval System (WATSTORE) for WY 1982 (October 1, 1981-September 30, 1982).

3.2 DESCRIPTION OF GAGING STATIONS

This study will focus on analyzing gaging and suspended sediment measurements obtained by the USGS at four gaging stations along a 27-mile reach of the Cowlitz-Toutle River system (Figure 1.1) for WY 1982.

The station farthest downstream is on the Cowlitz River, two stations are on the main stem Toutle River, and the farthest upstream station is on the North Fork Toutle River. Gaging station designations beginning downstream and proceeding upstream are (1) Cowlitz-Castle Rock; (2) Toutle-Highway 99; (3) Toutle-Tower Road; and (4) Toutle-Kidd Valley.

The Cowlitz-Castle Rock gage is at river mile (RM) 17.3 on the Cowlitz River, which is about 3 miles downstream of the Cowlitz-Toutle confluence. The channel bottom slope varies from 0.00098 at the Castle Rock gage to approximately 0.0057 at the Kidd Valley gage. Characteristics of the four gaging stations are shown in Table 3.1.

Table 3.1

Gaging Station Characteristics

Gage	River	Location	Bottom Slope ft/ft	Bottom Width ft
Castle Rock	Cowlitz	RM 17.3	0.00098	350
Highway 99	Toutle	RM 0.9	0.0010	150
Tower Road	Toutle	RM 6.5	0.0024	200
Kidd Valley	North Fork Toutle	RM 7.0	0.0057	100

The confluence of the main stem Toutle and North Fork rivers is at RM 17.3; therefore, the distance between Tower Road and Kidd Valley gages is 17.8 river miles.

3.3 GAGING DATA

Gaging data for the four stations as obtained from the USGS is shown in Appendix A. Hydraulic parameters such as top width, hydraulic depth, and mean flow velocity for a given discharge were determined from these data. Figures 3.1-3.4 are plots of these data showing the

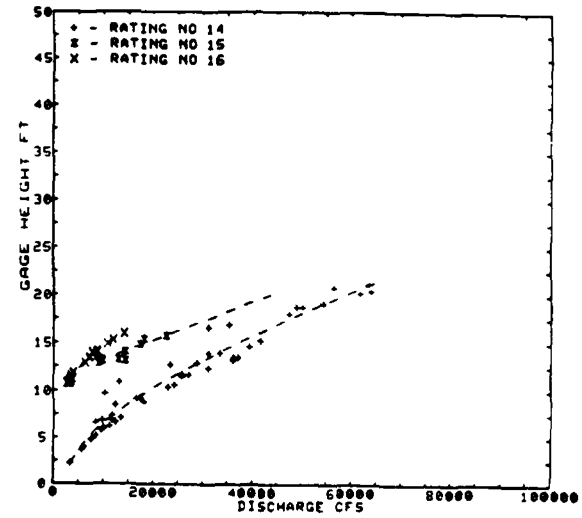

a. Discharge

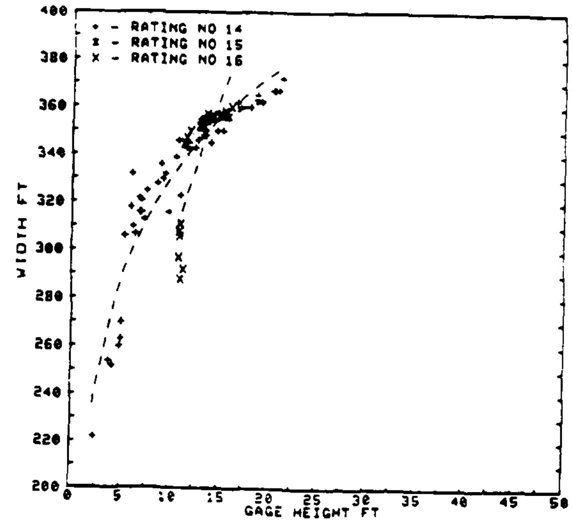

b. Top width

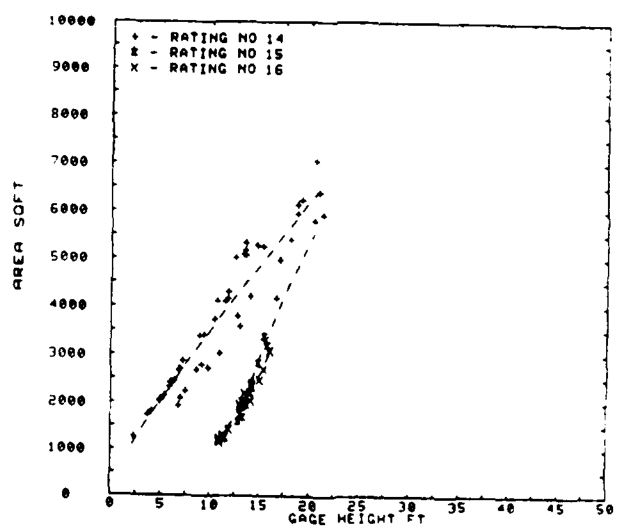

c. Cross-section area

Figure 3.1. Castle Rock gage: discharge, top width, and cross-section area versus gage height

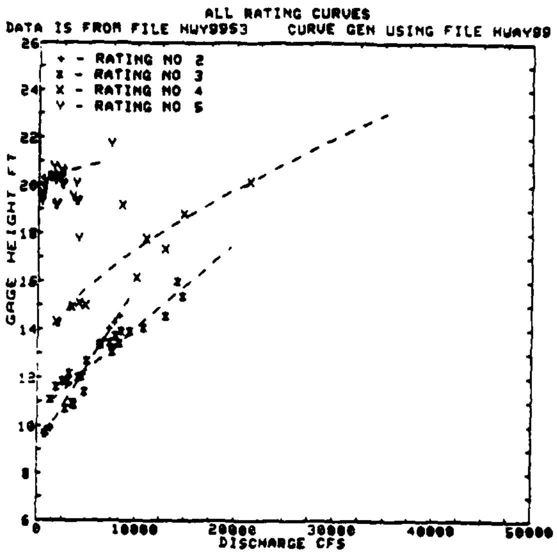

a. Discharge

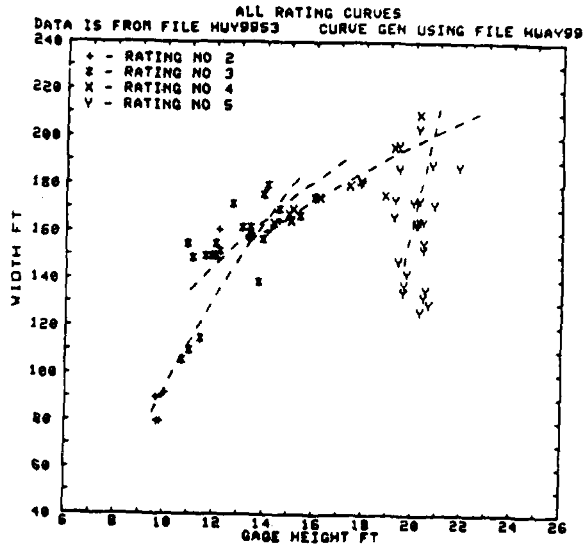

b. Top width

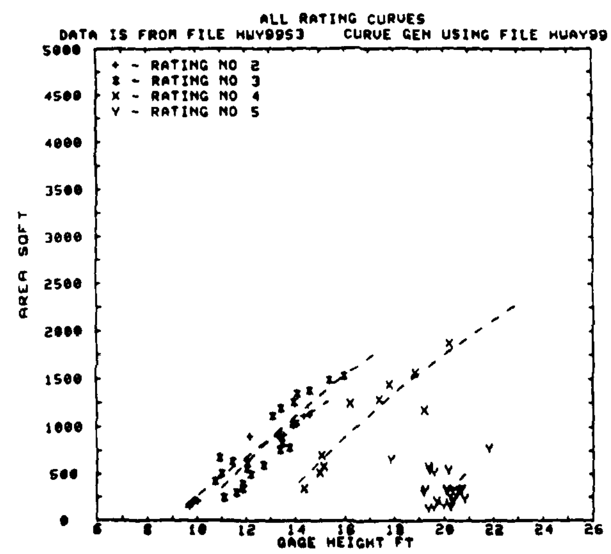

c. Cross-section area

Figure 3.2. Highway 99 Bridge gage: discharge, top width, and cross-section area versus gage height

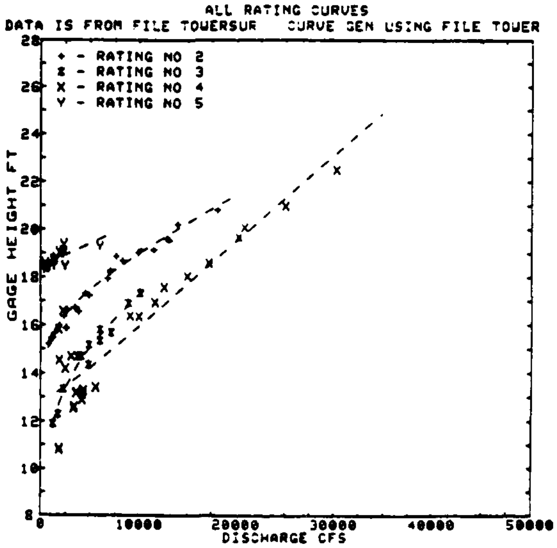

a. Discharge

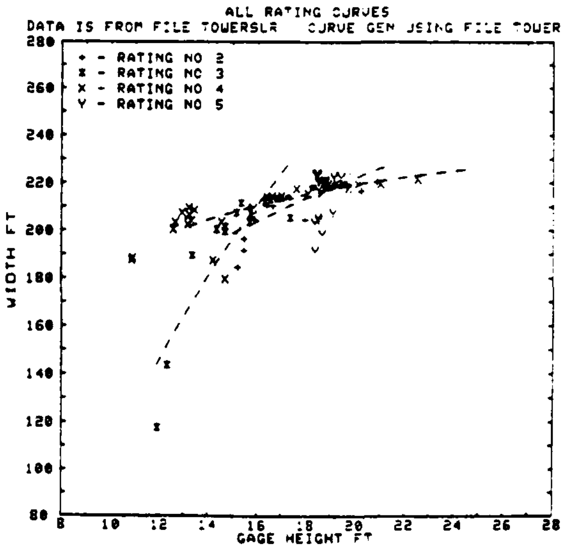

b. Top width

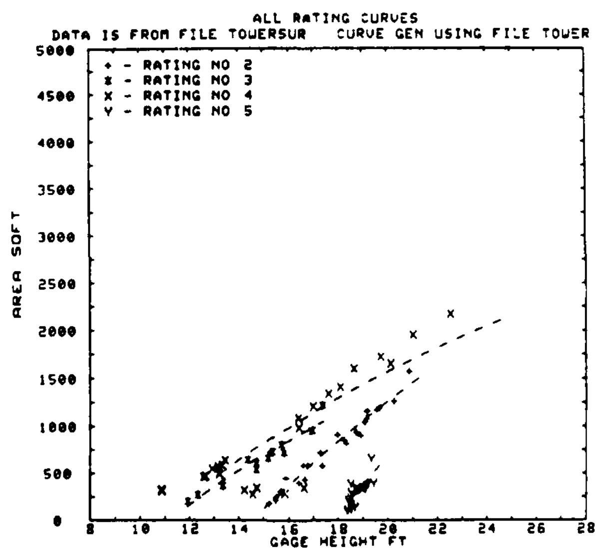

c. Cross-section area

Figure 3.3. Tower Road gage: discharge, top width, and cross-section area versus gage height

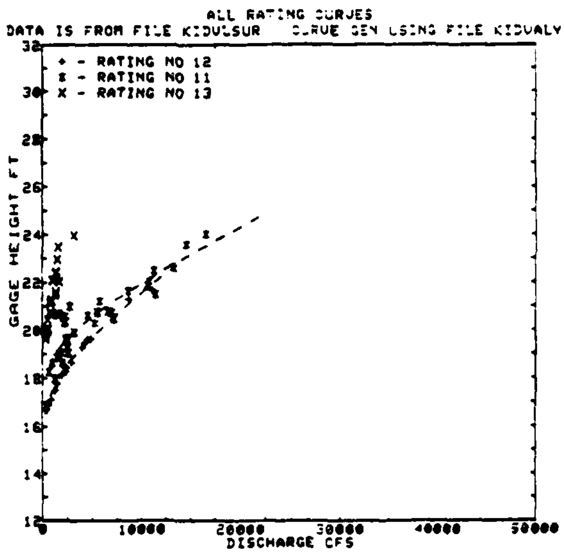

a. Discharge

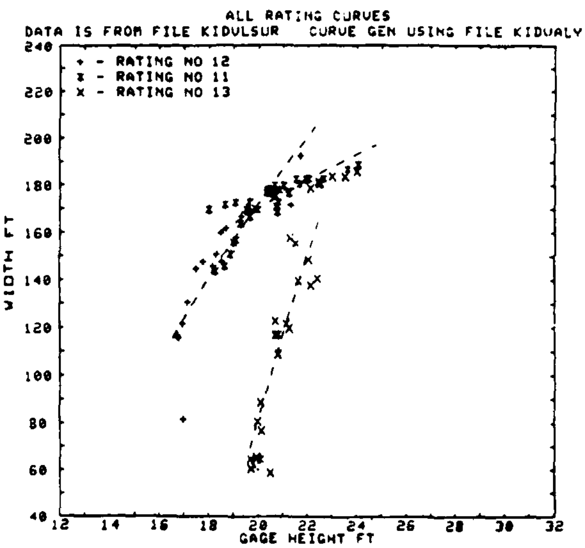

b. Top width

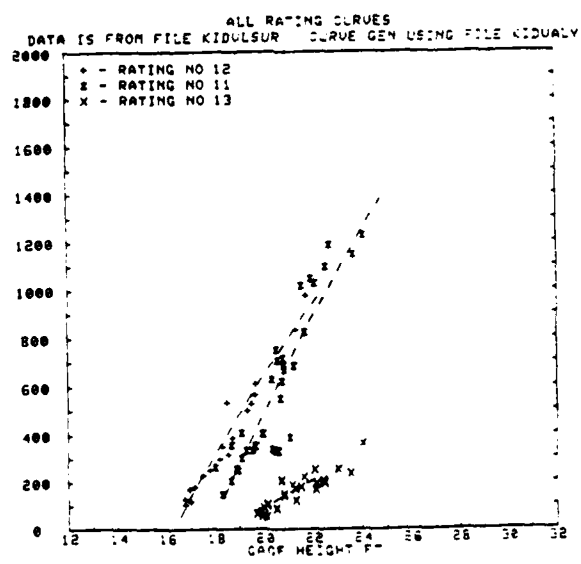

c. Cross-section area

Figure 3.4. Kidd Valley gage: discharge, top width, and cross-section area versus gage height

relation between the various hydraulic parameters as a function of gage height. The rating curves were not stable during the year because of the tremendous increase in the sediment supply and the river's sediment discharge. All gaging stations experienced dramatic shifts in the rating curves throughout the year, and the shifts were directly related to major storm events.

During WY 1982, six major storm events were monitored for sediment and water discharge. In most cases, the measured sediment discharge lagged behind the water discharge peaks. Peak water discharges for the six storm events are shown in Table 3.2 for the Toutle River-Highway 99 gage and a gage on the Cowlitz River near the confluence with the Columbia River at Kelso, Washington. The main difference in water discharge between the two stations is due to the flow contribution of the main stem Cowlitz River upstream of the confluence with the Toutle. The flow is regulated from the Mossy Rock Reservoir, which is a utility-owned dam. Detailed hydrographs of the six storm events are given in US Army Engineer District, Portland (1982).

3.4 SUSPENDED SEDIMENT DATA

Approximately 10,000 suspended sediment concentration samples were reported by the USGS at the four stations during WY 1982. Size distribution analysis of the samples consisted primarily of determining the sand break for each sample, i.e., the percent finer than 0.0625 mm. However, of major importance to this study, complete size distribution analysis was performed on approximately 100 samples. These data are listed in Appendix B for each gaging station.

Table 3.2

WY 1982 Major Storm Events

Storm Date	Peak Water Discharge cfs	
	Toutle River Highway 99	Cowlitz River Kelso, Washington
October 6-8, 1981	8,300	16,400
November 12-15, 1981	8,400	14,000
December 1-7, 1981	10,300[a]	37,000
	21,000	
January 15-18, 1982	16,000	32,000
January 23-25, 1982	36,000	65,000
February 13-22, 1982	38,000	66,000

[a] Two different peaks were noted: December 2 (10,300 cfs) and December 5 (21,300 cfs).

3.5 BED MATERIAL DATA

Size distribution of bed material samples collected and reported by the USGS for WY 1982 are shown in Appendix C.

CHAPTER 4

DATA ANALYSIS

4.1 BED MATERIAL

4.1.1 Size Distribution

Bed material samples were collected during WY 1982 at the four gaging stations. The particle size distribution analysis for the 269 samples reported is shown in Figure 4.1 and Table 4.1. In Figure 4.1, the arithmetic average size distribution for the bed material at each station as well as the average of all 269 samples is shown. These data illustrate that nearly all the bed material was in the sand size range and that there was very little variation in the bed material between the four stations. Results of the computed average size distribution analysis are shown in Table 4.1.

Table 4.1

Computed Average Analysis of Bed Material

Station	No. of Samples	d_{16} mm	d_{35} mm	d_{50} mm	d_{65} mm	d_{84} mm
Castle Rock	93	0.198	0.294	0.362	0.448	0.659
Highway 99	63	0.271	0.377	0.465	0.590	0.880
Tower Road	85	0.251	0.377	0.488	0.656	1.088
Kidd Valley	28	0.240	0.386	0.519	0.720	1.255
All stations	269	0.232	0.343	0.434	0.562	0.894

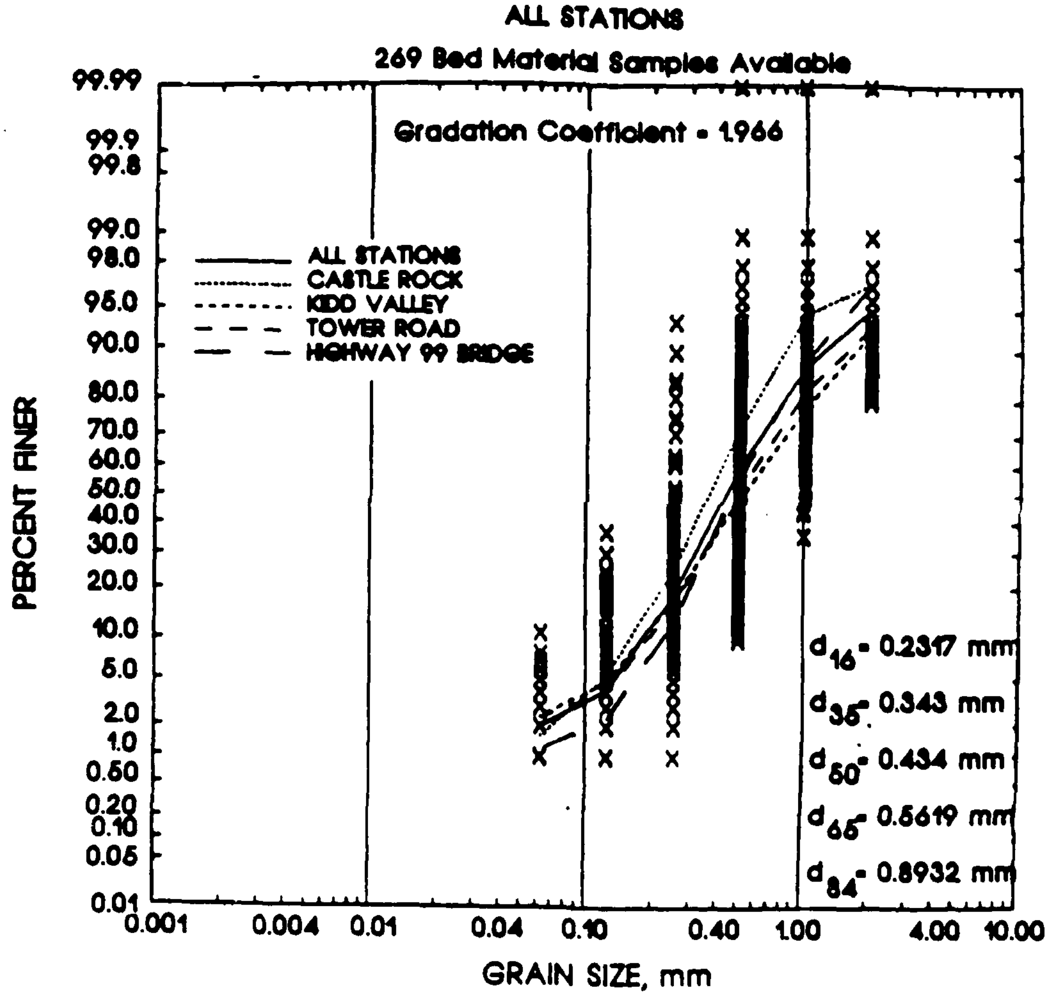

Figure 4.1. Bed material analysis

4.1.2 Specific Gravity

Individual particle specific gravities were computed by volumetric techniques by the US Army Engineer District, Portland (1982) on 150 bed material samples collected in the Cowlitz, Toutle, and North Fork Toutle rivers during the summer of 1981. The mean particle specific gravity of the 150 samples was 2.73.

4.2 MEASURED SUSPENDED SEDIMENT

4.2.1 Size Distribution

A summary of the size distribution analysis of the measured suspended sediment is shown for each of the gaging stations in Figure 4.2 and Table 4.2. The arithmetic average size distribution for each station is plotted in Figure 4.2 as well as the average for all stations. A summary of the results from the size distribution analysis is shown in Table 4.2, and as was the case with the bed material, there was little variation in the size distribution of the suspended material between the four gaging stations during WY 1982.

Table 4.2

Computed Average Analysis of Measured Suspended Sediment

Station	No. of Samples	d_{16} mm	d_{35} mm	d_{50} mm	d_{65} mm	d_{84} mm
Castle Rock	16	0.007	0.026	0.052	0.089	0.165
Highway 99	25	0.007	0.025	0.063	0.106	0.210
Tower Road	34	0.008	0.026	0.055	0.107	0.208
Kidd Valley	23	0.006	0.020	0.045	0.094	0.202
All stations	98	0.007	0.024	0.054	0.100	0.199

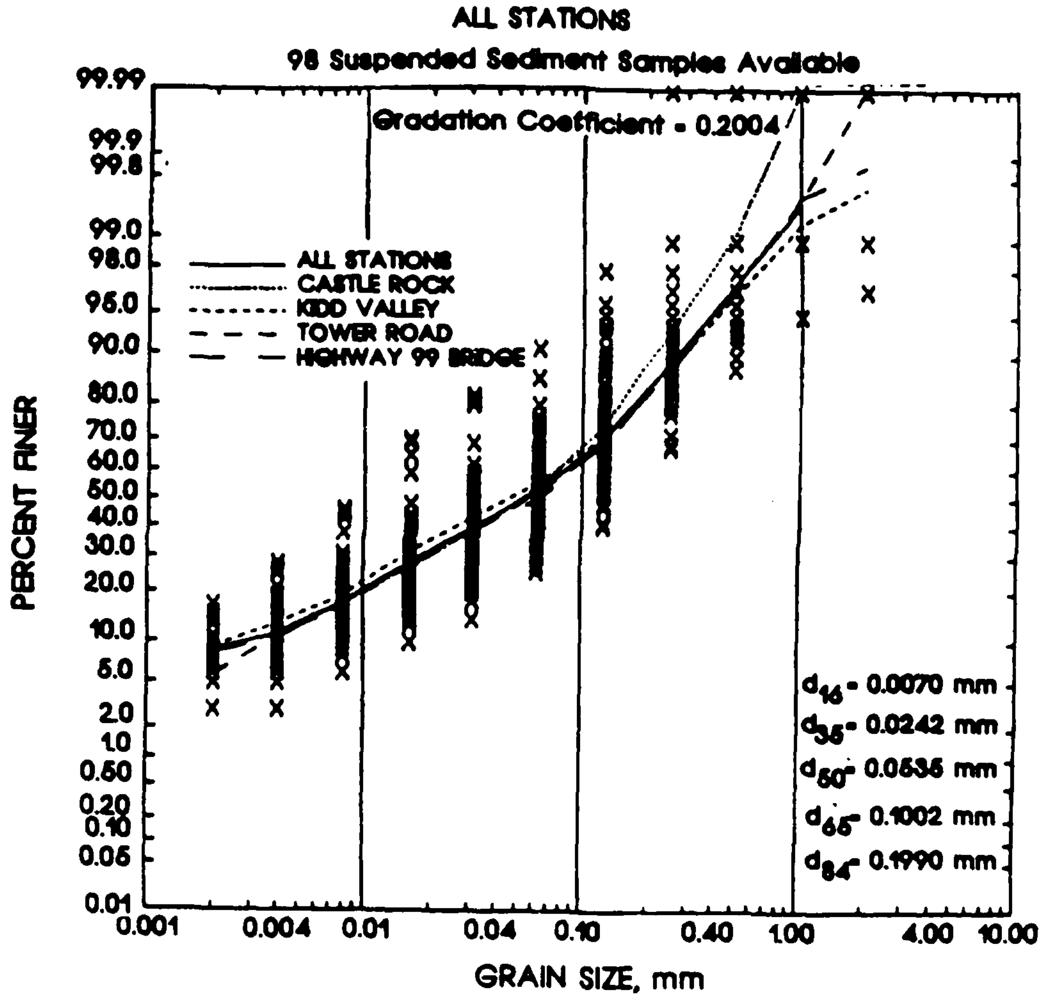

Figure 4.2. Suspended material analysis

4.2.2 Composition of Suspended Sediment

Figures 4.3 and 4.4 show the composition of the measured suspended sediment (expressed in terms of concentrations for particles larger than 0.0625 mm and those smaller than 0.004 mm) against total concentration for the four stations. It can be seen from Figure 4.3 that the suspended sediment becomes progressively coarser as the concentration increases. At suspended sediment concentrations in the water flood category ($C_v < 0.20$), the average percentage of particles greater than 0.0625 mm remained fairly constant at approximately 50 percent. However, as the concentration increased into the mud flood and lower mudflow category, the percent of particles increased to approximately 80 percent.

Figure 4.4 shows the clay content of the sediment and how it varies with concentration. Unfortunately, size distribution analysis was not obtained on the fine material for the extremely high concentrated flows, but as can be seen in Figure 4.4, the clay content of the total measured concentration was approximately 10 percent.

4.3 MEASURED SEDIMENT DISCHARGE

The measurements of suspended sediment concentrations shown in Appendix B are average concentrations in milligrams per litre of depth-integrated samples of suspended sediment for several verticals in the cross section. The measured suspended sediment discharge Q_{sm} was calculated by the product of the average concentration in milligrams per litre $C_{mg/\ell}$, the measured stream discharge in cubic feet per second Q , and a conversion factor K to obtain the suspended sediment discharge in tons per day, i.e.,

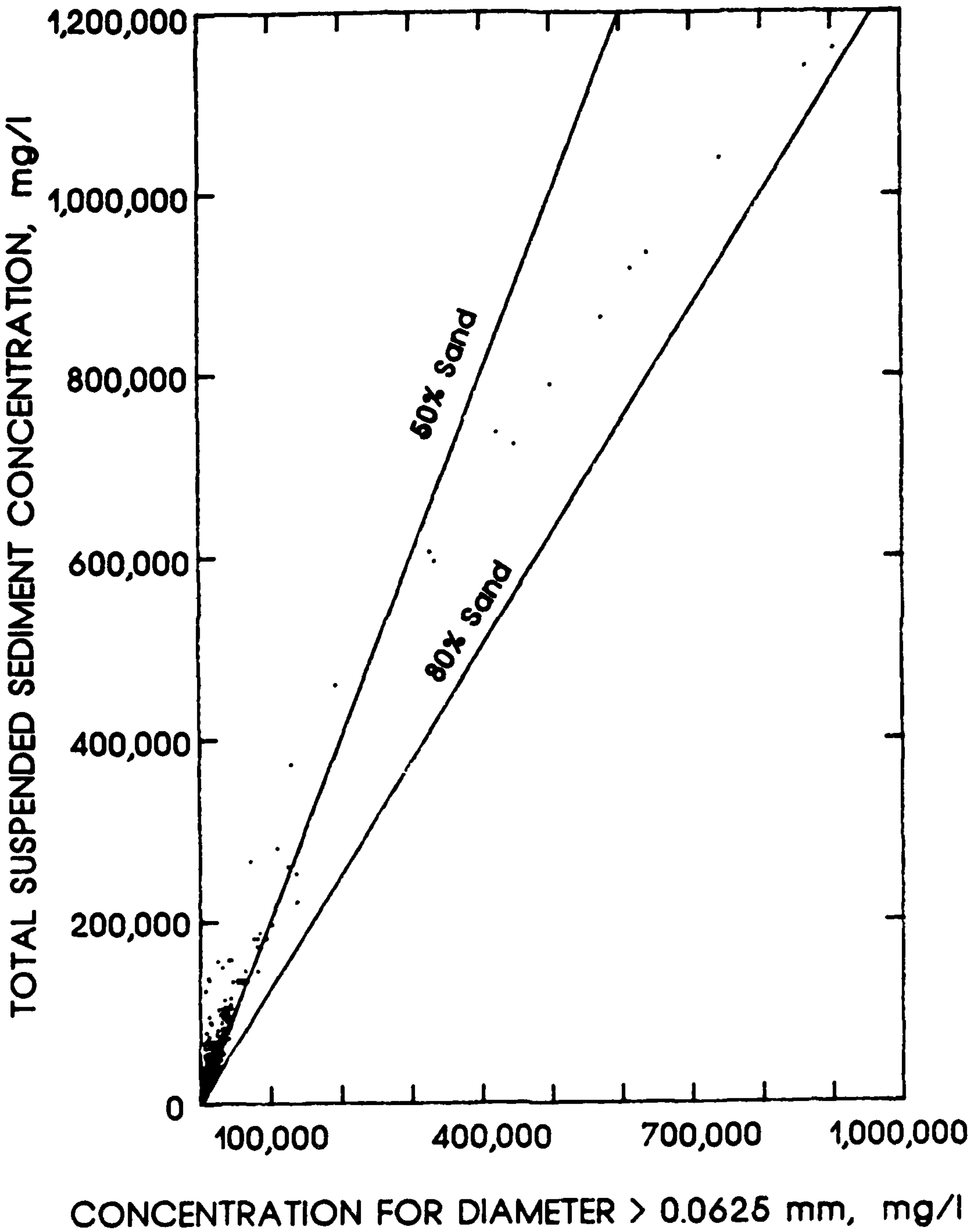

Figure 4.3. Composition of suspended material - sand

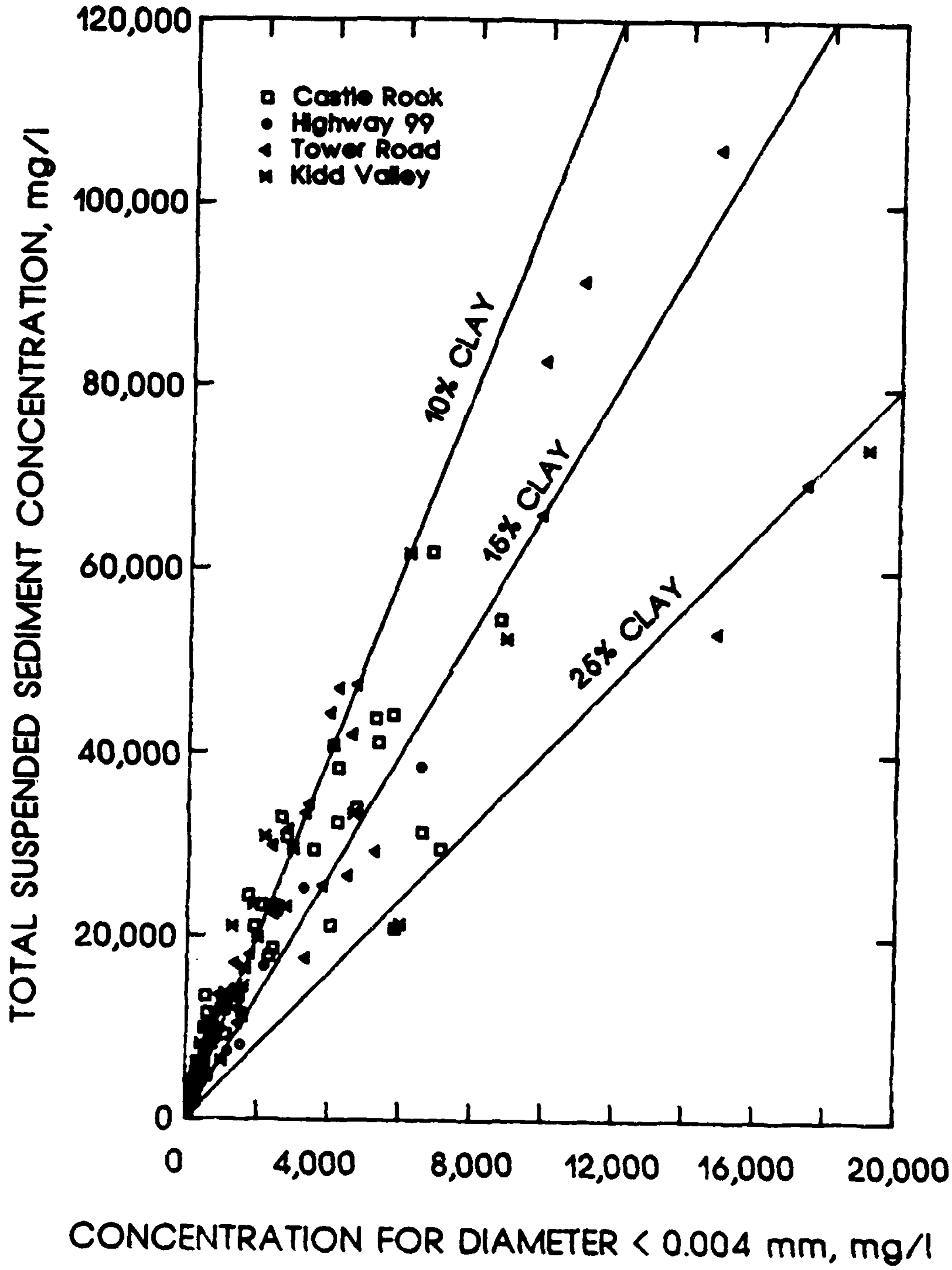

Figure 4.4. Composition of suspended material - clay

$$Q_{sm} = K \cdot C_{mg/\ell} \cdot Q \tag{4.1}$$

where the conversion factor K is equal to 0.0027.

The specific weight of the water-sediment mixture was calculated by a formula given by Simons, Richardson, and Haushild (1963):

$$\gamma_m = \frac{\gamma_w \gamma_s}{\gamma_s - (\gamma_s - \gamma_w) \frac{C_{ppm}}{10^6}} \tag{4.2}$$

where γ_s is the specific weight of the sediment. The concentration by weight C_{ppm} was calculated from

$$C_{ppm} = \frac{10^6}{\frac{10^6}{C_{mg/\ell}} - \frac{\gamma_w}{\gamma_s} + 1} \tag{4.3}$$

4.4 COMPUTED TOTAL LOAD

4.4.1 Introduction

A computer program developed for the Corps of Engineers computer-aided design system (CORPS) was used with some modification to compute the total sediment discharge. The computer program uses the modified Einstein procedure to estimate the total sediment discharge.

4.4.2 Viscosity and High Concentration Sediment Flows

4.4.2.1 Introduction. In the computation of total bed material discharge by the modified Einstein method, the viscosity of the transporting medium appears in two places: in the thickness of the laminar sublayer (Equation 2.60) and in the fall velocity of the sediment particles (Equation 2.29). Since direct measurements of the rheological parameters were not made on the Mount St. Helens material, a procedure to estimate the viscosity was developed based on the theoretical development of Woo (1985) and Naik (1983) and the experimental investigations of O'Brien (1986) and Mills (1983). Estimation of the rheological parameters of the water-sediment mixture was divided into two parts: for the basic fluid and for the dispersion of silt and larger particle sizes in the basic fluid.

4.4.2.2 Viscosity of the Basic Fluid. Viscometer measurements on slurries composed of bentonite and kaolin clays and fine material of mudflow deposits and water have been obtained by several investigators as discussed in Section 2.3.2. The data in Figure 4.5 illustrate the difficulty in adapting these data for practical application. The viscosity appears to be a function of not only the type of material but also the method of determining the yield stress from which the viscosity is determined. Of particular interest to this study is the data of Mills (1983) for fine sediment-water mixture ($d < 10$ microns) from Mount St. Helens (see Figure 2.5). The viscosity determined from shear stress measurements at high shear rates ($>100\ sec^{-1}$) is less than the viscosity determined from shear rates below $100\ sec^{-1}$. At the lower shear rates, the material behaves as a pseudoplastic material since the viscosity is a function of the shear rate but, as O'Brien (1986) observed, may be approximated by a straight line for simplicity. If shear rates in nature are in the lower range as suggested by several investigators (Section 2.3.2), then the complex procedure of Naik (1983) and Mills (1983) would overestimate the yield stress and underestimate the viscosity of the water-sediment mixture.

4.4.2.3 Viscosity of the Dispersion. The yield stress and plastic viscosity of the water-sediment mixture for the Mount St. Helens data were determined using the procedure developed by Naik (1983) and

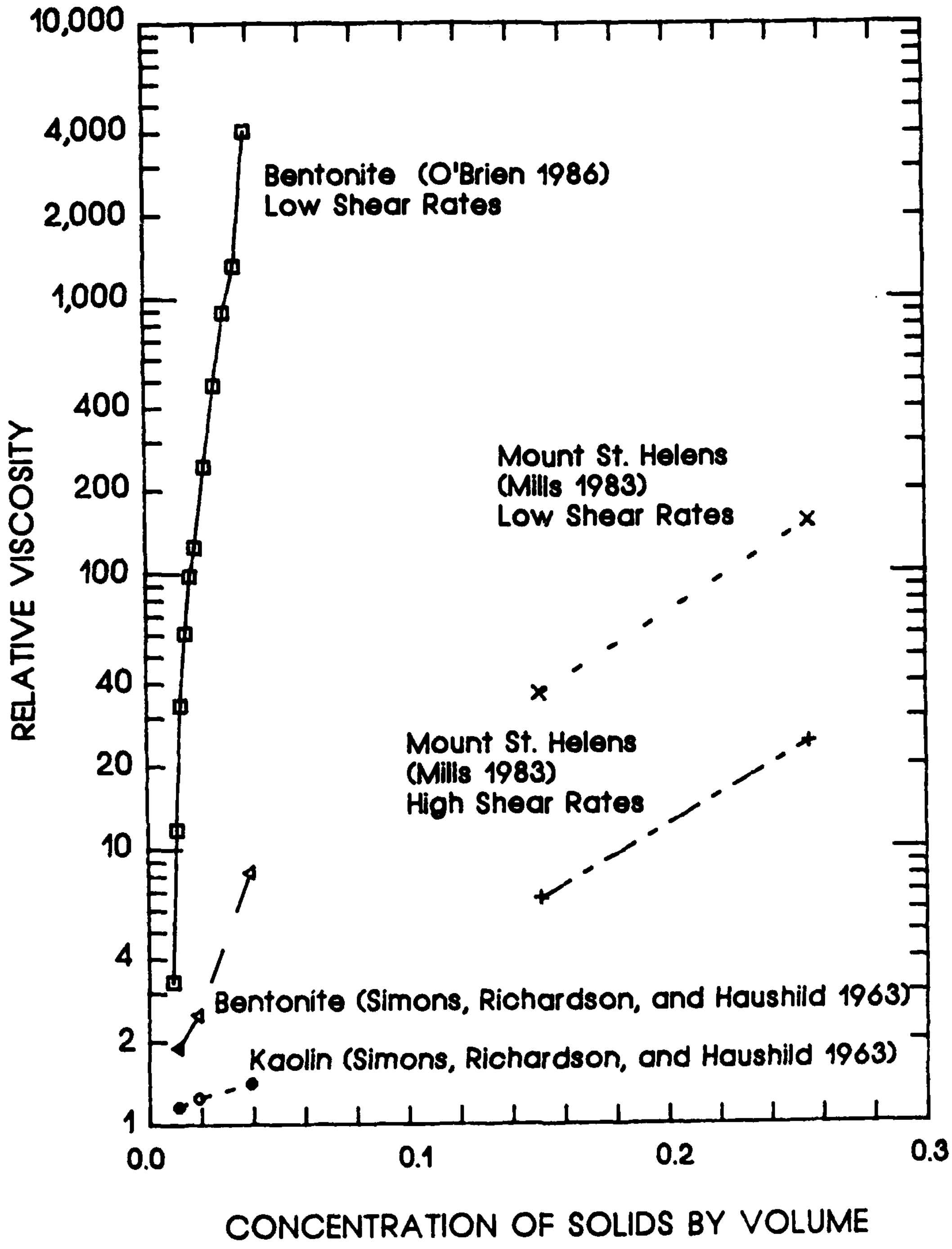

Figure 4.5. Relative viscosity of basic fluid

Mills (1983). The measured suspended sediment was divided into four discrete size fractions: 0-0.008 mm, 0.008-0.125 mm, 0.125-1.0 mm, and 1.0-10 mm. The geometric mean diameter of each fraction was 4 microns, 31.6 microns, 354 microns, and 3,160 microns, respectively. Other constants assumed were maximum volume fraction for all groups ϕ_m (Equation 2.24) = 0.68, and the ratio of specific surfaces S_p/S_o (Equation 2.17) = 2.0. The calculations were performed using the computer program listed in Naik's dissertation.

The relative viscosity of the water-sediment mixture was found to correlate best with the total solid concentration by volume C_v as shown in Figure 4.6. For comparison, Woo's (1985) simplified procedure (Section 2.3.2) was also used to estimate the relative viscosity of the mixture. The viscosity of the fine sediment-water mixture was calculated by relationships determined from Mill's (1983) Mount St. Helens data at the high shear rate (see Figure 4.5). The contribution of the silt and larger particle sizes were computed using Equation 2.10 in which μ_o was the viscosity of the fine sediment-water mixture and C_v the concentration of solids by volume greater than 0.008 mm in diameter. Both procedures underestimate the viscosity of the water-sediment mixture when compared to the data of O'Brien (1986) and Mills (1983) where the yield stresses were determined at low shear rates.

Figure 4.7 shows the comparison of the data of O'Brien and Mills at the low shear rates and the calculated relative viscosity using Naik's procedure for this study. Mills' data at the low shear rates compare well with those data of O'Brien, and it appears that Naik's theory, even with the correction by Mills, underestimates the viscosity. Validation

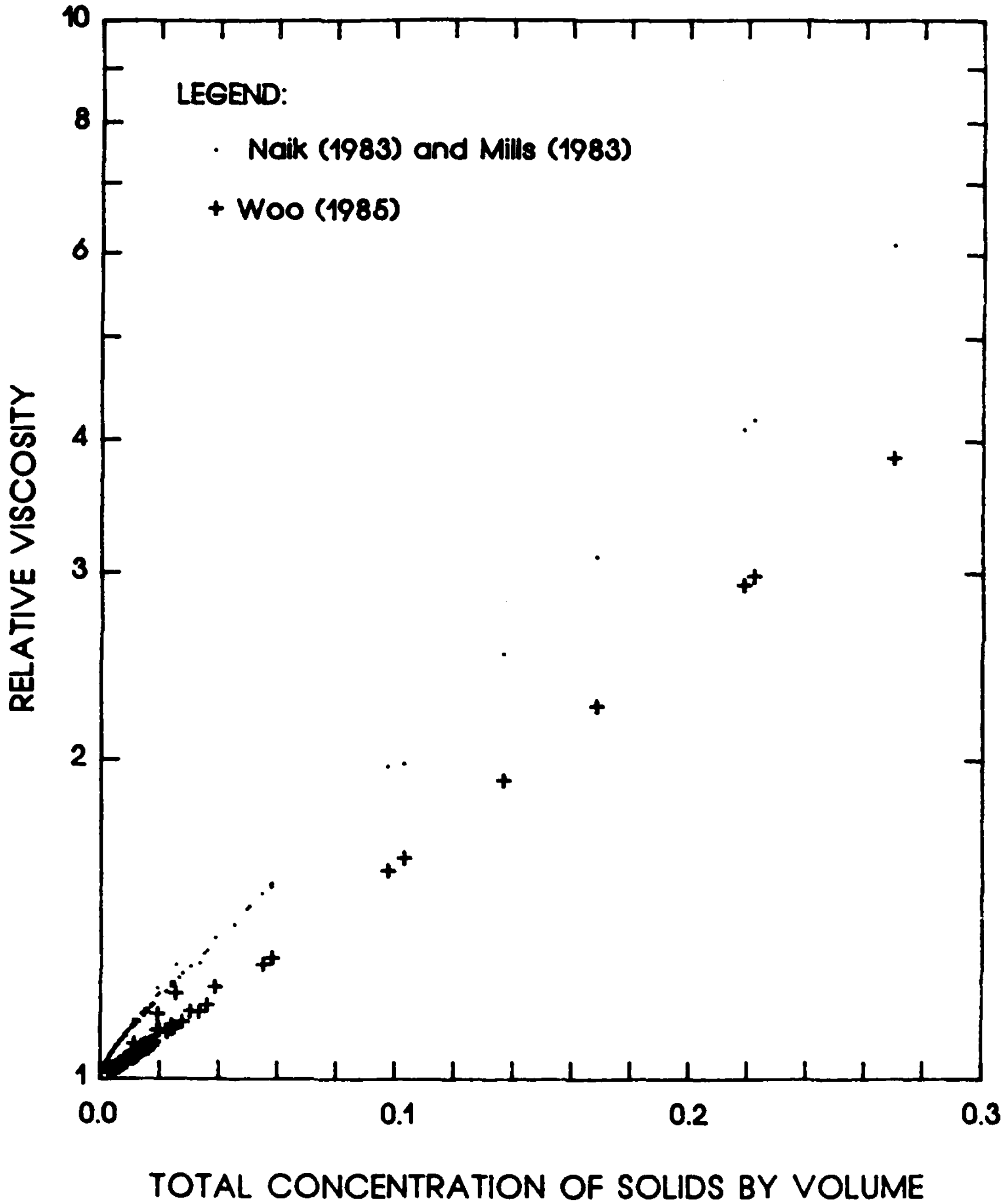

Figure 4.6. Relative viscosity versus total concentration of solids by volume

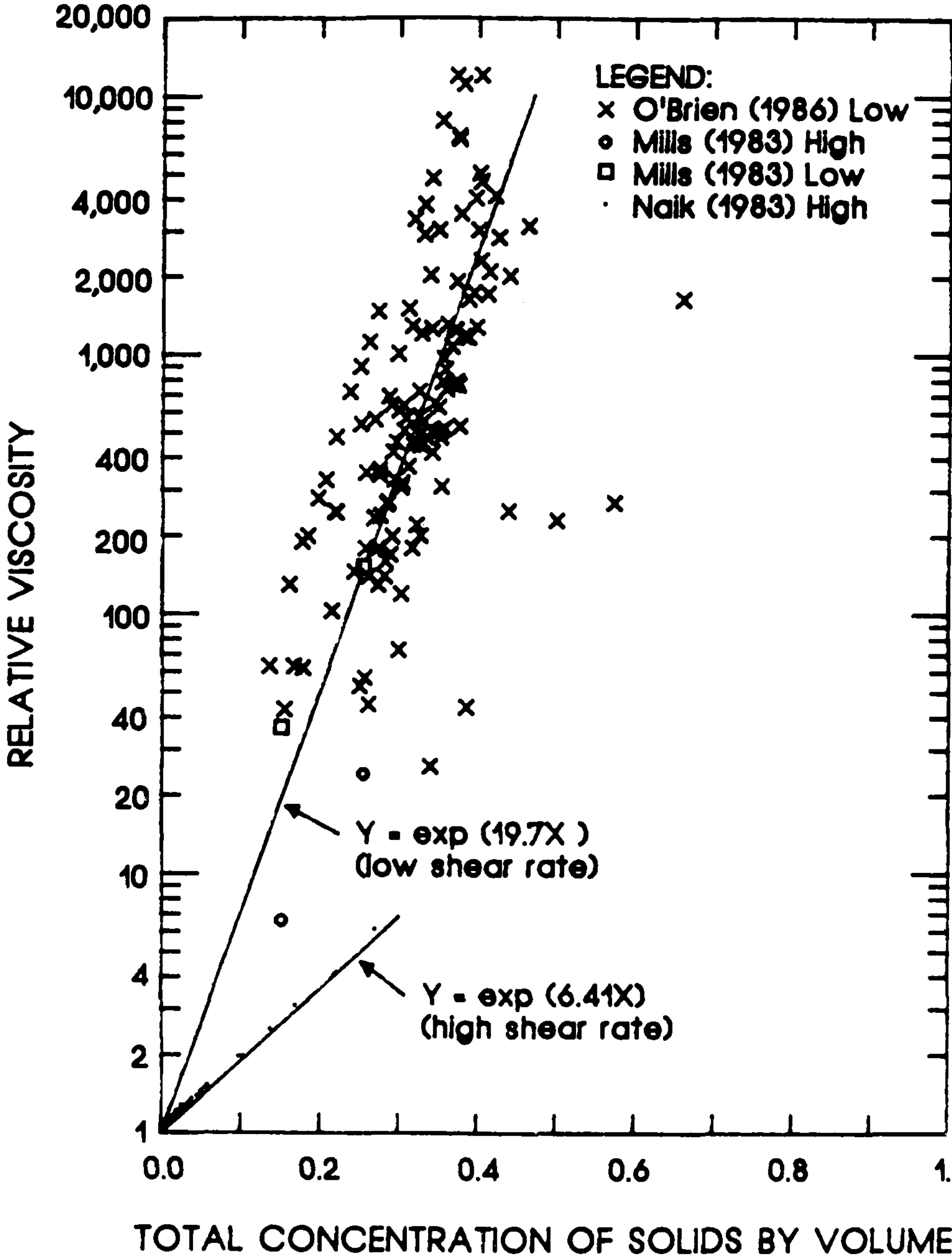

Figure 4.7. Relative viscosity versus total concentration of solids by volume (other investigators)

of these observations are only indirectly possible for this study since direct measurements of the rheological parameters were not made.

4.4.2.4 Effect of Viscosity on Computed Sediment Discharge. A sensitivity analysis was made of the effect of the viscosity on the computed total bed material discharge using the modified Einstein method. The Tower Road gaging station was selected for this analysis since size distribution analyses of the sand size particle range were reported on several extremely high concentration flows. The total bed material discharge was calculated by the modified Einstein method for three different kinematic viscosities of the water-sediment mixture: viscosity of clear water at measured temperature, apparent viscosity as calculated by Naik's procedure, and apparent viscosity as determined by the relation $\eta/\mu = \exp(19.7C_v)$ determined from O'Brien's and Mills' data at low shear rates (Figure 4.7), where μ is the viscosity of water and η is the apparent viscosity of the water-sediment mixture.

The results of the sensitivity analysis are shown in Figure 4.8. It appears that the viscosity of the water-sediment mixture has very little effect upon the total bed material discharge as computed by the modified Einstein method. The calculated versus measured bed material discharge for the three cases of viscosity essentially plot on top of one another except for the extremely high rates that correspond to the mudflow of March 20. Even in this case, the difference was only 2 percent. The departure of the calculated value from the line of perfect fit represents the unmeasured part of the total sediment load. However, because the viscometer data on actual mudflow deposits indicate that the apparent viscosity of the water-sediment mixture varies exponentially with the sediment concentration, this relationship (Figure 4.7)

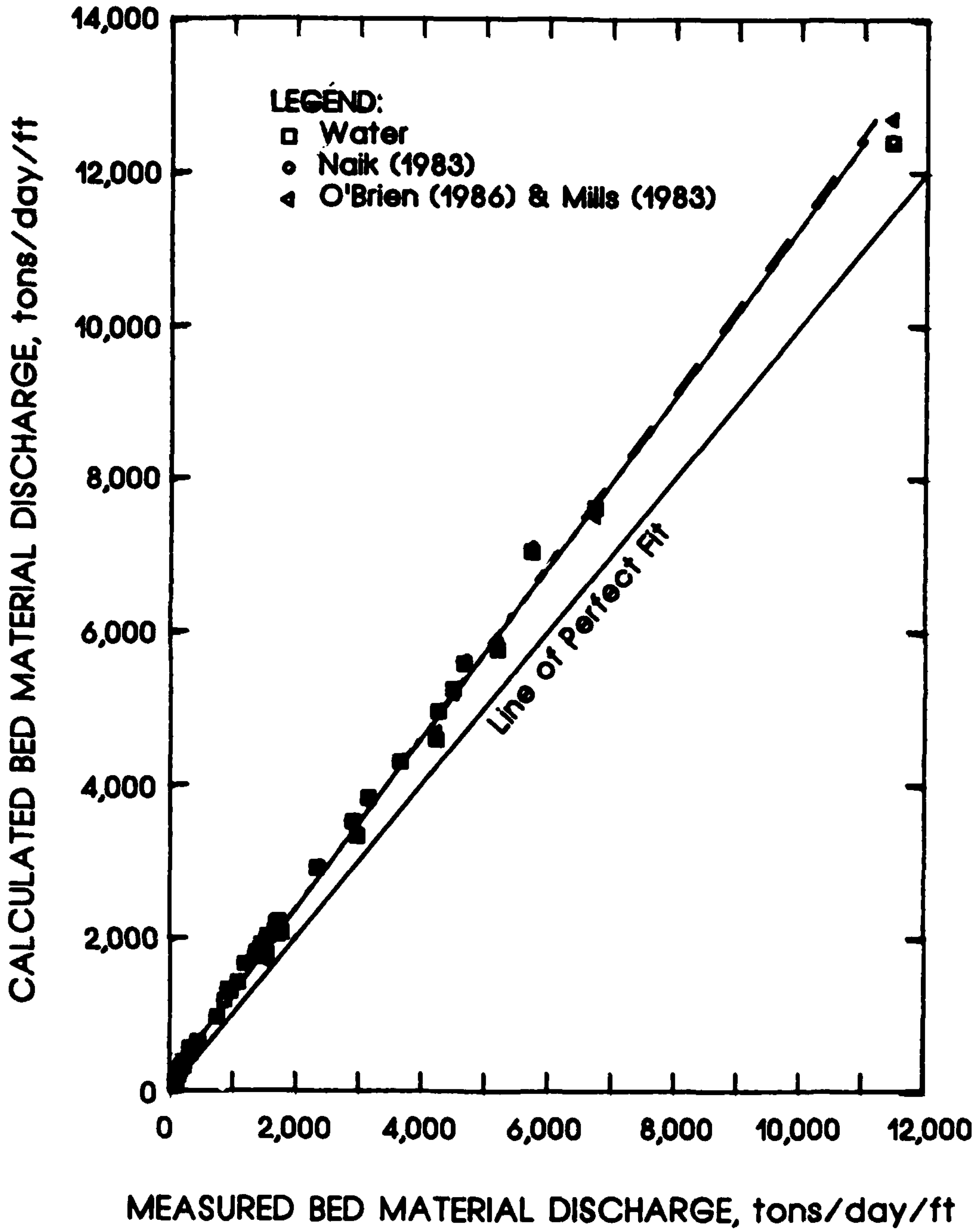

Figure 4.8. Sensitivity analysis of apparent viscosity on calculated total bed material discharge

was used to estimate the apparent kinematic viscosity of the water-sediment mixture that was used in the modified Einstein method to calculate the total bed material discharge for this study.

4.4.3 Unmeasured Sediment Discharge

The unmeasured bed material discharge per unit width, defined as the difference between the computed total bed material discharge and the measured bed material discharge, is plotted in Figure 4.9 as a function of the measured streamflow velocity for the four gaging stations. The relationship between the unmeasured bed material discharge per unit width is typical of that determined by Colby (1957), and his curves are also shown in Figure 4.9. Colby's relationship was determined from approximately 180 experimental data points from four sand-bed streams where the unmeasured sediment discharge was defined as the difference between the measured sediment discharge at a total load section and at a normal section. Individual points scatter widely from the curve, but the unmeasured sediment discharge increases on the average with about the third power of the mean velocity.

4.4.4 Suspended Sediment Distribution

The vertical distribution of suspended sediment concentration was not measured in the Cowlitz or Toutle rivers, but the variation of the exponent z', computed by trial and error from Equation 2.65, for the three size ranges, 0.125-0.250 mm, 0.250-0.500 mm, and 0.500-1.000 mm, with the calculated exponent z from Equation 2.37 and the fine sediment concentration is shown in Figures 4.10 and 4.11, respectively. In Equation 2.37, the fall velocity was computed from Rubey's (1933) equation (Equation 2.29) with the apparent viscosity from Figure 4.7,

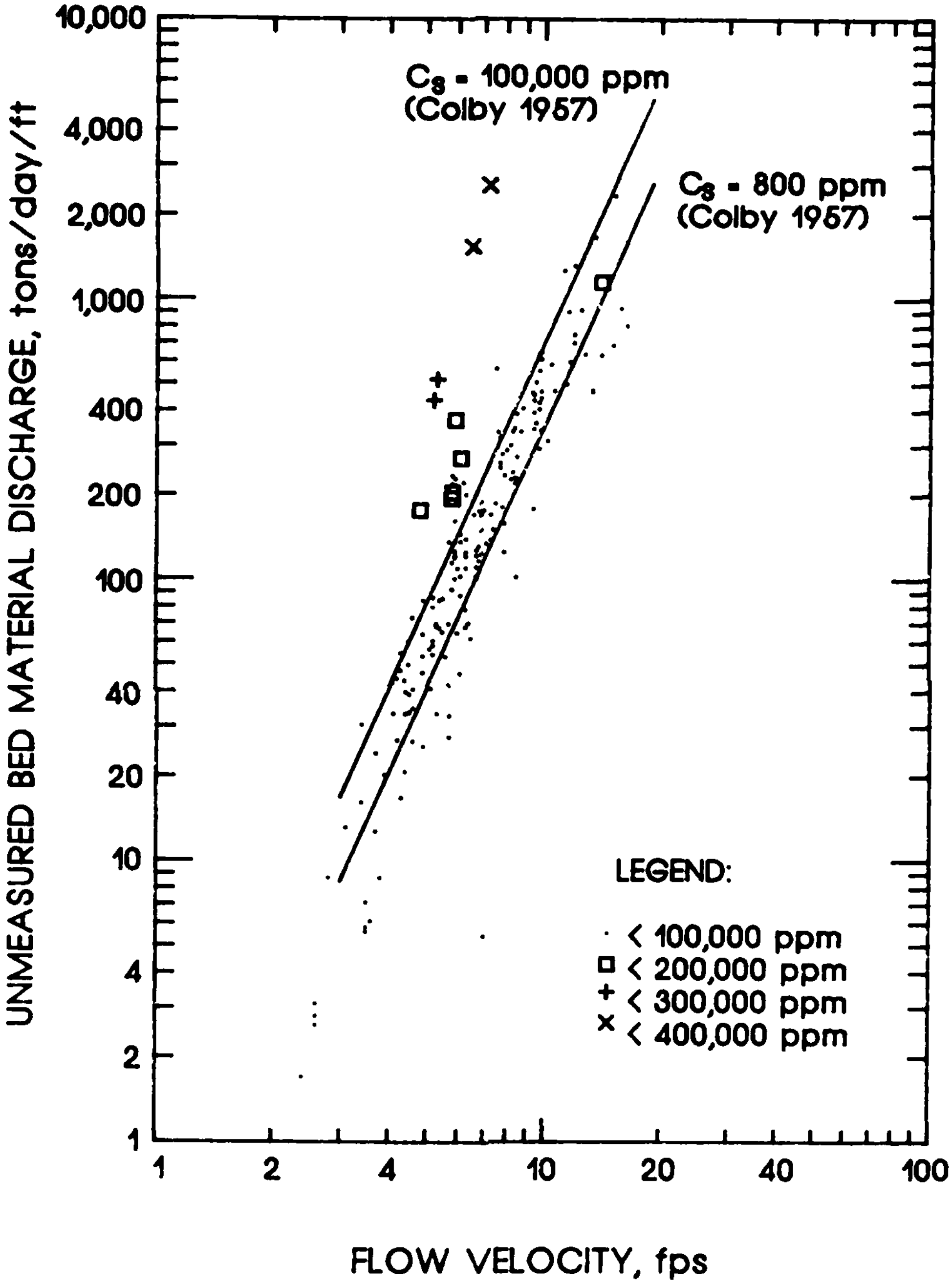

Figure 4.9. Relationship between unmeasured sediment discharge and mean flow velocity

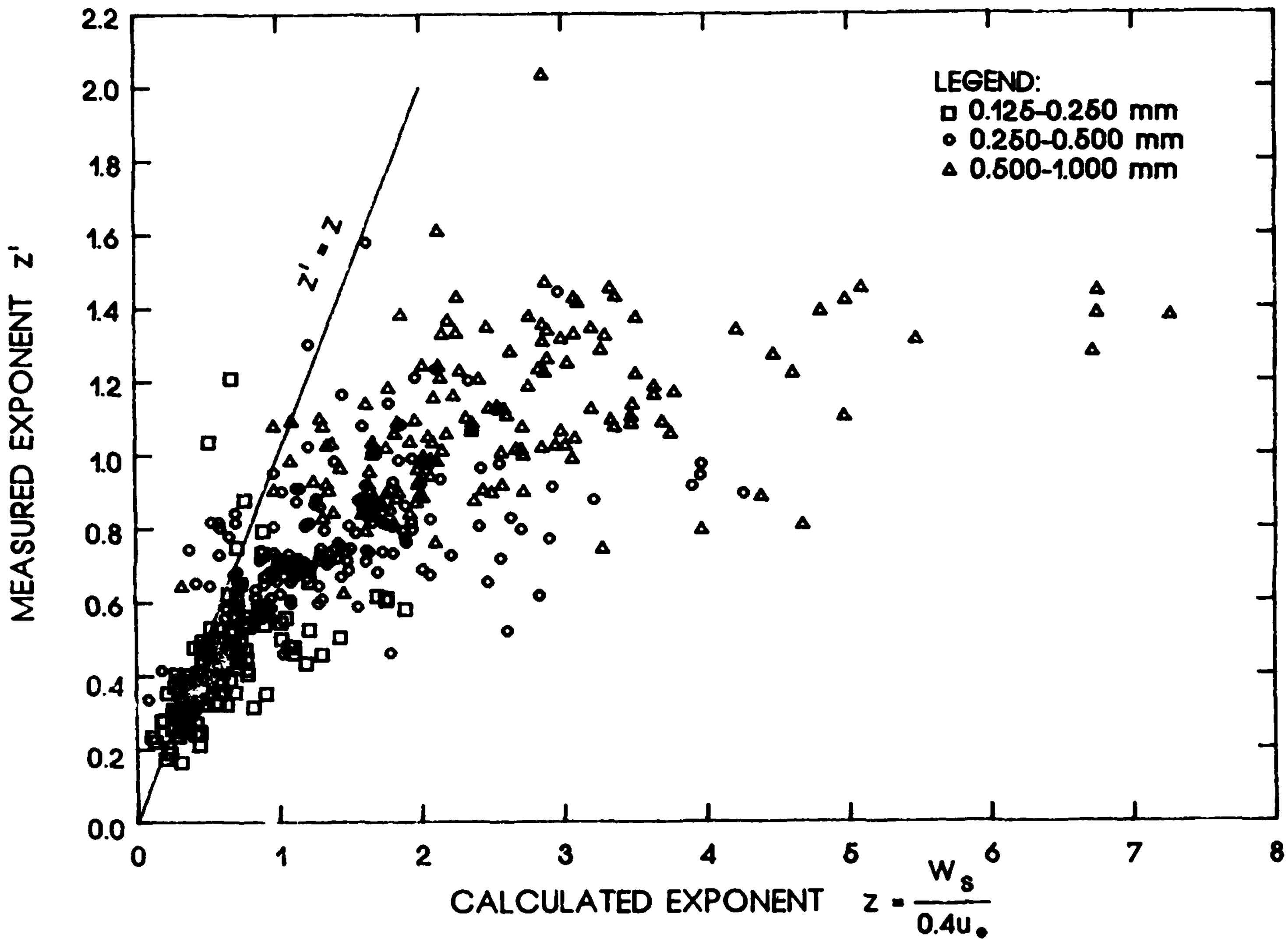

Figure 4.10. Variation of z' with z

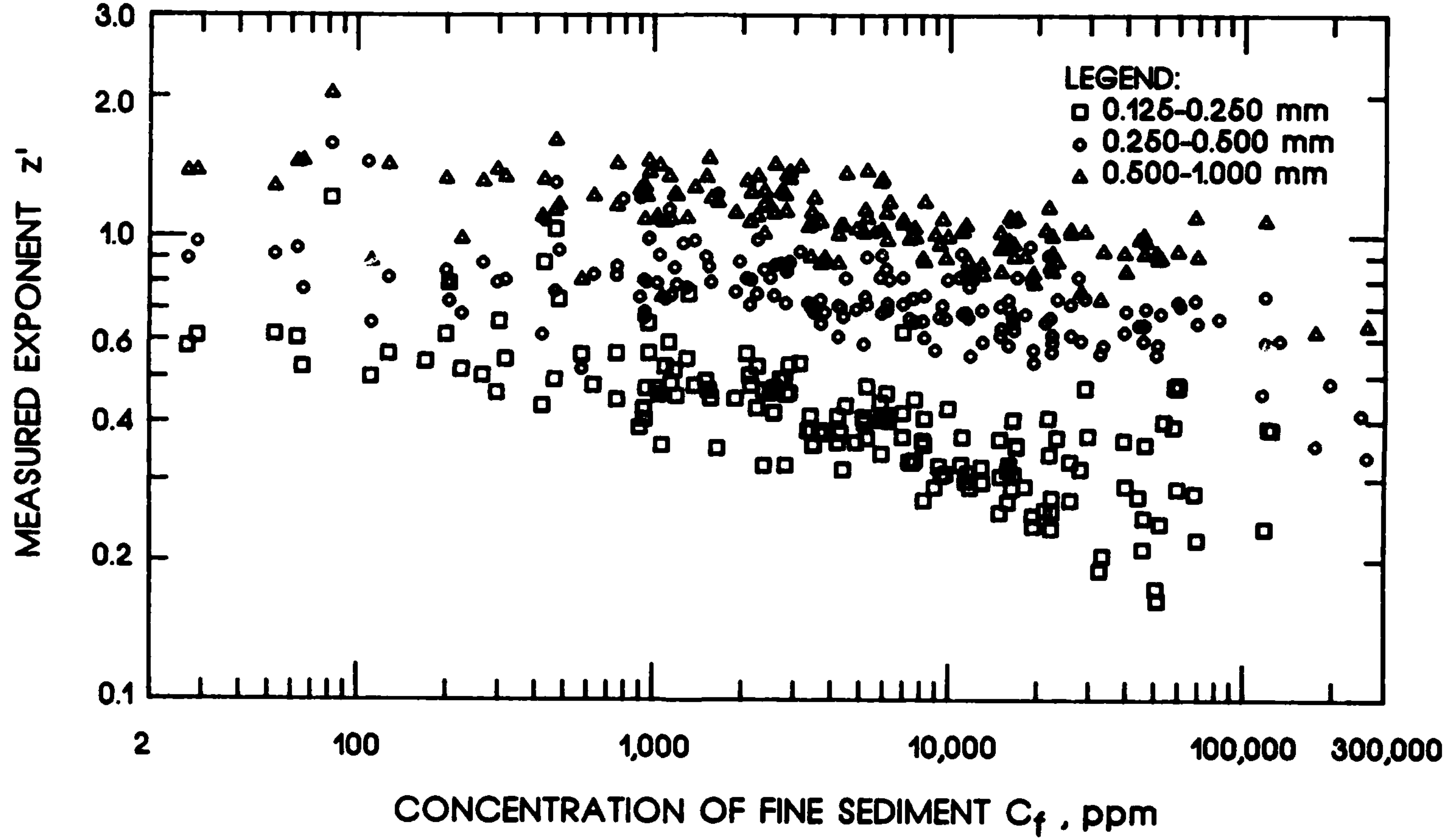

Figure 4.11. Variation of z' with concentration of fine sediment

the shear velocity from Equation 2.59, the von Karman constant equal to 0.4, and $\beta = 1.0$.

Figure 4.10 shows that the exponent of the concentration distribution curves z' computed by trial and error is generally less than the theoretical value. For small values, z' is generally in close agreement with z . Several z' values for the smaller particle size range were zero for the extremely high concentrations, and likewise, z approached zero. For large z values, z' is smaller than z , indicating the suspended sediment is distributed more uniformly than theory would predict. The deviation of the computed exponent from the measured exponent becomes greater with increasing particle size. This is typical of the results found by Anderson (1942), Colby and Hembree (1955), and Nordin and Dempster (1963).

As anticipated with increased fluid viscosity and a decrease in particle fall velocity, Figure 4.11 shows that as the concentration of fine sediment approaches the mudflow classification level, the sediment concentration profile becomes more uniform for all particle sizes.

4.4.5 Effects of High Concentrations on Fall Velocity

The variation of fall velocity for the three particle sizes with fine sediment concentration is shown in Figure 4.12. The fall velocity was computed with Rubey's equation using the apparent viscosity of the water-sediment mixture from Figure 4.7. Also plotted in Figure 4.12 is the variation of fall velocity with concentration as determined by Nordin (1963) from visual accumulation tube analyses of bed material in native water of the Rio Puerco with varying concentrations of suspended fine material (<0.053 mm). Nordin's curves show the apparent reduction

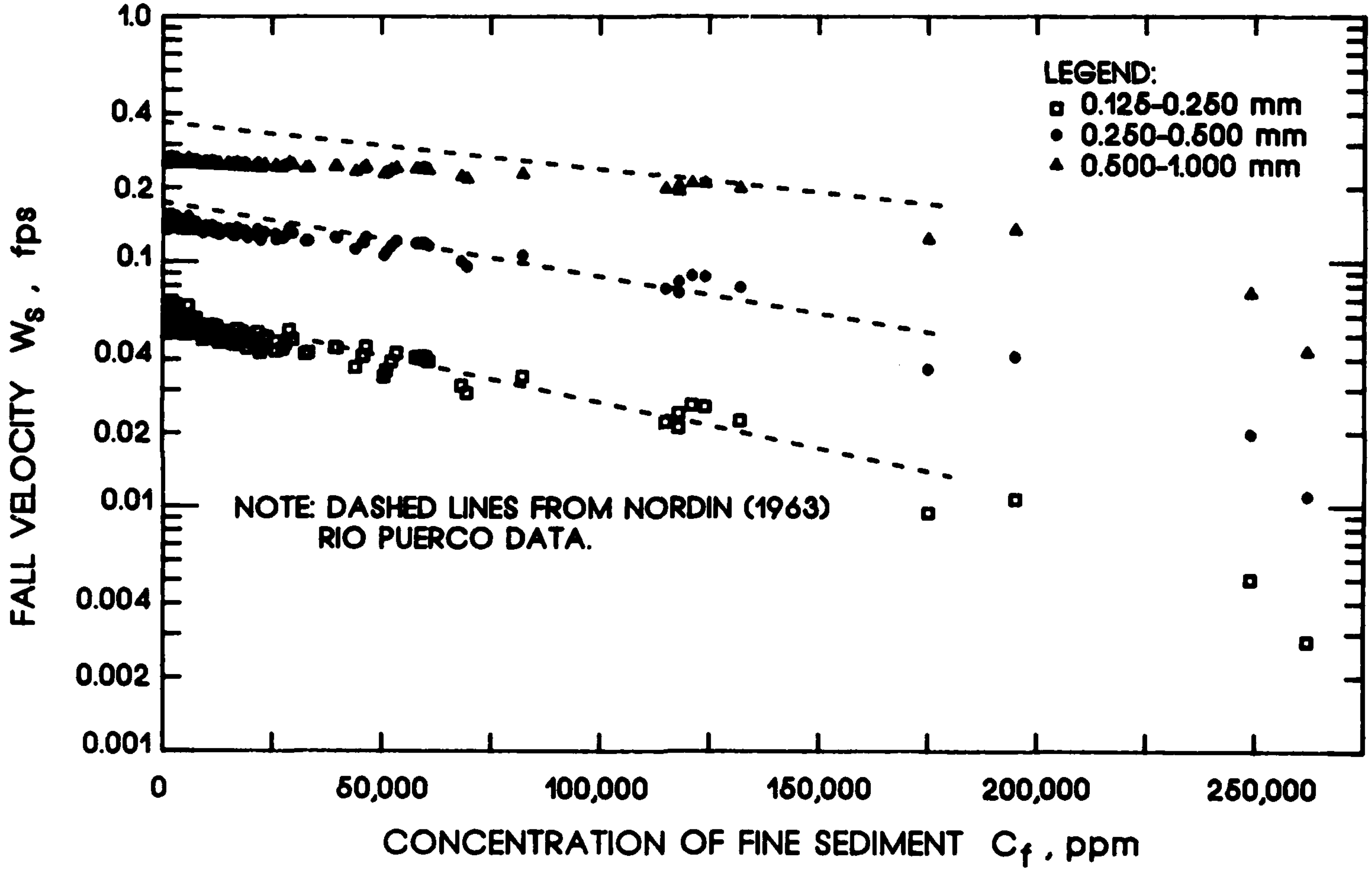

Figure 4.12. Variation of fall velocity with fine sediment concentration

in fall velocity at 24° C for various concentrations of fine material for the geometric mean diameter of the three size classes.

The agreement between the two fall velocities is reasonably good except for the two larger size classes at the low concentrations where Rubey's values are considerably lower than the measured value. Also Rubey's values begin to approach zero as the concentration approaches the mudflow level which is in agreement with the concept of a more uniform distribution of suspended sediment in hyperconcentrated sediment flow. As illustrated in Figure 2.11, Rubey's equation will result in lower fall velocity values for particle sizes over 0.50 mm, but as Woo (1985) suggested, the lower values may be closer to what actually occurs in natural streams due to the effects of hindered settling and flow turbulence.

4.5 SEDIMENT TRANSPORT EQUATIONS

4.5.1 Modified Einstein Method

The modified Einstein method was used to estimate the total bed material discharge for this study, and the results support, within limits, Woo's (1985) observation that the Einstein type of equation may be used for high fine material concentrations by varying the fluid properties. The sensitivity analysis conducted on the Tower Road gaging station data showed that the modified Einstein method underestimates the transport of the larger particle sizes (d > 1 mm) for total suspended concentrations over approximately 400,000 ppm by weight. For example, two samples of suspended sediment collected during the mudflow of March 20, 1982, had total concentrations of 627,000 and 587,000 ppm by weight and respective fines concentrations of 299,000 and 300,000 ppm by weight. The computed sediment discharge by the modified Einstein method for particle sizes greater than 1 mm was substantially less than the measured value for the same particle size range while the computed and measured values were essentially identical for the smaller particle sizes. However, Figure 4.9 illustrates the validity of using this method up to total concentrations of approximately 400,000 ppm by weight. The unmeasured bed material load in Figure 4.9 is essentially the bed load consisting of the larger particle sizes (d > 1 mm). For these data, the computed sediment discharge was always greater than the measured sediment discharge for the larger particle sizes.

4.5.2 Colby's Method

4.5.2.1 Introduction. The main objective of this study was to develop or adapt an existing sediment transport function for computing the sediment discharge in hyperconcentrated sediment flow. After a review of the literature, it became apparent that an empirical approach like Colby's (1964) would be the most viable solution with the present state of the art of hyperconcentrated sediment flow. The comparison between the total bed material discharge calculated by Colby's method and the Mount St. Helens data is shown in Figure 4.13. Similar to Woo's (1985) observations from his study using Colby's method with Simons, Richardson, and Haushild's (1963) data, the Colby procedure underestimated the total bed material discharge for the Mount St. Helens river system. Because Colby's method is widely used in the United States due to its proven reliability in sand-bed streams at low concentrations of fine sediment and because of Colby's own admission that his concentration of fines adjustment coefficient is only a guess, an attempt was made in this study to define the adjustment coefficients for the Mount St. Helens system. The utility of this approach would be to demonstrate

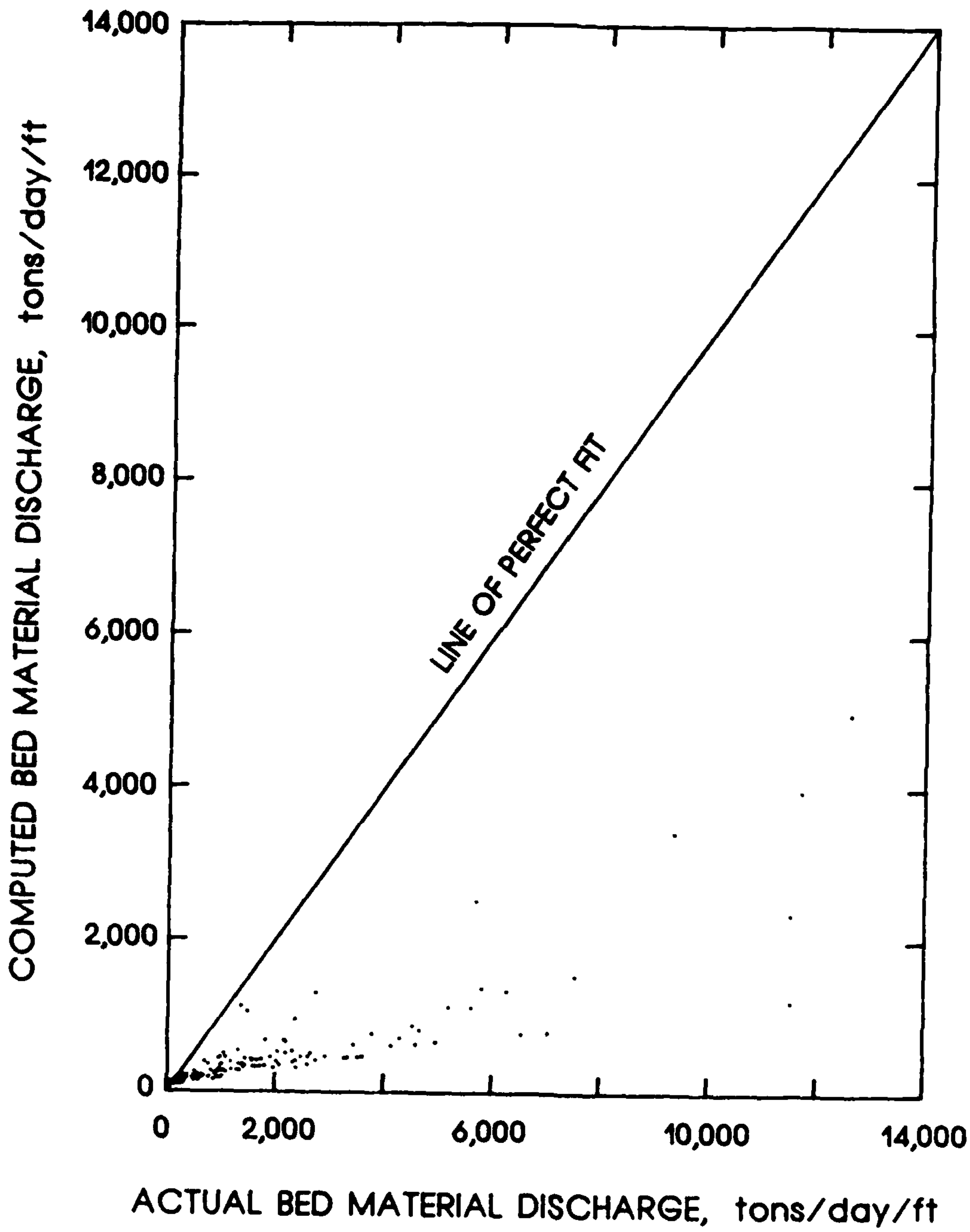

Figure 4.13. Comparison of total bed material discharge calculated by Colby's method with Mount St. Helens data

that for a given prototype system, a similar set of coefficients could easily be developed from data commonly collected and reported by the USGS.

4.5.2.2 Water Temperature and Median Bed Material Particle Size Adjustment Coefficients. As discussed in Section 2.7.2.3, Colby developed three adjustment coefficients that he applied to his empirical relationships of bed material discharge per unit width to flow velocity and flow depth in sand-bed streams. The three coefficients are (1) adjustment for water temperature from 60° F, (2) adjustment for median bed material particle size from 0.20 to 0.30 mm, and (3) adjustment for concentration of fine sediment (d_{50} < 0.0625 mm). Since the median bed material particle size was essentially constant at all stations and constant throughout the year, it was not possible to study the effect of particle size on the bed material discharge, and Colby's existing adjustment coefficients for particle size were used.

The water temperature varied from approximately 40° to 60° F in the Toutle and Cowlitz rivers, but the water temperature effect was not discernible as illustrated by Figure 4.14. Colby (1964) observed that the variation in bed material discharge at a given cross section is controlled by velocity and water temperature if the concentration of fine sediment is low, which is not the case with these data. Because the Mount St. Helens data were within the suggested range of median bed material particle size, of flow velocities, and of flow depths to which Colby suggested his adjustment coefficients apply, they were assumed applicable to this study. Furthermore, the temperature correction generally is rather small, and a large percentage error in the

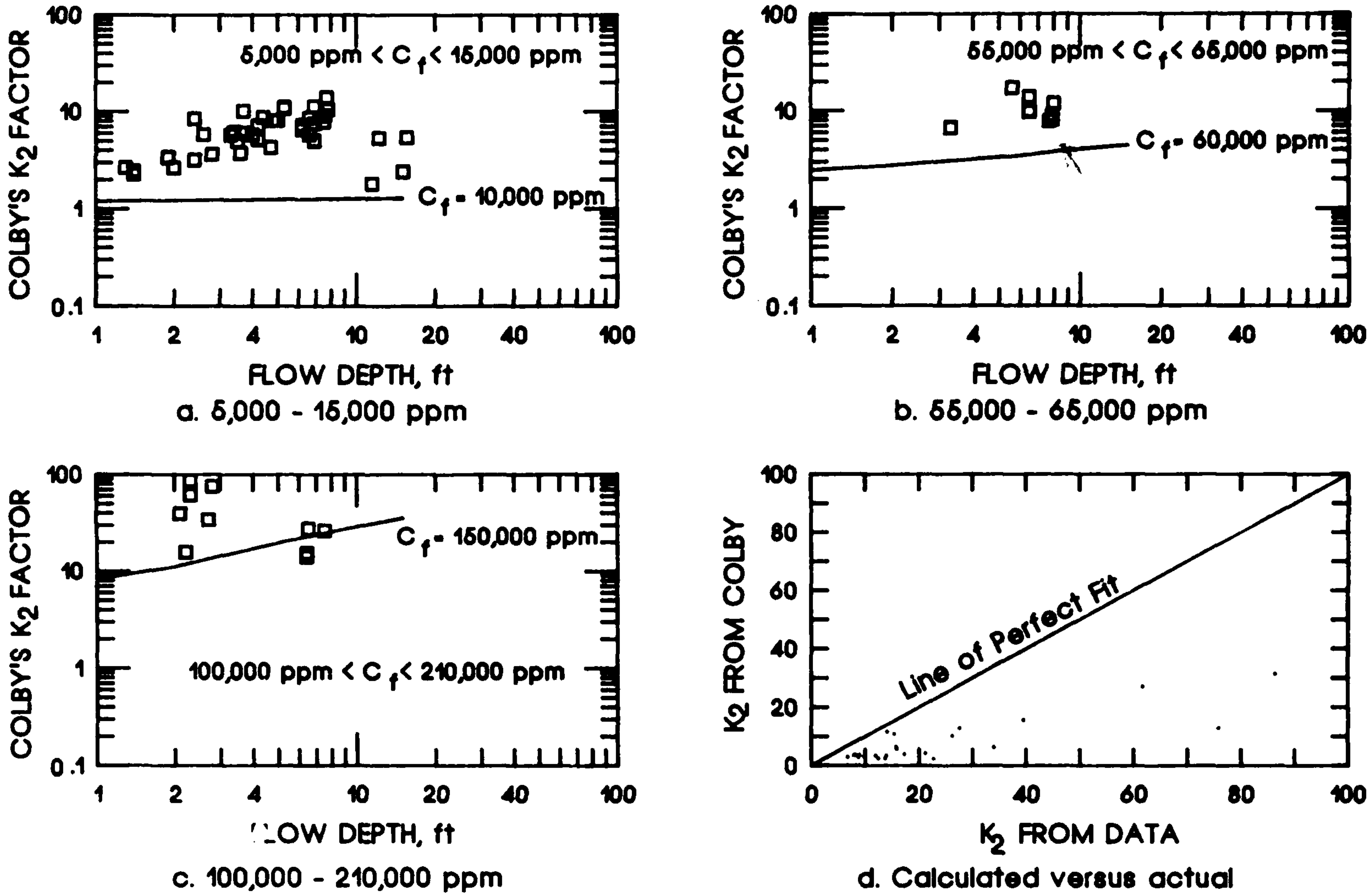

Figure 4.14. Effect of water temperature on bed material discharge for Mount St. Helens

correction usually causes only a moderate percentage error in bed material discharge (Colby 1964).

4.5.2.3 Adjustment Coefficient for Concentration of Fines. The three adjustment coefficients are applied to Colby's empirical bed material discharge per unit width q_{s1} by the equation

$$q_s = [1 + (K_1K_2 - 1)0.01K_3]\, q_{s1} \tag{4.4}$$

where

q_s = the adjusted bed material discharge per unit width

K_1 = adjustment coefficient for water temperature different from 60° F

K_2 = adjustment coefficient for concentration of fine sediment

K_3 = adjustment coefficient for median bed material particle size; reference size is 0.02-0.03 mm, i.e., K_3 = 100 expressed as percentage

It was assumed that Colby's K_1 and K_3 coefficients were valid for this study as discussed in Section 4.5.2.2; therefore, the adjustment coefficient for concentration of fines K_2 was calculated from

$$K_2 = \frac{100}{K_1K_2}\left(\frac{q_s}{q_{s1}} + K_3 - 1\right) \tag{4.5}$$

where K_1 , K_3 , and q_{s1} were determined by Colby's relationships, and q_s was the actual unit bed material discharge. The adjustment coefficient K_2 was determined by Equation 4.5 for the 186 data points where the size distribution of the measured suspended sediment was reported by the USGS and the total unit bed material discharge q_s was estimated by the modified Einstein method. Figure 4.15 shows the comparison between the K_2 coefficients for the Mount St. Helens data and the coefficient as determined by Colby. For each range of fine

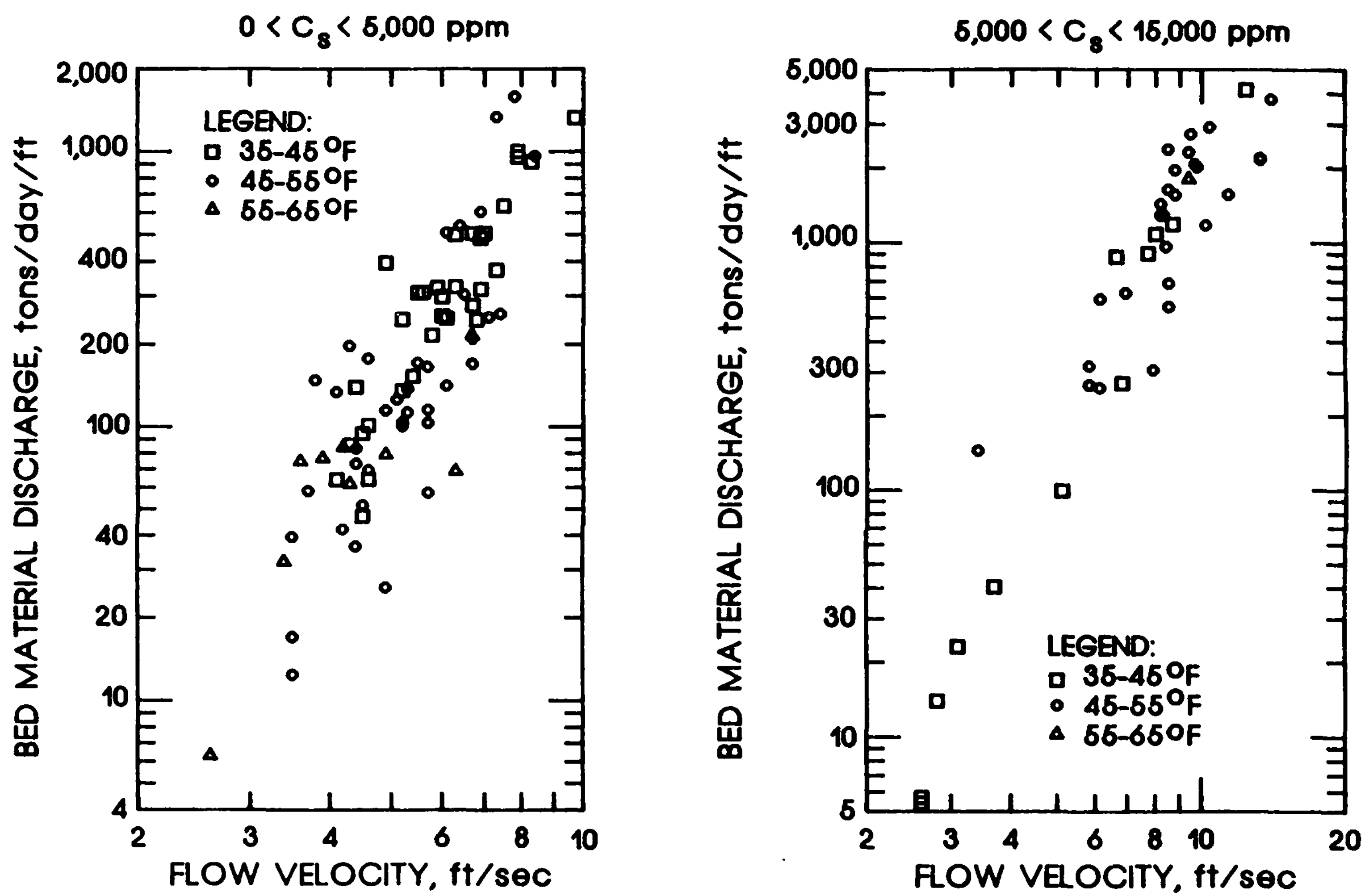

Figure 4.15. Colby adjustment coefficient for concentration of fine sediment

sediment concentration, the coefficients for the Mount St. Helens data were higher than the Colby values. The difference was greater for the lower concentrations, but as illustrated in Figure 4.15d, Colby's existing procedure would underestimate the bed material discharge for the entire range of fine sediment concentrations measured in the Toutle and Cowlitz rivers during WY 1982.

Colby (1964), in developing his graph for the adjustment coefficient for concentration of fine sediment K_2, apparently assumed that for a given flow depth, the coefficient varied linearly with the fine sediment concentration. An analysis of his curves shows that within the flow depth range of the Mount St. Helens data (0.1-25.0 ft), his graph can be represented by the equation

$$\log (K_2) = 0.63 \times 10^{-5} D^{0.185} C_f \qquad (4.6)$$

where D is the flow depth in feet and C_f is the fine sediment concentration in parts per million. The curves represented by Equation 4.6 are plotted in Figure 4.16 as a function of fine sediment concentration for flow depths of 2 and 3 ft. Also plotted in Figure 4.16 is the K_2 coefficient for the Mount St. Helens data for the same two flow depths. The data represented by the 2- and 3-ft depths actually covered the range from 1.5 to 2.5 and 2.5 to 3.5 ft, respectively. The mudflow of March 20, 1982, was not a large event in terms of stage and discharge, and therefore, the range of depths was narrow for this extremely high concentrated flow. These data were chosen to establish the relationship of the K_2 coefficient for the Mount St. Helens data because the scatter in the data for other depths at lower concentrations did not allow a more definitive variation in terms of depth. For the two depths, the variation in concentrations is sufficiently large, so that

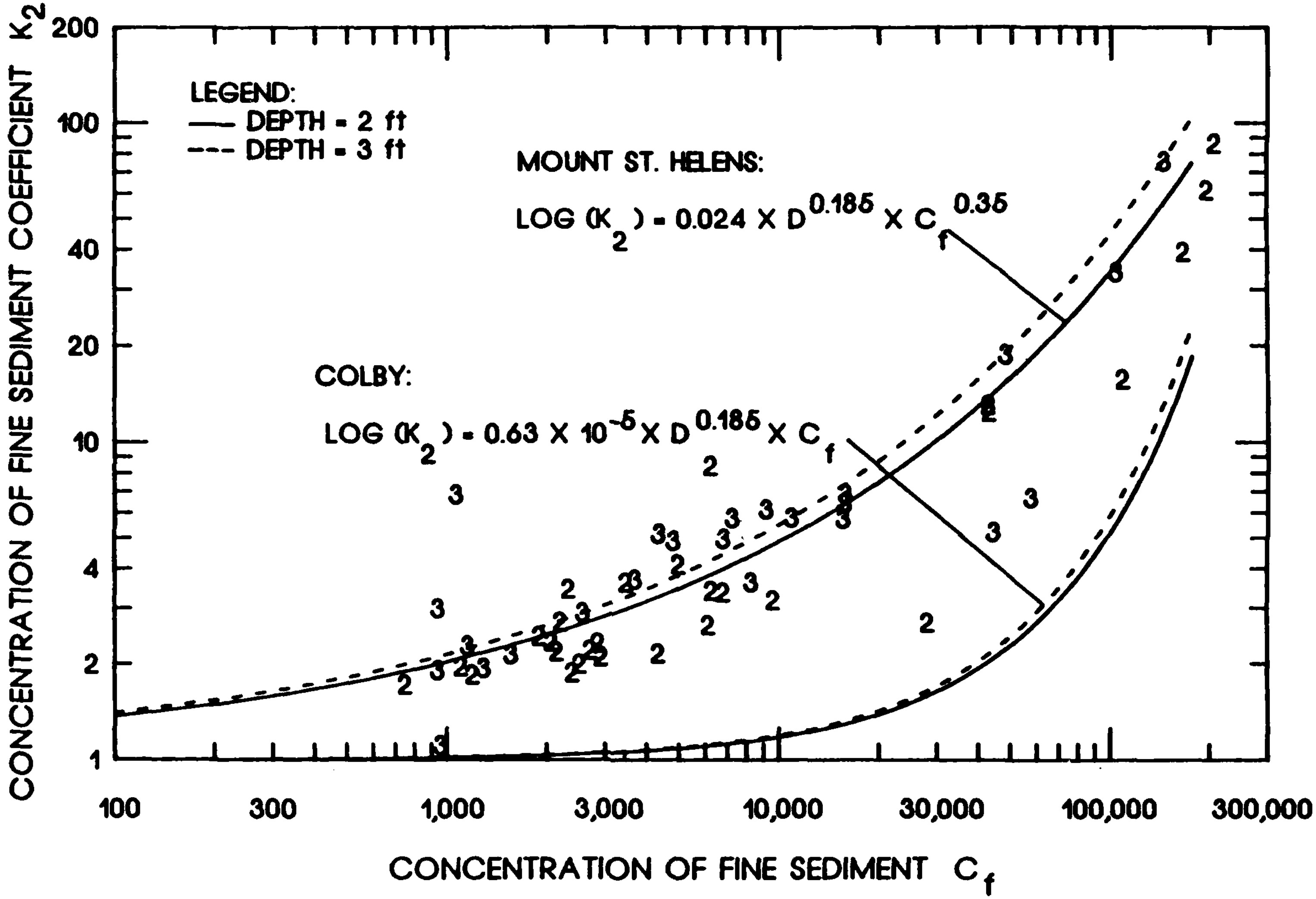

Figure 4.16. Empirical relationships for adjustment coefficient for fine sediment concentrations

using these data to modify Colby's curves should result in fairly accurate coefficients to account for high concentration of fine sediment.

The data were grouped into narrow ranges by concentration (10,000 ppm), i.e., 5,000-15,000 ppm, 15,000-25,000 ppm, etc.; and average values of each group were used to determine the coefficients in the empirical equation for K_2 as a function of depth and concentration of fine sediment. The resulting equation from the linear regression was

$$\log (K_2) = 0.024D^{0.185}C_f^{0.35} \qquad (4.7)$$

The curves for constant flow depths of 2 and 3 ft using Equation 4.7 are also plotted in Figure 4.16. The data indicate that the K_2 coefficient is greater than suggested by Colby's original relationship and that it varies with about the cube root of the fine sediment concentration.

Figure 4.17 is a plot of Equation 4.7 in Colby's original format, i.e., the adjustment coefficient, K_2 , is plotted as a function of flow depth for constant values of fine sediment concentration. Only selected concentrations are plotted in Figure 4.17 for clarity. They represent the concentration ranges that had the most data points. Although there is considerable scatter in the data, the coefficients represented by Equation 4.7 more accurately reflect the effect of fine sediment on bed material discharge in the Cowlitz and Toutle rivers during WY 1982.

The complete graph of the adjustment coefficient for fine sediment is shown in Figure 4.18 for flow depths from 0.1 to 25.0 ft and constant fine sediment concentration from 10,000 to 200,000 ppm in increments of 10,000 ppm. The lower and upper limits of Colby's curves for concentrations of 10,000 and 200,000 ppm, respectively, are shown for comparison. The new adjustment coefficient curves are not to be interpreted as being

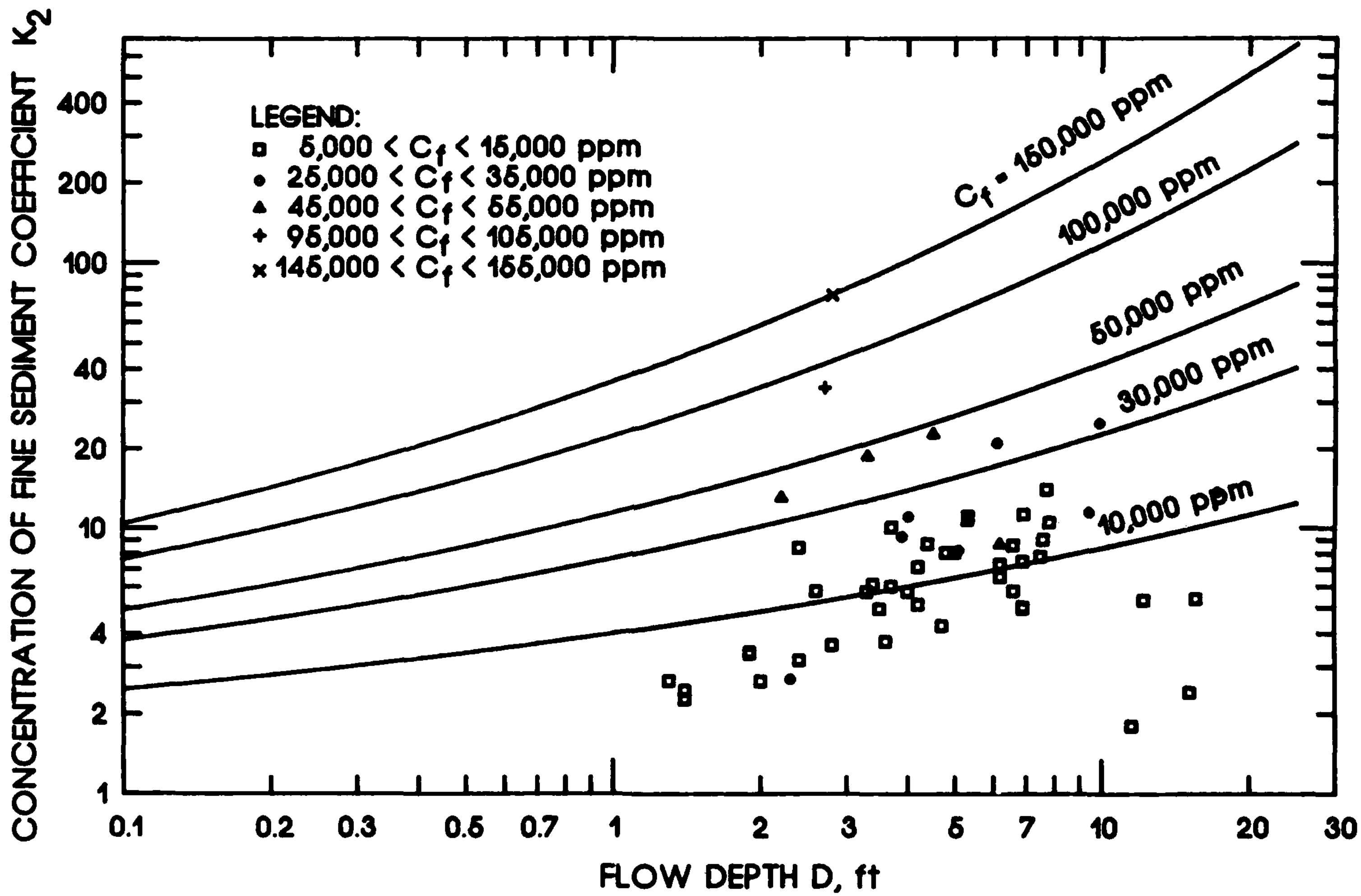

Figure 4.17. Adjustment coefficient for fine sediment concentration with Mount St. Helens data

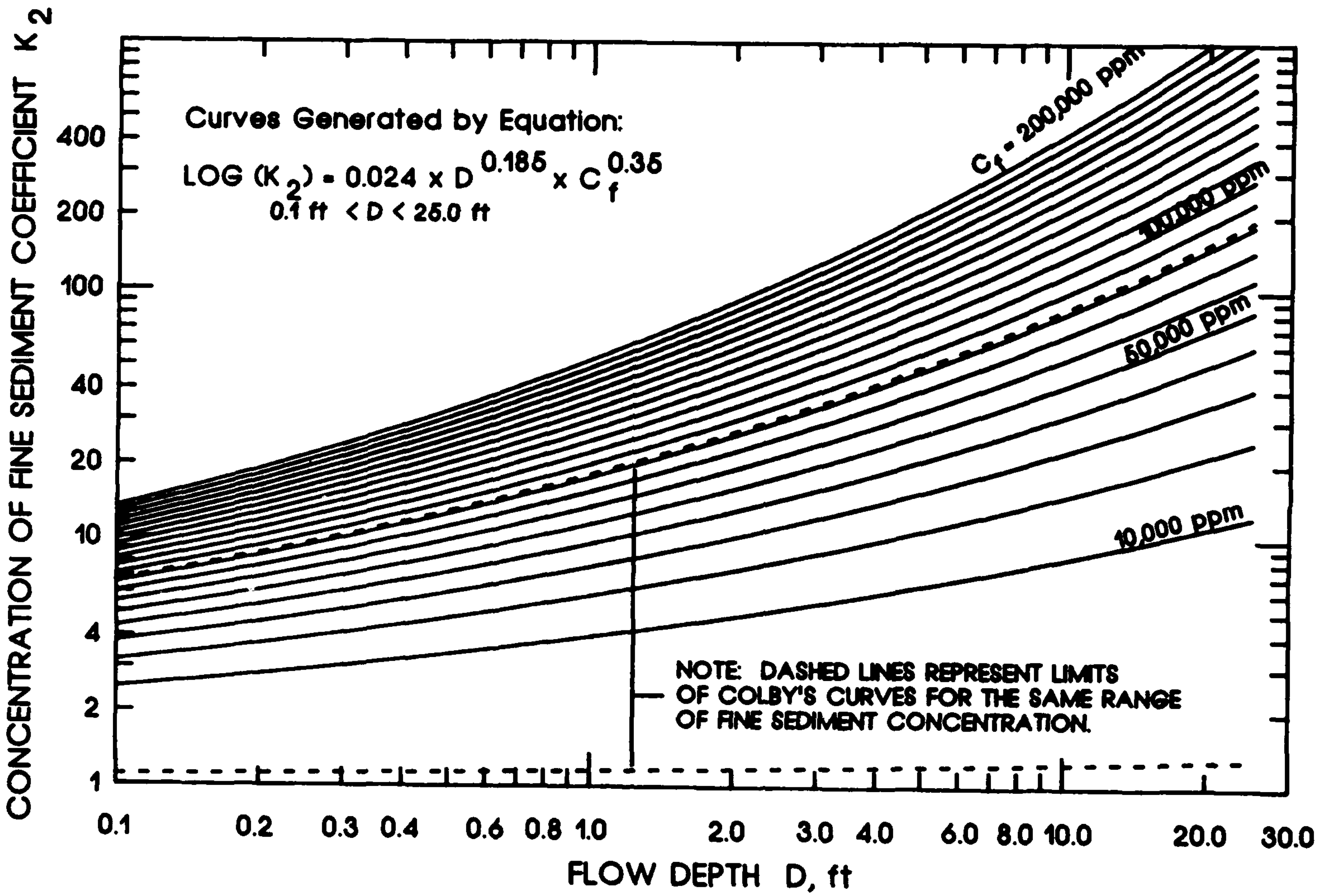

Figure 4.18. Graph for adjustment coefficient for concentration of fine sediment

universally applicable to all sand-bed streams but may be used by practicing engineers in the vicinity of Mount St. Helens, and in the absence of data from which a similar set of curves could be developed, may be used in other areas of the Cascade Mountain Range.

The adjustment coefficients for fine sediment concentration developed from the Mount St. Helens data were used in Colby's method with Simons, Richardson, and Haushild (1963) flume data, and the results are shown in Figure 4.19. The Colby method with the new adjustment coefficients overestimated the bed material discharge by approximately the same order of magnitude as the original Colby method underestimated it. The flume data are in the depth range $D < 1.0$ ft where both flume and field data that Colby used to develop his relationships showed the widest percentage difference and proportionally the fewest close agreements between observed and calculated values. Another reason for the inconsistency may be due, at least partly, to differences in bed configuration at about the same shallow depths and velocities.

4.6 BED FORMS

Perhaps the characteristic of the Cowlitz and Toutle river system that separates it from many of the sand-bed streams and flume studies that Colby used in his analysis is the energy level of the flow. The author observed flow conditions in the system during WY 1982 for both low and high flow conditions, and the flow was always characterized as very turbid, highly turbulent with standing waves that often moved upstream, even at low flows, indicating upper regime flow conditions. Although bed forms were not observed in the Mount St. Helens data set, Simons and Richardson's (1966) and Athaullah's (1968) bed form

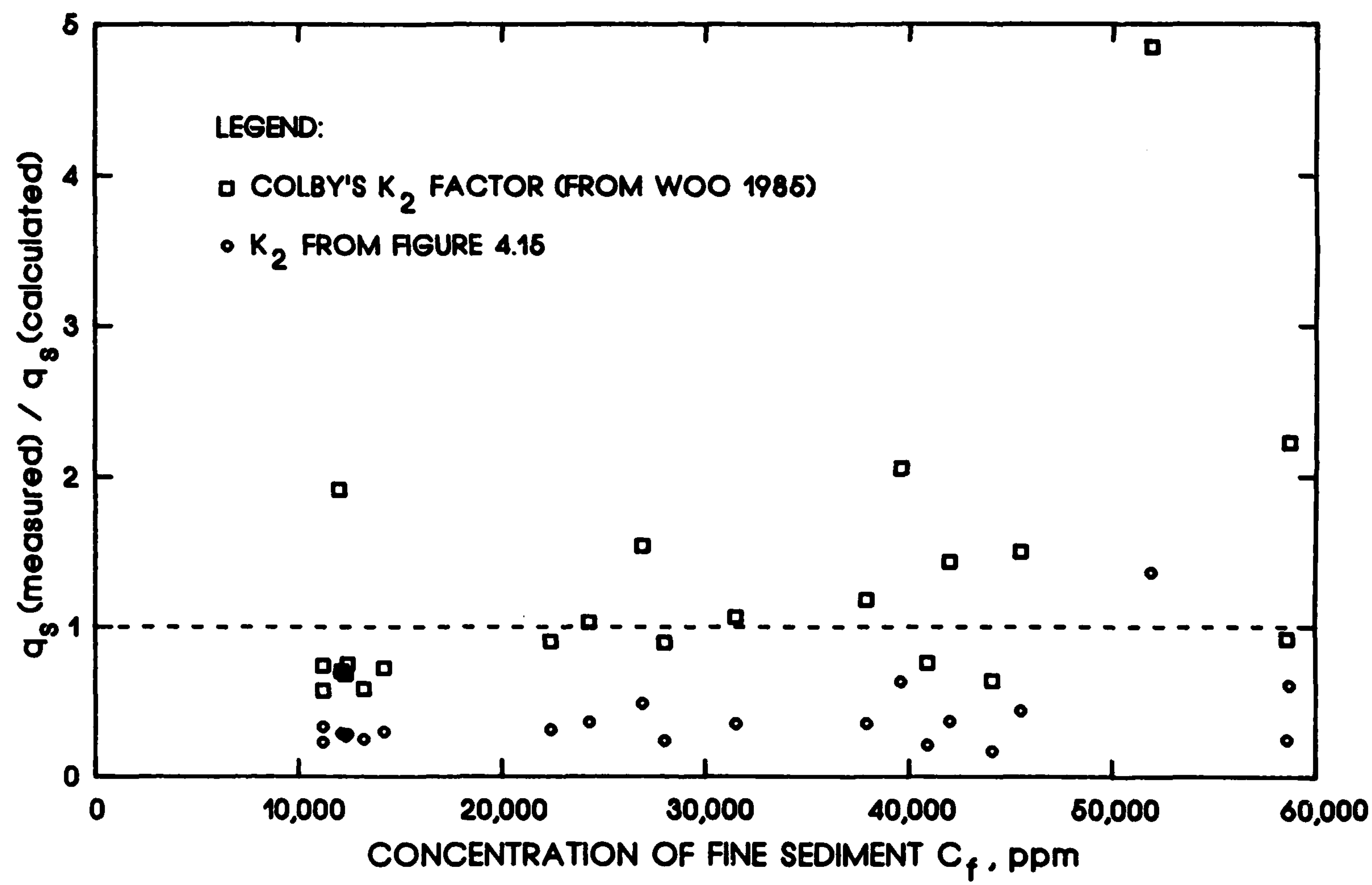

Figure 4.19. Comparison of tctal bed material discharge calculated by Colby's method with Simons, Richardson, and Haushild (1963) data

predictors were applied to the data to test the intuition that most flow conditions were in the upper regime.

The stream power function of Simons and Richardson (1966) predicted transition and upper regime flow for all flow conditions (see Figure 4.20). Athaullah's (1968) relationship based on Froude number and relative roughness also predicted, except for a few low Froude number flows at Castle Rock and Highway 99 Bridge gaging stations, transition and upper regime flow (see Figure 4.21). Figure 4.21 supports Bradley and Graham's (1983) observation of a change from dune bed to plane bed in the Cowlitz River that resulted in a substantial reduction in the resistance coefficient and subsequent reduction in flow depth (Section 2.6.5).

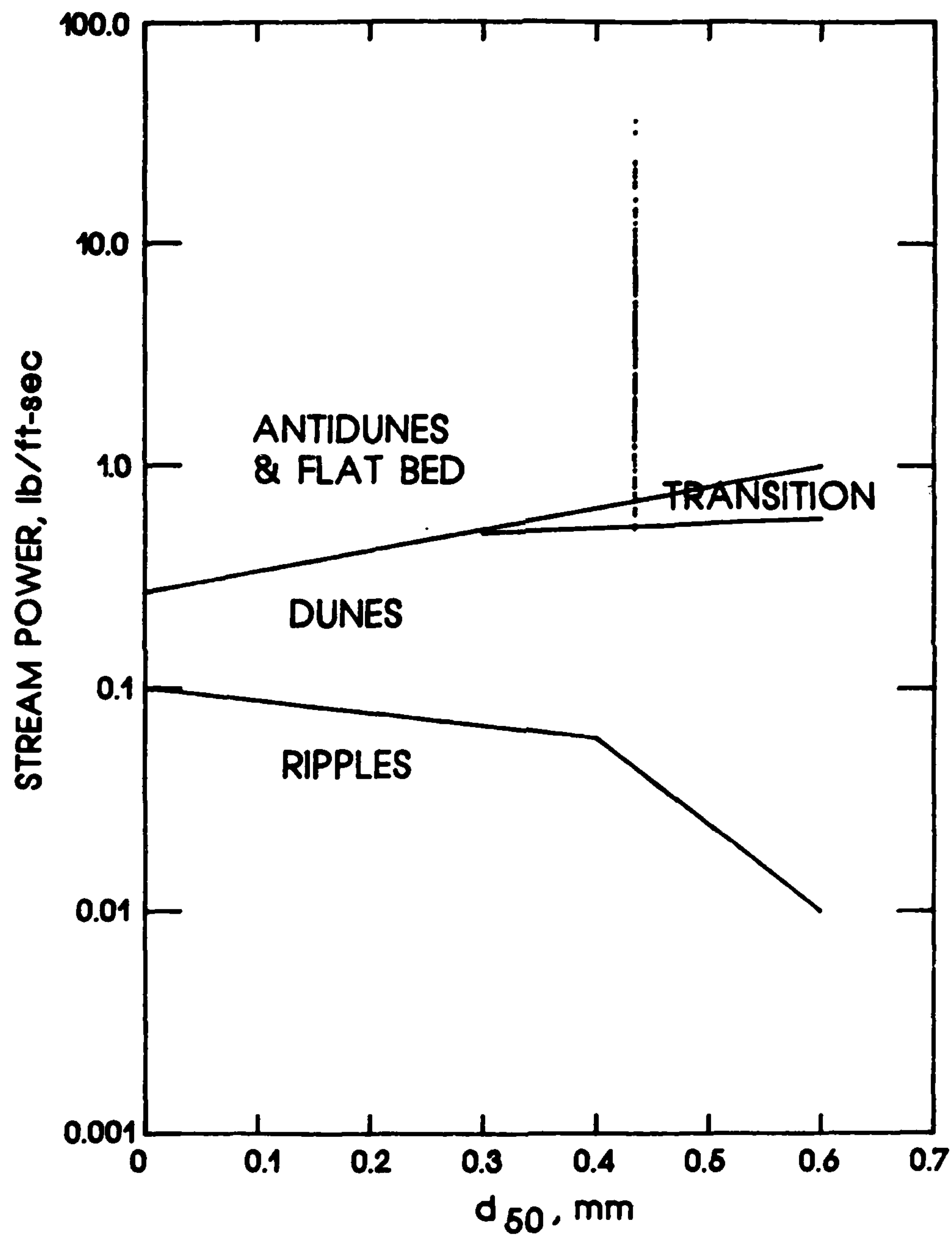

Figure 4.20. Simons and Richardson's bed predictor with Mount St. Helens data

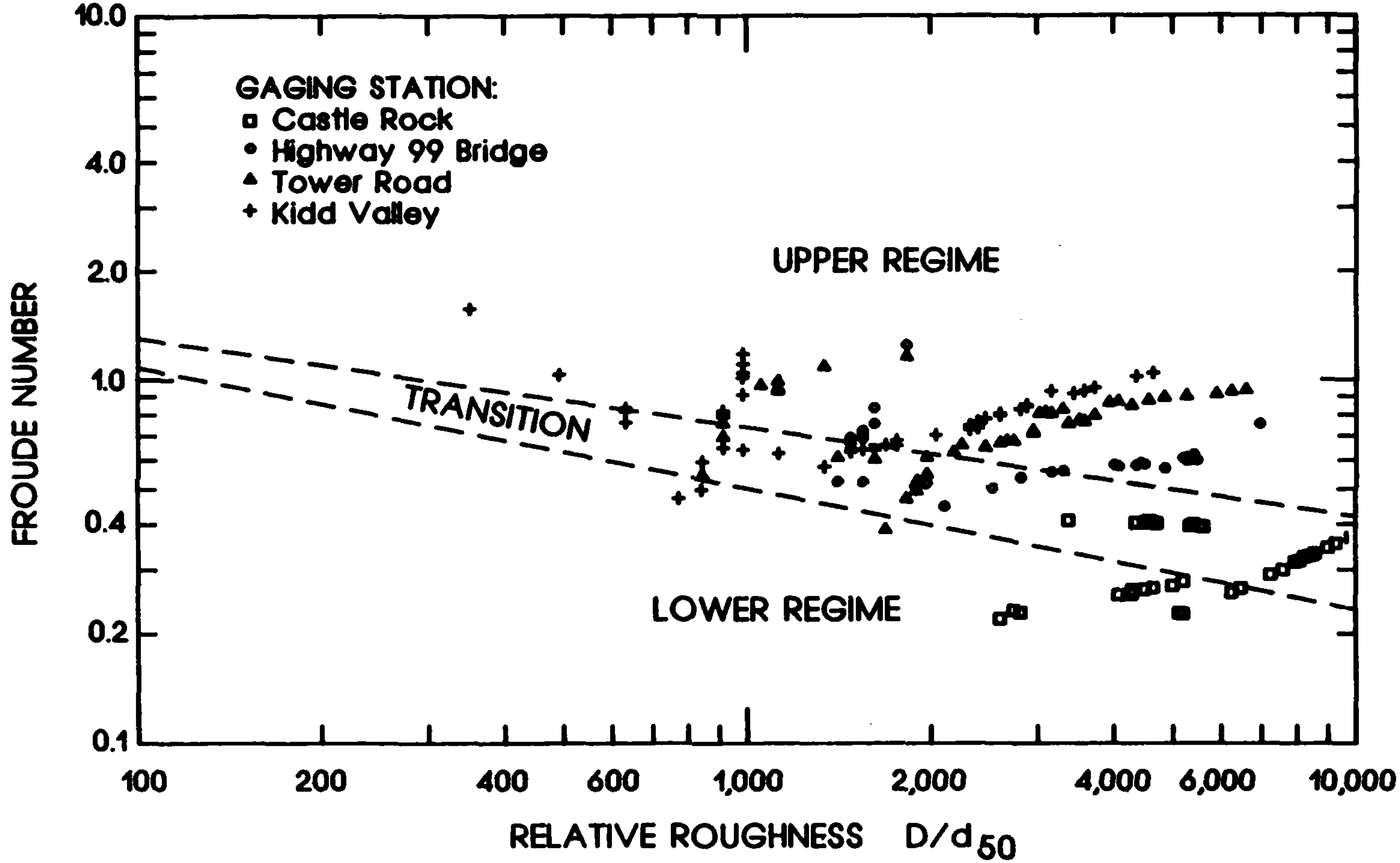

Figure 4.21. Athaullah's bed form predictor with Mount St. Helens data

CHAPTER 5

SUMMARY, CONCLUSIONS, AND RECOMMENDATIONS

5.1 SUMMARY

The purposes of this study were to test (1) recently developed theoretical concepts related to the effects of high concentration of suspended sediment on rheological properties of the water-sediment mixture and (2) the validity of using existing sediment transport formulas to predict total bed material discharge in sand bed streams of volcanic origin using stream gaging and suspended sediment data commonly available to the practicing engineer. The data set was collected by the USGS at four gaging and sediment sampling stations along a 27-mile reach of the Cowlitz and Toutle rivers, Washington, during October 1, 1981-September 30, 1982. The prototype data included stream gaging measurements, bed material samples, and depth-integrated suspended sediment measurements.

The required channel geometric and hydraulic parameters for testing sediment transport formulas were developed from the gaging data of this extremely dynamic river system, as manifested by several dramatic shifts in the stage-discharge rating curve of each gaging station during major storm events. The arithmetic average bed material size distribution was determined from 269 bed material samples since there was little variation in the bed material size between the four gaging stations and little variation throughout the year. Size distribution and composition of suspended sediment analyses were made on 98 suspended sediment samples.

The modified Einstein method was used to estimate the total bed material discharge. In the computations, the apparent viscosity and density of the water-sediment mixture were adjusted according to recently developed methodologies that take into account the increase in viscosity and density due to suspended sediment concentration. A sensitivity analysis using the modified Einstein method was performed on the data from one gaging station to study the effect of viscosity on the estimated total bed material discharge. The unmeasured bed material discharge as determined by the modified Einstein method was compared to the unmeasured sediment discharge from another investigator for the purpose of adding confidence to the estimated bed material discharges of this study.

An analysis was made of the exponent of the suspended sediment concentration distribution curves computed by trial and error from the modified Einstein method for the purpose of studying its variation with suspended sediment concentration and for comparing it to the theoretical value. Sediment particle fall velocities, computed by Rubey's equation within the modified Einstein method for the apparent viscosity of the water-sediment mixture, were compared to fall velocities of comparable bed material sizes determined from visual accumulation tube analyses in native water of the Rio Puerco, New Mexico, with varying concentrations of suspended fine sediment.

A comparison between total bed material discharge calculated by Colby's method and the Mount St. Helens data illustrated that Colby's adjustment coefficient for fine sediment concentration was inadequate for the Cowlitz and Toutle rivers. Colby's method consistently underpredicted the bed material discharge. The assumption was made that Colby's adjustment coefficients for median bed material size and temperature were applicable, and a new set of adjustment coefficients for fine sediment concentration has been developed that should be applicable to streams of similar geometry and flow conditions in the Mount St. Helens area and perhaps in the Cascade Mountain Range. The utility of developing a similar set of curves for any stream from data commonly available to the engineer has been demonstrated.

5.2 CONCLUSIONS

The following conclusions were reached:

1. The three flow processes that occurred in the Cowlitz and Toutle rivers during WY 1982 support the classification scheme proposed by the National Research Council (1982).

2. In heavy sediment-laden flow, the suspended sediment becomes progressively coarser as the concentration increases. In the Cowlitz-Toutle system, when the total suspended concentration increased into the mud flood and mudflow category ($C_v > 0.20$), the percentage of sand ($d > 0.0625$ mm) increased from an average value of approximately 50 percent upward to 75-80 percent. The percentage of clay ($d < 0.004$ mm) appeared to remain relatively constant at about 10 percent.

3. The modified Einstein method may be used to estimate the total bed material discharge without varying the fluid properties for total suspended concentration of approximately 40 percent by weight. At concentrations above this limit, the method accurately predicts the sediment discharge for the smaller size fractions but underpredicts the discharge of the larger particle sizes ($d > 1$ mm).

4. The exponent of the concentration distribution curves computed by trial and error in the modified Einstein method generally indicates that at high concentrations the suspended sediment is distributed more uniformly than theory predicts.
5. Particle fall velocities as computed by Rubey's equation with apparent viscosity of the water-sediment mixture as determined from viscometer tests at low shear rates appear reasonable when compared to visual accumulation tube tests of similar particle sizes in native water of the Rio Puerco.
6. Based on comments 4 and 5 above, at concentrations in the mud flood and mudflow categories, a reasonable estimate of the total bed material discharge would be equal to the measured bed material discharge.
7. Unmeasured sediment discharges as computed by the modified Einstein method for this study compared favorably with results of other investigators, and it is believed that the total bed material discharges reported herein for the Cowlitz-Toutle system are reasonably accurate.
8. Given the present state of the art of hyperconcentrated sediment flow, the most viable immediate solution to the problem of a method for predicting bed material discharge is an empirical approach such as Colby's method.
9. Colby's adjustment coefficients for fine sediment concentration consistently underestimated the bed material discharge in the Cowlitz and Toutle rivers and are not applicable to this high-energy system where the majority of flows is in the upper regime category.

10. The empirical adjustment coefficients for fine sediment concentration developed for the Cowlitz-Toutle system are not universal but should be applicable to other streams of comparable geometry, slope, and discharge in the Mount St. Helens area and perhaps in the Cascade Mountain Range. However, the utility of developing a similar set of adjustment coefficients for any river system has been demonstrated.

5.3 RECOMMENDATIONS

The following recommendations are made:

1. The existing methods for predicting the rheological parameters of a water-fine sediment mixture or of the overall water-sediment mixture are incomplete. As recommended by O'Brien (1986), the expansion of the viscometer data base for a wider range of mudflow deposits is sorely needed so that correction factors applied to theoretical procedures such as Naik's (1983) are based on native materials and on shear rates that actually occur in nature.
2. Improved methods for measuring the suspended sediment concentration profiles and flow velocity profiles in hyperconcentrated flow are needed in the laboratory and in the field.
3. Additional studies are needed of the variation of fall velocity with suspended sediment concentration, similar to those of Nordin (1963), where native bed materials, fine sediment, and water are used to obtain the results. In conjunction with these tests, viscometer measurements similar to those suggested in comment 1 above should be obtained on the native water-sediment mixtures so that theoretical procedures based on the rheological

parameters of the water-fine sediment mixture and hindered settling concepts due to larger sediment particles may be tested.

4. Other sediment transport equations need to be tested with the data set.
5. The data set needs to be expanded to include subsequent water years for the purpose of attempting to develop a method for predicting total bed material discharge by individual size fractions, which is a critical need for engineering purposes.

REFERENCES

Ackermann, N. L., and Shen, H. T. (1979). "Rheological characteristics of solid-liquid mixtures." American Institute of Chemical Engineers Journal, 25(2), 327-332.

Albertson, M. L. (1953). "Effect of shape on the fall velocity of gravel particles." Proceedings of the Fifth Hydraulics Conference, June 9-11, 1952, Iowa Institute of Hydraulic Research, State University of Iowa, Iowa City, Iowa, 243-261.

Anderson, A. G. (1942). "Distribution of suspended sediment in a natural stream." Transactions, American Geophysical Union, Part II: Twenty-Third Annual Meeting, April 3 and 4, 1942, Washington, D.C., 23, 678-683.

Andrade, E. N. da C. (1930, Mar 1). "The viscosity of liquids." Nature, 125(3148), 309-310. Comments are printed in Nature, 125(3154), 580-584.

Ansley, R. W., and Smith, T. N. (1967, Nov). "Motion of spherical particles in Bingham plastic." American Institute of Chemical Engineers Journal, 13(6), 1193-1196.

Athaullah, M. (1968). "Prediction of bed forms in erodible channels," Ph.D. Dissertation, Department of Civil Engineering, Colorado State University, Fort Collins, Colo.

Bagnold, R. A. (1954). "Experiments on a gravity-free dispersion of large solid spheres in a Newtonian fluid under shear." Proceedings of the Royal Society of London, Series A, 225, 49-63.

__________. (1956). "The flow of cohesionless grains in fluids." Philosophical Transactions of the Royal Society of London, Series A, 249, 235-297.

Beverage, J. P., and Culbertson, J. K. (1964). "Hyperconcentrations of suspended sediment." Journal of the Hydraulics Division, ASCE, 90(HY6), 117-128.

Bradley, J. B. (1986). "Hydraulics and bed material transport at high fine suspended sediment concentrations," Ph.D. Dissertation, Department of Civil Engineering, Colorado State University, Fort Collins, Colo.

Bradley, J. B., and Graham, J. D. (1983, Nov 8). "Effects of high sediment concentration on bedforms and river hydraulics." EOS, Transactions, American Geophysical Union, 64(45), 707 (abstract).

Brown, B. J., and Thomas, W. A. (1982, Apr). "Numerical model of sediment movement, Cowlitz-Toutle Rivers, Washington." Proceedings from the Conference, Mt. St. Helens: Effects on Water Resources, October 7-8, 1981, Jantzen Beach, Ore., Report No. 41, Washington State University, Pullman, Wash., 46-65.

Chen, C. L. (1986). "Non-Newtonian rheology and hydromechanics of debris flow." Presented at Fall Meeting of American Geophysical Union, December 5-9, 1983, San Francisco, Calif., EOS, Transactions, American Geophysical Union, 64(45), 704 (abstract).

Chu, J. (1980). "The viscosity of sediment-water mixture." Proceedings of the International Symposium on River Sedimentation, March 24-29, 1980, Beijing, China, Paper B6, I, 205-212.

Colby, B. R. (1957, Oct). "Relationship of unmeasured sediment discharge to mean velocity." Transactions, American Geophysical Union, 38(5), 708-717.

________. (1964). "Practical computations of bed-material discharge." Journal of the Hydraulics Division, ASCE, 90(HY2), 217-246.

Colby, B. R., and Hembree, C. H. (1955). "Computations of total sediment discharge, Niobrara River near Cody, Nebraska." Water-Supply Paper 1357, US Geological Survey, Washington, D.C.

Colby, B. R., and Scott, C. H. (1965). "Effects of water temperature on the discharge of bed material." Professional Paper 462-G, US Geological Survey, Washington, D.C.

Costa, J. E. (1984). "Physical geomorphology of debris flow." Development and Applications of Geomorphology, J. E. Costa and P. J. Fleisher, eds., Springer-Verlag, Berlin, 268-317.

Costa, J. E., and Jarrett, R. D. (1981, Aug). "Debris flows in small mountain stream channels of Colorado and their hydrologic implications." Bulletin of the Association of Engineering Geologists, XVIII(3), 309-322.

Curry, R. R. (1966, Jul). "Observation of alpine mudflows in the Tenmile Range, central Colorado." Geological Society of America Bulletin, 77(7), 771-776.

du Plessis, M. P., and Ansley, R. W. (1967, Jul). "Settling parameters in solids pipelining." Journal of the Pipeline Division, ASCE, 93(PL2), 1-17.

Einstein, A. (1906). "A new determination of molecular dimensions." Annaler der Physik, Reprinted in Theory of The Brownian Movement, E. P. Hutton & Company, 19, 289-306.

Einstein, H. A. (1950). "The bed-load function for sediment transportation in open channel flows." Technical Bulletin No. 1026, US Department of Agriculture, Soil Conservation Service, Washington, D.C.

Einstein, H. A., and Chien, N. (1955, Aug). "Effects of heavy sediment concentration near the bed on velocity distribution." Missouri River Division Series No. 8, University of California, Institute of Engineering Research and US Army Engineer Division, Missouri River, Omaha, Nebr.

Fan, J., and Dou, G. (1980). "Sediment transport mechanics." Proceedings of the International Symposium on River Sedimentation, March 24-29, 1980, Beijing, China, Paper B(I), I, 1167-1177.

Gagoshidze, M. S. (1969). "Mudflows and floods and their control." Soviet Hydrology: Selected Papers, 4, 410-422.

Gibbs, R. J., Matthews, M. D., and Link, D. A. (1971, Mar). "The relationship between sphere size and settling velocity." Journal of Sedimentary Petrology, 41(1), 7-18.

Govier, G. W., and Aziz, K. (1972). The flow of complex mixtures in pipes. Van Nostrand Reinhold Company, New York, N.Y.

Guy, H. P., Simons, D. B., and Richardson, E. V. (1966). "Summary from alluvial channel data from flume experiments, 1956-61." Professional Paper 462-I, US Geological Survey, Washington, D.C.

Hanks, R. W. (1963a). "Laminar-turbulent transition for flow in pipes, concentric annuli, and parallel plates." American Institute of Chemical Engineers Journal, 9(1), 45-48.

_________. (1963b). "Laminar-turbulent transition for fluids with a yield stress." American Institute of Chemical Engineers Journal, 9(3), 306-309.

Hanks, R. W., and Pratt, D. R. (1967, Dec). "On the flow of Bingham plastic slurries in pipes and between parallel plates." Journal of the Society of Petroleum Engineering, 342-346.

Hanks, R. W., and Dadia, B. H. (1971). "Theoretical analysis of turbulent flow of non-Newtonian slurries in pipes." American Institute of Chemical Engineers Journal, 17(3), 554-557.

Higgins, J. D., Naik, B., Mills, S. V., Copp, H., and Roberson, J. A. (1983, Oct). "The mechanics of mud flow." Report 51, State of Washington Water Research Center, Washington State University, Pullman, Wash.

Howard, C. D. D. (1962, Nov). Discussion of "Sediment transport mechanics: introduction and properties of sediment," Progress Report by the Task Committee on Preparation of Sedimentation Manual of the Committee on Sedimentation, Journal of the Hydraulics Division, ASCE, 88(HY6), 235-237.

________. (1963, Sept). "Flow of clay-water suspension." Journal of the Hydraulics Division, ASCE, 89(HY5), 89-97.

Inter-Agency Committee on Water Resources. (1957, Dec). "A study of methods used in measurement and analysis of sediment loads in streams; report no. 12, some fundamentals of particle size analysis." St. Anthony Falls Hydraulic Laboratory, Minneapolis, Minn.

Johnson, A. M. (1970). Physical processes in geology. Freeman, Cooper & Company, San Francisco, ch 12-14, 432-534.

Johnson, A. M., and Hampton, M. A. (1969). "Subaerial and subaqueous flow of slurries." Final Report to US Geological Survey, Branner Library, Stanford University, Stanford, Calif.

Kennedy, J. F. (1963, Aug). "The mechanics of dunes and antidunes in erodible-bed channels." Journal of Fluid Mechanics, Part 4, 16, 521-544.

Keulegan, G. H. (1938, Dec). "Laws of turbulent flow in open channels." Journal of Research of the National Bureau of Standards, Paper No. RP1151, 21, 707-741.

Kozicki, W., and Tiu, C. (1967). "Non-Newtonian flow through open channels." Canadian Journal of Chemical Engineering, 45, 127-134.

Lara, J. M. (1966). "Change in the modified Einstein procedure to compute 'z.'" Sedimentation Section, Hydrology Branch, Bureau of Reclamation, US Department of the Interior, Denver, Colo.

Maude, A. D., and Whitmore, R. L. (1958, Dec). "A generalized theory of sedimentation." British Journal of Applied Physics, 9.

McNown, J. S., and Lin, P. N. (1952). "Sediment concentration and fall velocity." Proceedings, Second Midwestern Conference on Fluid Mechanics, Ohio State University, Columbus, Ohio, 401-411.

Mills, S. V. (1983). "An experimental study of the rheology of mud flows," M.S. Thesis, Washington State University, Pullman, Wash.

Moshev, V. V. (1979, Mar-Apr). "Viscosity relationships for heavily filled suspensions." Fluid Mechanics--Soviet Research, 8(2), 88-96.

Naik, B. (1983). "Mechanics of mudflows treated as the flow of a Bingham fluid," Ph.D. Dissertation, Department of Civil and Environmental Engineering, Washington State University, Pullman, Wash.

National Research Council. (1982). "Selecting a methodology for delineating mudslide hazard areas for the National Flood Insurance Program." Academy Press, Washington, D.C.

Nordin, C. F., Jr. (1963). "A preliminary study of sediment transport parameters, Rio Puerco near Bernardo, New Mexico." Professional Paper 462-C, US Geological Survey, Washington, D.C.

Nordin, C. F., Jr., and Dempster, G. R., Jr. (1963). "Vertical distribution of velocity and suspended sediment, Middle Rio Grande, New Mexico." Professional Paper 462-B, US Geological Survey, Washington, D.C.

O'Brien, J. S. (1986). "Physical processes, rheology and modeling mudflows," Ph.D. Dissertation, Department of Civil Engineering, Colorado State University, Fort Collins, Colo.

O'Brien, J. S., and Julien, P. Y. (1985). "Physical properties and mechanics of hyperconcentrated sediment flows." Proceedings of Delineations of Landslide, Flashflood and Debris Flow Hazards in Utah, D. S. Bowles, ed., Logan, Utah, June 14-15, 1984, 260-279.

Okuda, S., Suwa, H., Okunishi, K., Nakano, M., and Yokoyama, K. (1977). "Synthetic observation on debris flow, part 3, observations at Valley Kamikamihorizawa of Mt. Yakedake in 1976." Annuals, Disaster Prevention Research Institute, Kyoto University, Kyoto, Japan, 20B-1, 237-263.

Oliver, D. R., and Ward, S. G. (1959, Jul). "Studies of the viscosity and sedimentation of suspensions, part 5: the viscosity of settling suspensions of spherical particles." British Journal of Applied Physics, 10.

Pazwash, H. (1970). "Drag forces on bodies moving through aqueous clay suspensions," Ph.D. Dissertation, University of Illinois, Urbana, Ill.

Pierson, T. C., and Costa, J. E. (1984). "A rheological classification of subaerial sediment-water flows." Abstracts with Programs, Ninety-seventh Annual Meeting, Geological Society of America, 16(6), 623.

Qian, Y., Yang, W., Zhao, W., Cheng, X., Zhang, L., and Xu, W. (1980). "Basic characteristics of flow with hyperconcentration of sediment." Proceedings of the International Symposium on River Sedimentation, March 24-29, 1980, Beijing, China, Paper B3, I, 175-184.

Richardson, J. F., and Zaki, W. N. (1954). "Sedimentation and fluidization, part I." Transactions, Institute of Chemical Engineers, London, 32.

Rodine, J. D., and Johnson, A. M. (1976). "The ability of debris, heavily freighted with coarse clastic materials, to flow on gentle slopes." Sedimentology, 23(2), 213-234.

Roscoe, R. (1953). "Suspensions." Flow Properties of Disperse Systems, J. J. Hermans, ed., Interscience Publications, Inc., New York, 1-38.

Rouse, H. (1937). "Modern concepts of the mechanics of fluid turbulence." Transactions of the American Society of Civil Engineers, Paper No. 1965, 102, 463-505 (discussion, 506-543).

________. (1946). Elementary mechanics of fluids. John Wiley & Sons, New York, N.Y.

Rubey, W. W. (1933). "Settling velocities of gravel, sand, and silt particles." American Journal of Science, Fifth Series, 25(148), 325-338.

Simons, D. B., and Richardson, E. V. (1966). "Resistance to flow in alluvial channels." Professional Paper 422-J, US Geological Survey, Washington, D.C.

Simons, D. B., Richardson, E. V., and Haushild, W. L. (1963). "Some effects of fine sediment on flow phenomena." Water-Supply Paper 1498-G, US Geological Survey, Washington, D.C.

Simons, D. B., and Senturk, F. (1977). Sediment transport technology. Water Resources Publications, Fort Collins, Colo.

Simons, Li, and Associates. (1982). Engineering analysis of fluvial systems. BookCrafters, Inc., Chelsea, Mich.

Stokes, G. G. (1851). "On the effect of the internal friction of fluids on the motion of pendulums." Transactions, Cambridge Philosophical Society, 9.

Swanson, V. F. (1967, Jun). "The development of formula for direct determination of free settling velocity of any size particle." Transactions of the Society of Mining Engineers, 238, 160-166.

Takahashi, T. (1981). "Debris flow." Annual Review of Fluid Mechanics, Annual Reviews, Inc., Palo Alto, Calif., 13, 57-77.

Thomas, D. G. (1961, Sept). "Laminar-flow properties of flocculated suspensions." American Institute of Chemical Engineers Journal, 7(3).

________. (1965). "Transport characteristics of suspension: VIII. A note on the viscosity of Newtonian suspensions of uniform spherical particles." Journal of Colloid Science, 20.

US Army Engineer District, Portland. (1982, Dec). "Mount St. Helens, Cowlitz and Toutle Rivers, sedimentation study, 1980-1982." Portland, Oreg.

Valentik, L., and Whitmore, R. L. (1965). "The terminal velocity of spheres in Bingham plastics." British Journal of Applied Physics, 16.

Vanoni, V. A. (1981). "Recent development in sediment transport in rivers and estuaries." School of Engineering, California State University, Los Angeles, Calif.

Vinogradov, Y. B. (1969). "Some aspects of the formation of mudflows and methods of computing them." Soviet Hydrology: Selected Papers, 5, 480-500.

Ward, S. G. (1955). "Properties of well-defined suspensions of solids in liquids." Journal of Oil and Colour Chemists' Association, 38.

Watson, R. L. (1969, Oct). "Modified Rubey's law accurately predicts sediment settling velocities." Water Resources Research, 5(5), 1147-1150.

Woo, H. (1985). "Sediment concentration in hyperconcentrated flow," Ph.D. Dissertation, Colorado State University, Fort Collins, Colo.

Yano, K., and Daido, A. (1965, Feb). "Fundamental study on mud-flow." Bulletin of the Disaster Prevention Research Institute, Kyoto University, Kyoto, Japan, Part 2, 14(80), 69-83.

Zhang, H., Ren, Z., Jiang, S., Sun, D. H., and Lu, N. (1980). "Settling of sediment and the resistance to flow at hyperconcentration." Proceedings of the International Symposium on River Sedimentation, March 24-29, 1980, Beijing, China, Paper B4, I, 185-194.

APPENDIX A

USGS GAGING DATA

Water Year 1982 (October 1, 1981-September 30, 1982)

Date	Width ft	Area sq ft	Flow cfs	Gage Height ft	Velocity fps
Castle Rock Gaging Data					
Rating No. 14, 49 Points					
10 05	222.0	1280.0	3160.0	2.30	2.47
10 06	318.0	2340.0	9480.0	5.87	4.05
10 06	316.0	2720.0	11500.0	6.94	4.23
10 07	310.0	2420.0	9880.0	6.07	4.08
10 13	270.0	2070.0	7660.0	4.98	2.76
10 20	252.0	1830.0	6140.0	4.10	3.35
10 26	254.0	1750.0	5640.0	3.75	3.22
10 28	306.0	2150.0	8460.0	5.28	3.93
11 02	260.0	2050.0	7480.0	4.83	3.65
11 09	263.0	2060.0	7560.0	4.95	3.67
11 12	332.0	2430.0	9760.0	5.88	4.02
11 16	307.0	2470.0	11000.0	6.29	4.45
11 20	316.0	2680.0	12200.0	6.74	4.55
11 23	336.0	3400.0	18000.0	8.87	5.28
11 30	313.0	2880.0	13300.0	7.20	4.62
12 02	346.0	4110.0	24300.0	10.72	5.91
12 05	350.0	5180.0	36200.0	13.45	6.99
12 05	348.0	5340.0	37100.0	13.56	6.95
12 06	348.0	5100.0	36000.0	13.29	7.06
12 06	350.0	5080.0	36100.0	13.52	7.11
12 06	343.0	5030.0	31000.0	12.47	6.16
12 08	343.0	4170.0	27100.0	11.79	6.50
12 10	343.0	4110.0	25800.0	11.57	6.28
12 15	339.0	3730.0	23000.0	10.44	6.17
12 18	330.0	2800.0	16500.0	9.16	5.89
12 21	332.0	3410.0	17300.0	9.32	5.07
12 28	325.0	2250.0	11500.0	7.44	5.11
01 06	321.0	2100.0	9610.0	6.94	4.58
01 11	322.0	1940.0	8340.0	6.72	4.30
01 17	345.0	4310.0	25700.0	11.83	5.96

(Continued)

APPENDIX A (Continued)

Date		Width ft	Area sq ft	Flow cfs	Gage Height ft	Velocity fps
01	20	328.0	2690.0	12200.0	8.57	4.54
01	23	350.0	5290.0	39300.0	14.70	7.43
01	23	350.0	5260.0	41500.0	15.30	7.91
01	24	367.0	6400.0	56500.0	20.92	8.83
01	24	367.0	7060.0	63900.0	20.56	9.05
01	24	362.0	6240.0	54300.0	19.22	8.82
01	25	355.0	3590.0	28800.0	13.00	7.88
01	27	345.0	4220.0	31100.0	14.05	7.42
01	27	345.0	4220.0	33400.0	14.05	7.91
02	01	346.0	3800.0	23300.0	12.75	6.13
02	05	323.0	3030.0	13100.0	10.98	4.32
02	08	316.0	2730.0	10300.0	9.77	3.77
02	16	360.0	5410.0	47300.0	18.09	8.74
02	16	363.0	5950.0	50000.0	18.78	8.40
02	17	365.0	6140.0	48800.0	18.78	7.95
02	19	360.0	4984.0	35300.0	16.98	7.08
02	20	367.0	5800.0	61700.0	20.35	10.47
02	20	372.0	5920.0	63400.0	21.28	10.71
02	20	362.0	4180.0	31100.0	16.70	7.44
Rating No. 15, 10 Points						
03	03	356.0	3200.0	22600.0	15.83	7.06
03	10	356.0	2840.0	17300.0	14.90	6.09
03	15	357.0	3390.0	18100.0	15.45	5.34
03	20	352.0	2040.0	14200.0	13.22	6.96
03	23	355.0	1920.0	12800.0	13.34	6.67
03	29	352.0	1610.0	8980.0	12.90	5.58
04	05	354.0	1910.0	9830.0	13.18	5.15
04	12	355.0	2420.0	14200.0	14.16	5.87
04	19	352.0	1700.0	9530.0	13.35	5.60
04	26	354.0	1950.0	8630.0	13.68	4.43
Rating No. 16, 19 Points						
05	03	356.0	2040.0	8660.0	14.10	4.24
05	11	356.0	2200.0	7840.0	14.10	3.56
05	17	356.0	2350.0	8520.0	14.20	3.63
05	24	356.0	2180.0	7710.0	14.02	3.54
06	01	357.0	2480.0	10700.0	14.98	4.31

(Continued)

APPENDIX A (Continued)

Date		Width ft	Area sq ft	Flow cfs	Gage Height ft	Velocity fps
06	08	357.0	2000.0	7160.0	13.60	3.58
06	15	358.0	2700.0	11800.0	15.41	4.37
06	21	360.0	3090.0	14000.0	16.09	4.53
06	30	353.0	2200.0	7100.0	13.47	3.23
07	06	352.0	1960.0	6300.0	13.00	3.21
07	19	292.0	1320.0	3720.0	11.34	2.82
07	27	288.0	1230.0	3350.0	11.00	2.72
08	09	297.0	1230.0	3220.0	10.88	2.62
08	18	311.0	1160.0	3190.0	11.02	2.75
08	25	306.0	1200.0	2810.0	10.95	2.34
08	31	308.0	1210.0	2650.0	10.88	2.19
09	16	345.0	1240.0	3350.0	11.35	2.70
09	20	347.0	1260.0	3440.0	11.61	2.73
09	28	350.0	1430.0	3850.0	11.97	2.69

Highway 99 Bridge Gaging Data

Rating No. 2, 12 Points

09	28	80.0	213.0	805.0	9.83	3.78
10	06	157.0	905.0	6300.0	13.37	6.96
10	06	158.0	931.0	6540.0	13.54	7.02
10	06	160.0	1040.0	7140.0	14.05	6.86
10	06	165.0	1140.0	8280.0	14.54	7.26
10	06	163.0	1130.0	7710.0	14.30	6.82
10	07	161.0	917.0	4610.0	12.15	5.03
10	13	91.0	232.0	1340.0	9.90	5.78
10	19	90.0	162.0	822.0	9.67	5.07
11	03	92.0	220.0	1300.0	10.01	5.91
11	09	90.0	182.0	852.0	9.65	4.68

Rating No. 3, 23 Points

11	12	106.0	432.0	2740.0	10.73	6.48
11	14	162.0	1210.0	8280.0	13.41	6.84
11	14	162.0	1130.0	7540.0	13.08	6.67
11	16	155.0	686.0	3610.0	10.91	5.26
11	19	110.0	519.0	3540.0	11.00	6.82

(Continued)

APPENDIX A (Continued)

Date		Width ft	Area sq ft	Flow cfs	Gage Height ft	Velocity fps
11	23	115.0	648.0	4760.0	11.44	7.34
12	02	180.0	1360.0	10700.0	14.09	7.87
12	02	176.0	1270.0	9280.0	13.95	7.31
12	05	167.0	1504.0	14700.0	15.40	9.77
12	06	175.0	1540.0	14100.0	16.00	9.16
12	06	170.0	1390.0	13000.0	14.57	9.35
12	07	157.0	1040.0	8380.0	13.93	8.05
12	09	172.0	609.0	4960.0	12.72	8.14
12	11	155.0	634.0	4400.0	12.05	6.94
12	14	150.0	410.0	3000.0	11.86	7.32
12	16	158.0	846.0	7300.0	13.47	8.62
12	18	150.0	580.0	4120.0	12.04	7.10
12	22	152.0	510.0	3160.0	12.20	6.20
12	29	150.0	359.0	2480.0	11.87	6.91
01	06	149.0	258.0	1260.0	11.11	4.88
01	12	150.0	312.0	1820.0	11.63	5.83
01	16	160.0	776.0	6310.0	13.38	8.13
01	18	139.0	797.0	7770.0	13.75	9.75
Rating No. 4, 10 Points						
01	24	210.0	1883.0	21400.0	20.20	11.36
01	25	175.0	1260.0	9950.0	16.20	7.90
01	29	165.0	720.0	4820.0	15.03	6.69
02	02	170.0	600.0	4130.0	15.13	6.88
02	04	168.0	536.0	3420.0	14.95	6.38
02	09	164.0	361.0	1810.0	14.33	5.01
02	14	180.0	1300.0	12900.0	17.39	9.96
02	17	176.0	1580.0	14800.0	18.85	9.37
02	19	182.0	1450.0	11000.0	17.82	7.59
02	22	196.0	1190.0	8480.0	19.20	7.11
Rating No. 5, 25 Points						
02	25	181.0	677.0	4100.0	17.84	6.06
03	02	187.0	595.0	4020.0	19.37	6.75
03	05	197.0	558.0	3770.0	19.40	6.76
03	09	204.0	561.0	3830.0	20.15	6.83
03	16	138.0	534.0	3460.0	19.59	6.48

(Continued)

APPENDIX A (Continued)

Date		Width ft	Area sq ft	Flow cfs	Gage Height ft	Velocity fps
03	24	167.0	315.0	1660.0	19.19	5.27
03	30	174.0	348.0	1830.0	19.24	5.26
04	07	189.0	356.0	2190.0	20.70	6.15
04	13	188.0	793.0	7280.0	21.80	9.18
04	20	164.0	346.0	2470.0	20.06	7.14
04	27	164.0	333.0	2280.0	20.10	6.25
05	03	165.0	341.0	2270.0	20.35	6.66
05	10	174.0	274.0	1620.0	20.23	5.91
05	17	130.0	341.0	2340.0	20.60	6.86
05	24	136.0	296.0	1860.0	20.45	6.28
06	02	153.0	244.0	1350.0	20.38	5.53
06	10	156.0	246.0	1470.0	20.40	5.98
06	18	172.0	252.0	1470.0	20.82	5.83
06	22	133.0	234.0	1150.0	20.37	4.91
06	29	127.0	160.0	724.0	20.25	4.52
07	08	165.0	190.0	584.0	20.21	3.07
07	20	173.0	171.0	518.0	19.97	3.03
07	28	143.0	224.0	431.0	19.71	1.92
08	13	135.0	154.0	381.0	19.57	2.47
08	27	148.0	143.0	323.0	19.36	2.26

Tower Road Gaging Data

Rating No. 2, 23 Points

10	06	218.0	825.0	7010.0	18.30	8.50
10	06	218.0	913.0	7570.0	18.89	8.29
10	07	214.0	585.0	4510.0	17.34	7.71
10	13	210.0	319.0	1370.0	15.67	4.29
10	19	185.0	190.0	725.0	15.22	3.82
10	27	192.0	227.0	1010.0	15.47	4.45
10	28	211.0	441.0	2580.0	16.63	5.85
11	04	197.0	259.0	1170.0	15.48	4.52
11	12	211.0	408.0	2280.0	16.38	5.59
11	14	219.0	859.0	6950.0	18.23	8.09
11	14	205.0	919.0	6720.0	17.95	7.31
11	16	214.0	599.0	3410.0	16.74	5.69
11	18	215.0	727.0	4870.0	17.25	6.70

(Continued)

APPENDIX A (Continued)

Date		Width ft	Area sq ft	Flow cfs	Gage Height ft	Velocity fps
11	24	214.0	595.0	3760.0	16.57	6.32
12	01	205.0	458.0	2520.0	15.87	5.50
12	02	219.0	946.0	8260.0	18.71	8.73
12	05	221.0	1580.0	18100.0	20.85	11.46
12	05	217.0	1270.0	14000.0	20.23	11.02
12	06	220.0	1180.0	13100.0	19.55	11.10
12	06	220.0	1200.0	12900.0	19.64	10.67
12	06	219.0	1168.0	11500.0	19.16	9.84
Rating No. 3, 12 Points						
12	08	207.0	734.0	5890.0	15.81	8.02
12	10	208.0	672.0	4840.0	15.18	7.20
12	15	212.0	744.0	5900.0	15.36	7.93
12	15	214.0	964.0	8820.0	16.93	9.15
12	18	202.0	617.0	4070.0	14.71	6.59
12	21	200.0	550.0	3710.0	14.70	6.74
12	29	190.0	377.0	2290.0	13.35	6.07
01	08	118.0	210.0	1200.0	11.91	5.71
01	12	144.0	277.0	1710.0	12.32	6.17
01	16	204.0	821.0	7040.0	15.70	8.57
01	17	206.0	1230.0	10100.0	17.35	8.21
01	19	201.0	653.0	4820.0	14.36	7.38
Rating No. 4, 25 Points						
01	23	218.0	1730.0	20200.0	19.70	11.68
01	23	220.0	1660.0	20800.0	20.11	12.53
01	24	222.0	2180.0	30200.0	22.52	13.85
01	24	220.0	1960.0	25000.0	21.01	12.76
01	26	215.0	1100.0	9940.0	16.37	9.04
01	29	204.0	595.0	4270.0	13.31	7.18
02	02	203.0	581.0	4190.0	13.15	7.21
02	04	201.0	467.0	3280.0	12.56	7.02
02	09	189.0	324.0	1830.0	10.87	5.65
02	12	188.0	327.0	1810.0	10.82	5.54
02	14	215.0	1220.0	11600.0	16.97	9.51
02	16	221.0	1610.0	17200.0	18.62	10.68
02	17	216.0	1420.0	15000.0	18.07	10.56
02	19	214.0	996.0	9000.0	16.40	9.04
02	21	218.0	1350.0	12600.0	17.60	9.33
02	24	209.0	647.0	5470.0	13.43	8.45

(Continued)

APPENDIX A (Continued)

Date		Width ft	Area sq ft	Flow cfs	Gage Height ft	Velocity fps
03	01	207.0	501.0	3600.0	13.21	7.19
03	05	204.0	479.0	3360.0	12.65	7.01
03	09	210.0	507.0	3540.0	13.20	6.98
03	15	208.0	557.0	4140.0	12.92	7.43
03	20	180.0	353.0	3040.0	14.71	8.61
03	20	188.0	329.0	2470.0	14.21	7.51
03	22	204.0	282.0	1840.0	14.55	6.52
03	29	210.0	293.0	1760.0	15.83	6.01
04	06	215.0	354.0	2170.0	16.60	6.19
Rating No. 5, 21 Points						
04	12	219.0	673.0	5910.0	19.33	8.78
04	26	219.0	348.0	2200.0	19.00	6.32
05	03	223.0	381.0	2270.0	19.12	5.96
05	10	220.0	326.0	1550.0	18.88	4.75
05	17	223.0	409.0	2310.0	19.42	5.65
05	24	208.0	342.0	1880.0	19.09	5.50
06	01	221.0	336.0	1530.0	18.79	4.55
06	08	218.0	305.0	1320.0	18.51	4.33
06	14	221.0	332.0	1320.0	18.75	3.98
06	21	221.0	353.0	1450.0	18.71	4.11
06	28	224.0	252.0	852.0	18.49	3.38
07	06	224.0	230.0	724.0	18.40	3.15
07	13	224.0	204.0	605.0	18.43	2.97
07	19	224.0	179.0	538.0	18.50	3.01
08	04	222.0	170.0	430.0	18.50	2.53
08	13	199.0	148.0	411.0	18.65	2.78
08	24	205.0	131.0	288.0	18.51	2.20
09	01	204.0	107.0	320.0	18.35	2.99
09	08	192.0	126.0	315.0	18.37	2.50
09	28	206.0	173.0	521.0	18.48	3.01
Kidd Valley Gaging Data						
Rating No. 12, 18 Points						
10	06	168.0	567.0	4530.0	19.64	7.99
10	06	169.0	530.0	4190.0	19.49	8.90
10	07	151.0	353.0	2320.0	18.32	6.57

(Continued)

APPENDIX A (Continued)

Date		Width ft	Area sq ft	Flow cfs	Gage Height ft	Velocity fps
10	19	82.0	119.0	469.0	16.98	3.94
10	26	116.0	107.0	330.0	16.77	3.08
10	28	148.0	254.0	1410.0	17.80	5.55
11	02	122.0	172.0	648.0	16.94	3.77
11	09	117.0	130.0	460.0	16.74	3.54
11	12	145.0	231.0	1230.0	17.52	5.32
11	14	167.0	503.0	4020.0	19.32	7.99
11	14	162.0	389.0	2880.0	18.70	7.40
11	16	146.0	303.0	1930.0	18.19	6.37
11	23	148.0	320.0	2180.0	18.55	6.81
11	30	131.0	181.0	862.0	17.15	4.76
12	02	170.0	614.0	4850.0	19.67	7.90
12	03	160.0	537.0	2410.0	18.48	4.49
12	05	193.0	978.0	11100.0	21.72	11.31
12	05	172.0	835.0	8710.0	21.34	10.43
Rating No. 11, 35 Points						
12	05	169.0	717.0	7000.0	20.78	9.26
12	06	173.0	685.0	6590.0	20.81	9.62
12	06	171.0	623.0	5580.0	20.75	8.96
12	08	170.0	406.0	3200.0	19.94	7.88
12	09	170.0	336.0	2480.0	19.55	7.38
12	14	156.0	252.0	1660.0	18.98	6.59
12	17	167.0	352.0	2300.0	19.67	6.51
12	18	164.0	337.0	2480.0	19.29	7.36
12	21	157.0	304.0	1900.0	19.10	6.25
12	28	151.0	260.0	1470.0	18.90	5.65
01	06	144.0	150.0	646.0	18.30	4.31
01	12	146.0	208.0	1000.0	18.67	4.61
01	17	178.0	671.0	5500.0	20.84	8.19
01	23	181.0	1100.0	11300.0	22.54	10.27
01	23	183.0	1030.0	10800.0	22.08	10.48
01	24	183.0	1190.0	13300.0	22.67	11.18
01	24	183.0	1020.0	11400.0	21.55	11.18
01	25	177.0	632.0	5260.0	20.33	8.32
01	29	173.0	357.0	2460.0	19.64	6.89
02	02	173.0	411.0	2590.0	19.09	6.30

(Continued)

APPENDIX A (Continued)

Date		Width ft	Area sq ft	Flow cfs	Gage Height ft	Velocity fps
02	04	172.0	359.0	1980.0	18.68	5.52
02	08	170.0	267.0	1210.0	18.01	4.53
02	14	178.0	708.0	7140.0	20.54	10.08
02	15	177.0	753.0	7150.0	20.49	9.50
02	16	183.0	1050.0	10600.0	21.93	10.10
02	17	181.0	826.0	8610.0	21.69	10.42
02	19	177.0	685.0	5750.0	21.24	8.39
02	20	189.0	1230.0	16500.0	24.07	13.42
02	20	187.0	1150.0	14500.0	23.64	12.68
02	22	180.0	551.0	4590.0	20.66	8.33
03	01	180.0	390.0	2750.0	21.04	7.05
03	04	177.0	333.0	2220.0	20.60	6.67
03	04	177.0	332.0	2080.0	20.55	6.26
03	09	178.0	343.0	2170.0	20.35	6.33
03	15	178.0	335.0	2310.0	20.40	6.40
Rating No. 13, 29 Points						
03	20	117.0	205.0	1570.0	20.70	7.65
03	20	123.0	206.0	1660.0	20.70	8.06
03	20	177.0	212.0	1360.0	20.72	6.42
03	23	156.0	181.0	1280.0	21.51	7.07
03	31	179.0	169.0	965.0	22.12	5.71
04	05	181.0	198.0	1370.0	22.47	6.93
04	08	182.0	204.0	1310.0	22.44	6.42
04	14	186.0	366.0	3130.0	24.01	8.55
04	19	184.0	240.0	1530.0	23.53	6.38
04	29	184.0	257.0	1500.0	23.01	5.84
05	07	141.0	212.0	1320.0	22.42	6.23
05	12	138.0	196.0	1070.0	22.14	5.46
05	17	149.0	255.0	1660.0	22.07	6.51
05	24	140.0	225.0	1310.0	21.64	5.82
06	04	158.0	124.0	813.0	21.28	5.14
06	07	122.0	190.0	834.0	21.15	4.39
06	14	120.0	172.0	969.0	21.27	5.63
06	23	109.0	142.0	798.0	20.80	5.62
07	01	89.0	105.0	532.0	20.09	5.07
07	06	77.0	110.0	498.0	20.12	4.53

(Continued)

APPENDIX A (Concluded)

Date	Width ft	Area sq ft	Flow cfs	Gage Height ft	Velocity fps
07 13	81.0	95.0	421.0	19.98	4.43
07 22	62.0	76.0	306.0	19.86	4.03
07 29	61.0	70.7	293.0	19.71	4.14
08 06	65.0	66.2	246.0	19.69	3.72
08 17	65.0	60.8	219.0	19.95	3.60
08 31	65.0	57.8	207.0	20.07	3.58
09 07	66.0	56.8	200.0	19.91	3.52
09 13	59.0	90.0	515.0	20.48	5.72
09 20	117.0	153.0	816.0	20.81	5.34

APPENDIX B

USGS WATER AND SEDIMENT DATA

Water Year 1982 (October 1, 1981-September 30, 1982)

Date	Time	Temp °C	Flow cfs	Sed. Susp mg/ℓ	Percent Finer Sediment Suspension 0.002 mm	0.004 mm	0.008 mm	0.016 mm	0.031 mm	0.062 mm	0.125 mm	0.250 mm	0.500 mm	1.00 mm	2.00 mm
Castle Rock - Cowlitz River Gage															
October															
05	1155	10.5	3160	43						90					
06	1330		10400	6680						97					
06	1810	13.0	11900	14400						99					
07	1655		9830	5200						97					
13	1200		7700	212						61					
21	1210	11.0	7090	159						40					
26	1240	10.5	5700	109						43					
28	1220	11.0	8460	8770						97					
28	1240	11.0	8420	9340						98					
28	1255	11.0	8380	8210						97					
November															
02	1120	10.0	7480	497						67					
02	1145	10.0	7480	445	15	18	26	35	48	68	88	100			
02	1205	10.0	7480	441						68					
09	1335	11.0	7560	234						50					
09	1400	11.0	7560	206						53	81	99	100		
09	1410	11.0	7560	239						47					
12	0900	10.0	9920	5170						86					
12	0945	10.0	9850	4600						86					
12	1035	10.0	9810	3570						89					
12	1150	10.0	9700	3240						82					
12	1215	10.0	9700	2820						84					
12	1235	10.0	9630	2860						83					
12	1330	10.0	9590	2500						80					
13	1125	10.0	8600	748						64					
14	2130		13600	13700						92					
15	0800	9.0	12000	4180						82					
15	1545	9.5	11400	2740						82					
16	0920		11100	4460						79					
16	1030		11100	4240						78					
16	1130	9.0	11000	4300						75					
16	1255	9.0	10900	3940						76					
16	1320	9.0	10800	3760						78					
16	1335		10800	3860						76					
17	0940	9.5	12000	2040						64					
17	1745	9.0	13300	4540						83					
18	1410	9.0	14300	3880						66					

(Continued)

APPENDIX B (Continued)

Date	Time	Temp °C	Flow cfs	Sed. Susp mg/ℓ	Percent Finer Sediment Suspension 0.002 mm	0.004 mm	0.008 mm	0.016 mm	0.031 mm	0.062 mm	0.125 mm	0.250 mm	0.500 mm	1.00 mm	2.00 mm
19	1420	8.5	12800	1340						81					
20	1340	9.0	12200	1380		11	18	28	41	57	82	99	100		
23	1025		15000	2120						54					
23	1330	9.5	17900	1660						52					
23	1355	9.5	17800	1610		11	17	27	40	56	83	99	100		
23	1415		17800	1720						51					
24	0935	8.0	16700	812						78					
30	1200		13400	612						23					
30	1233	8.0	13300	548	10	10	13	16	21	31	54	96	100		
30	1240	8.0	13400	725						20					
December															
01	1445	9.0	13300	757						50					
02	1020	7.5	22600	8240						91					
02	1030	7.5	22600	4900						85					
02	1115	7.5	23700	6710						89					
02	1145	7.5	24400	9260						89					
02	1215	7.5	24500	9870						89					
02	1245	7.5	24800	10200						87					
02	1315	7.5	24900	9310						91					
02	1345	7.5	24600	9230						92					
02	1505	7.5	23700	8100		19	31	48	69	86	98	100			
02	1545	7.5	23000	6600						89					
05	1230		34400	20400						94					
05	1300		35400	22200						92					
05	1330		35800	22200						92					
05	1400		36000	22300						93					
05	1430		36600	22400						91					
05	1500		37400	22300						91					
05	1515		38000	21700						92					
05	1600		38400	20300						92					
05	1630		38200	18500						92					
05	1700		38200	17200						89					
05	1730		38200	15500						90					
05	1800		38300	16600						88					
05	1830		38200	14000						91					
05	2000		37900	11600						92					
05	2030		37500	11700						93					
05	2100		37000	12100						90					
05	2130		36700	10600						93					
05	2200		36300	10500						90					
05	2230		36000	10400						89					
05	2300		35800	10000						88					
05	2330		35600	8890						89					

(Continued)

APPENDIX B (Continued)

Date	Time	Temp °C	Flow cfs	Sed. Susp mg/ℓ	Percent Finer Sediment Suspension 0.002 mm	0.004 mm	0.008 mm	0.016 mm	0.031 mm	0.062 mm	0.125 mm	0.250 mm	0.500 mm	1.00 mm	2.00 mm
06	0005		35200	8670						86					
06	0030		35200	8090						86					
06	0100		35100	7880						86					
06	0130		35500	7490						85					
06	0200		35600	7670						84					
06	0330		36000	7140						85					
06	0405		36000	7120						82					
06	0500		36400	6500						85					
06	0535		36600	6680						82					
06	0600		36700	6610						82					
06	0605		36700	6740						83					
06	0700		36700	6380						82					
06	0800	8.5	35800	6210						79					
06	0900		34200	5560						81					
06	1050		35000	5210						84					
06	1115		33500	14800						94					
06	1135		33400	4950						81					
06	1200		33200	5140						80					
06	1230		32800	4750						85					
06	1300		32400	5110						77					
06	1330		32000	4580						81					
06	1400		31900	4900						80					
06	1430		31800	4480						82					
06	1500		31400	4900						80					
06	1530		31300	4620						82					
06	1600		31000	4540						85					
07	1655	8.0	26000	5730						38					
08	1000		27200	1700						73					
08	1220		27000	4840						25					
08	1305		27000	2190		8	14	22	33	48	75	98	100		
08	1345		27000	1640						62					
09	1400	9.5	24800	2220						30					
10	1300	8.5	25800	3660						26					
10	1340	8.5	25800	3200		5	8	13	18	28	48	85	99	100	
10	1415	8.5	25800	3150						26					
15	0930	9.0	22000	1740						73					
15	1215	9.0	24200	1620						70					
15	1300	9.0	25000	1870						68					
15	1330	9.0	25500	4020	4	6	11	16	31	39					
15	1350	9.0	25900	2110						71					
21	1210	8.0	17300	1140						46					
21	1235	8.0	17200	1800	5	8	12	20	28	33					
28	1030	6.0	11400	1700						17					

(Continued)

APPENDIX B (Continued)

Date	Time	Temp °C	Flow cfs	Sed. Susp mg/ℓ	Percent Finer Sediment Suspension 0.002 mm	0.004 mm	0.008 mm	0.016 mm	0.031 mm	0.062 mm	0.125 mm	0.250 mm	0.500 mm	1.00 mm	2.00 mm
28	1400	6.0	11400	1910						14					
28	1415	6.0	11500	1420						23					
28	1440	6.0	11500	1550						16					
January															
06	1315	4.0	9390	640						8					
06	1325	4.0	9390	1350						8					
06	1335	4.0	9390	602						10					
11	1320	6.0	8460	799						32					
11	1335	6.0	8460	785						39					
11	1350	6.0	8460	938						30					
17	1308	5.5	25100	4080		10	13	21	32	48	74	96	100		
17	1355		25000	2980						57					
18	1330	6.0	20000	2500		7	11	17	24	37	59	89	99	100	
18	1335	6.0	19900	2130						44					
20	1145	5.0	12000	1260						28					
20	1220	5.0	12000	1760						29					
20	1300	5.0	11900	1320						26					
23	1900	9.0	38800	6440						85					
23	2010	8.5	38700	6260						86					
23	2140	8.5	40200	6180						84					
23	2400		41200	5700						80					
24	0140		44500	5900						76					
24	0228	8.0	46800	7370		16	23	37	56	77	95	99	100		
24	0300	8.0	48300	8200						82					
24	0710	8.0	58900	14400						83					
24	0900	8.0	64800	11200						84					
24	1305		62700	7100						75					
24	1525		56800	6110						72					
24	1640	7.0	51500	6250						68					
25	1220	6.0	29000	6230						59					
25	1320	6.0	28000	11600	10	14	25	39	56	72	91	100			
25	1335	6.0	27800	11900						78					
26	1140	6.0	33800	3480						66					
27	1315	6.0	31400	1610						53					
27	1345	6.0	31200	3010	3	3	6	10	14	31	41	72	99	100	
27	1435	6.0	31000	1730						47					
February															
01	1330	7.0	23000	1060						22					
01	1400	7.0	22800	1500						15	22	47	90	100	
01	1430	7.0	22500	1190						20					
05	1125		13400	1160						24					
05	1145		13400	1040						12	26	29	63	99	100
05	1200		13300	1100						24					

(Continued)

APPENDIX B (Continued)

Date	Time	Temp °C	Flow cfs	Sed. Susp mg/l	0.002 mm	0.004 mm	0.008 mm	0.016 mm	0.031 mm	0.062 mm	0.125 mm	0.250 mm	0.500 mm	1.00 mm	2.00 mm
					Percent Finer Sediment Suspension										
08	1220	4.0	10200	885						22					
08	1235	4.0	10200	1640						16					
08	1250	4.0	10200	1340						10					
16	0935	8.0	43600	7860						70					
16	1140	8.0	48000	6610						70					
16	1350	8.0	50300	9740	7	10	15	27	41	63	77	90	98	100	
16	1445	8.0	50200	7800						74					
16	1715	8.0	50200	7710						70					
16	1735	8.0	50200	7870						72					
16	1750	8.0	50500	8740						62					
16	1810	8.0	50700	6580						74					
17	1035	8.0	49900	16700						84					
17	1230		48000	10900						79					
17	1320	8.0	47100	13600						55					
17	1340	8.0	46900	8380						73					
18	2105	8.0	39200	8990	8	9	14	24	36	47	68	81	96	100	
18	2125	8.0	39200	5260						82					
19	0715		35700	3630						77					
19	1135		33600	7320	6	7	8	15	23	38	58	91	99	100	
19	1200		34200	3140						73					
20	1040		58100	26600						88					
20	1355		54800	43200						78					
20	1400		55800	32300						93					
20	1415		56500	32400						90					
20	1550		62500	32400						90					
20	1615		62500	38500	11	17	29	44	62	77	95	100			
20	1630		62800	31500						84					
20	1835		63700	19200						80					
20	1850		61300	25200	10	13	21	34	48	66					
20	1905		61300	17200						85					
20	2000		60400	17800						82					
20	2050		59300	19900						78					
20	2310		52300	29000						82					
20	2325		50300	29600						85					
20	2355		48000	31800						65					
21	0100		45600	19100						84					
21	0125		44600	19000						82					
21	0155		43900	16000						84					
21	0250		42000	16000						81					
21	1040	6.5	32200	12500						66					
21	1205	6.0	31700	11000						64					
21	1230	6.5	31700	11600						62					
21	1300	6.5	31500	11100						64					

(Continued)

APPENDIX B (Continued)

Date	Time	Temp °C	Flow cfs	Sed. Susp mg/ℓ	0.002 mm	0.004 mm	0.008 mm	0.016 mm	0.031 mm	0.062 mm	0.125 mm	0.250 mm	0.500 mm	1.00 mm	2.00 mm
					Percent Finer Sediment Suspension										
21	1320	6.5	31700	13400						56					
21	1335	6.5	31000	11700						60					
23	1245	5.0	35900	2380						45					
25	1330	7.0	36000	9100						31					
25	1350	7.0	36000	7990						34					
March															
03	1255	6.0	22900	1830						25					
10	1230	8.5	16800	2080						46					
15	1215	6.0	17600	1920						20					
20	0035		12600	987						13	25	60	96	98	100
20	0037		12600	837						24	34	61	96	100	
20	0130		12600	1640						81	95	100			
20	0145		13600	36700						97	100				
20	0218		17200	65800						90	99	100			
20	0220		17600	67100						89	99	100			
20	0225		17800	66700						90	99	100			
20	0235		18000	67600						86	98	100			
20	0325		14200	124000						93	100				
20	0328		13900	124000						93	100				
20	0335		13600	157000						84	97	99	100		
20	0346		13300	136000						90	99	100			
20	0350		13300	138000						91	99	100			
20	0445		16700	95400						86	98	99	100		
20	0540		13600	73200						83	98	99	100		
20	0542		13600	66900						87	99	100			
20	0545		13600	68200						87	99	100			
20	0650		12500	60600						88	98	100			
20	1210		14000	22400						76	92	100			
20	1545		13900	18100						61	85	98	99	100	
20	1600		13700	16100						70	88	98	100		
23	1155	7.0	12800	4800						41					
29	1145	8.0	8980	3540						39					
April															
05	1100	6.5	9830	1950						52					
05	1110	6.5	9830	5300						23					
12	0915	8.0	14400	24200						58					
12	1140	8.0	13900	18800						61					
19	0920	9.0	9530	2300						36					
19	1215	9.0	9530	3870						26					
26	1235	9.0	8640	2040						37	46	86	99	100	
May															
03	0825	8.0	8700	1440					46						
03	0845	8.0	8700	2670						21	34	40	87	98	100
11	1215	9.0	7840	809						48					

(Continued)

APPENDIX B (Continued)

Date	Time	Temp °C	Flow cfs	Sed. Susp mg/ℓ	0.002 mm	0.004 mm	0.008 mm	0.016 mm	0.031 mm	0.062 mm	0.125 mm	0.250 mm	0.500 mm	1.00 mm	2.00 mm
					Percent Finer Sediment Suspension										
11	1225	9.0	7840	1050						28	51	82	99	100	
17	1235	11.5	9150	1640						54					
May															
17	1300	11.5	9280	1440						44	65	87	98	100	
24	1235	11.5	7750	1570						27	37	61	97	100	
June															
01	1205	9.5	10600	1390						8	23	44	84	99	100
08	1305	11.0	7170	671						10	45	71	99	100	
15	1203	11.5	11800	637						38	47	73	98	100	
21	1215	11.0	14000	1750						18					
July															
06	1130	13.0	6300	344						17					
19	1255	15.0	3720	232						28					
27	1150	16.5	3350	173						37	58	82	98	100	
August															
09	1315	14.5	3220	166						31	52	75	95	100	
18	1140	17.0	3190	123						23	44	77	96	100	
25	1250	16.5	2810	121						23	44	74	97	100	
31	1050	15.0	2650	188						21					
31	1115	15.0	2650	159						21					
September															
16	1250	15.0	3350	323						34					
20	1155	13.0	3730	629						59					
20	1540	14.0	3360	2950						87					
28	1310	12.5	3850	324						41					
							Highway 99 Bridge - Toutle River Gage								
October															
05	1340	10.0	700	1300						24					
05	1505	10.0	700	1130						39	43	53	72	82	93
06	0920		5300	8140						75					
06	0930		5650	9100						70					
06	0955		6200	9440						73					
06	1020		6400	11900						68					
06	1025		6300	11800						71					
06	1030		6200	13000						71					
06	1050		6500	13400						74					
06	1100	12.0	6600	14000						78					
06	1115		6900	14400						77					
06	1145		7500	14100						78					
06	1205		7850	14300						78					
06	1225		8000	15500						74					
06	1325		8250	17300						79					

(Continued)

APPENDIX B (Continued)

Date	Time	Temp °C	Flow cfs	Sed. Susp mg/ℓ	0.002 mm	0.004 mm	0.008 mm	0.016 mm	0.031 mm	0.062 mm	0.125 mm	0.250 mm	0.500 mm	1.00 mm	2.00 mm
					Percent Finer Sediment Suspension										
06	1345		8300	18900						79					
06	1505		8200	24500						85					
06	1510		8100	26200						84					
06	1555		7700	28500						83					
06	1600		7650	27600						86					
06	1610		7650	28800						84					
06	1615		7700	32100						83					
06	1745		7900	31600						86					
06	1845		7700	39300						89					
06	1915		7750	39300						89					
06	1925		7800	39400						89					
06	2005		9000	52500						72					
06	2030		9300	53000						86					
06	2130		8650	89600						84					
06	2215		8350	78100						89					
07	0930		4900	36200						89					
07	1000		4800	31000						89					
07	1030		4700	32500						87					
07	1100		4600	27000						89					
07	1130		4550	26500						88					
07	1200		4450	23300						91					
07	1250		4350	21900						90					
07	1305		4300	21400	16	28	46	68	80	86					
07	1320		4300	20600						89					
13	1520		1340	1240						46					
13	1535		1340	1910						32					
13	1550		1340	1090						63					
19	1615	11.0	822	1250						34					
26	1535	12.0	531	820						31					
November															
03	1200	10.5	1300	2420						60					
03	1215	10.5	1300	2930		10	15	22	32	44	56	72	93	99	100
03	1230	10.5	1300	2140						60					
09	1340	10.5	852	2020		8	12	18	26	37	52	72	94	100	
11	1810	11.5	1490	5340						16					
11	2040		2050	3660						44					
12	0930	11.0	2920	15300						80					
12	0955	11.0	2340	16300						81					
12	1005	11.0	2310	14100						80					
12	1105	11.0	2670	12700						76					
12	1200	11.0	2400	11100						78					
12	1220	11.0	2740	11200		14	24	39	56	68	82	91	98	100	
12	1240	11.0	2180	10900						71					

(Continued)

APPENDIX B (Continued)

Date	Time	Temp °C	Flow cfs	Sed. Susp mg/ℓ	Percent Finer Sediment Suspension 0.002 mm	0.004 mm	0.008 mm	0.016 mm	0.031 mm	0.062 mm	0.125 mm	0.250 mm	0.500 mm	1.00 mm	2.00 mm
13	0945	9.0	1550	3640						59					
14	1405		7840	50200						83					
14	1415		7910	51900						84					
14	1435		8250	61400						80					
14	1455		8500	64000						77					
14	1505		8550	68100						76					
14	1525		8270	54800						82					
14	1605		8400	53400						80					
14	1630		8700	52500		17	27	43	62	75	90	95	99	100	
14	1640		8850	50800						78					
14	1655		8870	48100						79					
14	1735		8460	53600						78					
14	1805		8200	47500						80					
14	1905		7800	48600						74					
14	2215		6450	34100						75					
14	2220		6400	38100						66					
15	0850	8.0	4400	14300						58					
15	1515	8.0	4120	9960						66					
16	1205	7.5	3730	14400						67					
16	1355	7.5	3640	13900						60					
16	1430	7.5	3530	14500		11	17	28	41	52	71	91	97	99	100
16	1455	8.0	3590	17300						53					
17	1015	8.5	3650	9200						61					
17	1710		4960	20500						67					
18	1340	8.0	4550	11700						61					
19	1025	7.5	3540	9970						40					
19	1110		3540	8030						48					
19	1225		3540	8150						42					
19	1230		3540	9320		9	15	23	31	41	59	80	93	99	100
19	1250	6.0	3540	8160						46					
23	1220	8.0	4760	8180		9	14	21	30	41	58	78	92	99	100
24	1110	6.0	3640	9380						37					
December															
01	1415	7.0	3030	4640						42					
02	0810	8.0	8720	17700						59					
02	0820	8.0	8960	19900						61					
02	0845	8.0	8840	16300						53					
02	0900	8.0	9080	16800						56					
02	0920		9780	19800						55					
02	0930		9780	18900						60					
02	0950		10500	21000						62					
02	1000		11000	23600						60					
02	1010		10500	25000						62					

(Continued)

APPENDIX B (Continued)

Date	Time	Temp °C	Flow cfs	Sed. Susp mg/ℓ	Percent Finer Sediment Suspension 0.002 mm	0.004 mm	0.008 mm	0.016 mm	0.031 mm	0.062 mm	0.125 mm	0.250 mm	0.500 mm	1.00 mm	2.00 mm
02	1020		11100	23200						68					
02	1030		11600	26100						68					
02	1040		11100	27500						71					
02	1050		11700	28400						72					
02	1100		11700	28400						75					
02	1110		11800	31500						71					
02	1120		11200	31800						72					
02	1130		12000	33400		14	22	36	52	70	87	95	98	100	
02	1135		12000	31400						73					
02	1140		11700	33600						72					
02	1150		11400	33600						72					
02	1200		11200	33400						73					
02	1210	8.0	11000	35700						67					
02	1215		10800	35000						67					
02	1220		10700	33000						72					
02	1235		10300	34400						69					
02	1305		10000	40900						63					
02	1340		9320	29600						72					
02	1420		8840	29200						68					
02	1440		8390	26800						68					
02	1530		8100	23200		12	22	34	49	64	82	93	98	100	
02	1550	7.5	7260	22200						63					
05	1245		17300	67000						70					
05	1310		17400	67800						69					
05	1345		18600	64900						72					
05	1405		19000	64100						72					
05	1410	9.0	19100	64200						71					
05	1455		19600	64100						69					
05	1510		19000	60700						70					
05	1515		18800	68100						62					
05	1540	9.0	18200	47500						63					
05	1740		16500	54400						64					
05	1900		17400	65700						52					
05	1945	9.0	16600	47800						59					
05	2045		15600	67300						50					
05	2100		15300	43200						61					
05	2205		14500	34300						65					
05	2210	8.0	14400	37900						63					
05	2340	8.0	13900	32900						58					
06	0050	8.0	13900	31600						56					
06	0135	8.0	14000	28600						59					
06	0220	7.5	14100	28400						58					
06	0305	7.5	14100	38200						48					

(Continued)

APPENDIX B (Continued)

Date	Time	Temp °C	Flow cfs	Sed. Susp mg/ℓ	Percent Finer Sediment Suspension 0.002 mm	0.004 mm	0.008 mm	0.016 mm	0.031 mm	0.062 mm	0.125 mm	0.250 mm	0.500 mm	1.00 mm	2.00 mm
06	0350	8.0	13900	28000						56					
06	0455	7.5	13500	25800						58					
06	0555	7.5	13600	24800						56					
06	0645	7.5	13200	23600						53					
06	0900	7.5	14800	35600						40					
06	1020	7.5	13200	41200						34					
06	1110	8.0	13100	23400		10	15	24	36	49	72	93	99	100	
06	1245		13000	26900						45					
06	1250		13000	19900						51					
06	1335		12900	20800						51					
06	1500	8.0	12700	21900						49					
06	1620		12400	19800		10	14	23	34	48	70	93	99	100	
07	1205		8300	18100						36					
07	1245	8.0	8450	16400						37					
07	1350	8.0	8380	17400						36					
07	1505	8.0	8100	13700		8	12	20	30	43	64	87	97	99	100
07	1525	8.0	8000	22100						27					
09	1230	8.5	8400	16900						23					
09	1245	8.5	8450	8480		8	12	20	28	39	57	84	97	100	
09	1255	8.5	8480	18400						22					
11	1050	5.5	4400	18600						20					
11	1250	5.5	4400	15600						23					
11	1320	5.5	4400	8090		8	13	21	31	42	60	85	98	100	
11	1345	5.5	4400	16600						22					
14	1320	6.0	3000	5000	6	6	13	21	30	40					
15	1550	8.5	9950	14100						56					
15	1620	8.5	10300	14700						59					
16	1025	7.0	7840	15400						30					
16	1235	7.0	7380	12400						34					
16	1310	7.0	7130	10500		7	11	19	28	40	61	86	97	100	
16	1345	7.0	7320	12200						34					
18	1000	7.0	4120	5880						36					
18	1250	7.0	4120	5820						36					
18	1310	7.0	4120	6150	6	7	8	16	24	35					
18	1325	7.0	4120	6290						32					
22	1010	5.5	3160	7700						32					
22	1300	5.5	3160	6670						34					
22	1315	5.5	3160	6200	6	6	8	17	25	40					
22	1330	5.5	3160	7200						28					
29	0945	4.0	2480	3840						25					
29	1150	4.0	2480	3590						23					
29	1210	4.0	2480	3800						22					
29	1225	4.0	2480	4460						19					

(Continued)

APPENDIX B (Continued)

Date	Time	Temp °C	Flow cfs	Sed. Susp mg/ℓ	Percent Finer Sediment Suspension 0.002 mm	0.004 mm	0.008 mm	0.016 mm	0.031 mm	0.062 mm	0.125 mm	0.250 mm	0.500 mm	1.00 mm	2.00 mm
January															
06	1200	5.0	1260	1340						30					
12	1135	5.0	1820	3400						23					
12	1150	5.0	1820	3620		5	8	13	18	26	42	72	96	100	
12	1205	5.0	1820	3490						24					
14	1320	6.5	2960	4250						33					
16	1245		6500	12400						31					
16	1355	6.0	6900	9260						38					
16	1505	6.0	6600	11100						32					
16	1530		7100	10400		6	9	14	22	34	59	85	98	99	100
16	1650	6.0	8800	14000						35					
17	1505	5.5	9000	12300						34					
18	1015	6.5	9400	6980						29					
18	1310	6.5	6900	6340						30					
18	1335	6.5	6850	8200	4	5	7	12	19	23					
18	1355	6.5	6829	5880						32					
23	1210	6.5	21100	19400						61					
23	1255	7.0	22700	14400						56					
23	1300		22800	21900						57					
23	1345		22800	21500						55					
23	1355		22700	21600						59					
23	1400		22700	21500						55					
23	1410		21500	21200						57					
23	1435		19500	20600						59					
23	1505		20600	19900						55					
23	1515		20500	20000						53					
23	1520		20500	21000						51					
23	1545		20200	18700						59					
23	1605		20200	19600						55					
23	1645		20300	19700						55					
23	2050		19500	20800						55					
23	2100		19600	17000						67					
23	2330		21000	18400						53					
24	0125		23200	23500						46					
24	0145		23500	22500						48					
24	0245		26700	30800						51					
24	0315	7.0	29000	34400						42					
24	0320	7.0	29400	30000						51					
24	0425		31800	42000						52					
24	0445		32500	46700						47					
24	0530		35100	46500						52					
24	0625		33700	26100						60					
24	0715		32300	44900						53					

(Continued)

APPENDIX B (Continued)

Date	Time	Temp °C	Flow cfs	Sed. Susp mg/ℓ	Percent Finer Sediment Suspension 0.002 mm	0.004 mm	0.008 mm	0.016 mm	0.031 mm	0.062 mm	0.125 mm	0.250 mm	0.500 mm	1.00 mm	2.00 mm
24	0725		32100	42300						58					
24	0825		31100	45700						47					
24	0830		30800	39900						52					
24	0900		29400	52200						46					
24	0930		28800	43100						47					
24	0940		28700	43200						44					
24	1110		26700	38200						44					
24	1220		26200	32600						43					
24	1300		25700	32200						40					
24	1445		22700	28300						42					
24	1615		21700	23700						48					
25	1500	7.0	10700	19500						58					
25	1630	7.0	10800	15400						50					
25	1655	7.0	10800	16400		10	15	23	34	47	67	88	98	100	
26	1245	6.5	10700	12300						48					
29	1150	6.5	4820	6080						25					
29	1200	6.5	4820	4960						29					
29	1215	6.5	4820	5830						24					
February															
02	0920	7.5	4130	4940						33					
02	1150	7.5	4130	4620						38					
02	1215	7.5	4130	6160	4	5	9	15	22	28					
02	1235	7.5	4130	4760						36					
04	1300		3420	2880						35					
04	1320		3420	3600						30					
04	1335		3420	3140						33					
09	1200		1810	1880						33					
09	1210		1810	2120	4	6	10	14	21	32					
09	1225		1810	1740						32					
12	0835	5.0	2310	2010						29					
14	1220	8.5	13200	26400						61					
14	1240	8.5	13300	28400						57					
14	1300	8.5	13300	25700						62					
15	1235	8.5	13500	18400						60					
17	1020	8.5	15500	57300						68					
17	1100		15300	46200						67					
17	1215		14700	35900						64					
17	1335		14000	29000						61					
17	1435		13400	24100						59					
17	1535		13000	21700						57					
17	1620.		13000	22700						60					
17	1730		13000	23400	6	8	16	26	41	80	96	99	100		
17	1800	8.0	13000	21800						49					

(Continued)

APPENDIX B (Continued)

Date	Time	Temp °C	Flow cfs	Sed. Susp mg/ℓ	0.002 mm	0.004 mm	0.008 mm	0.016 mm	0.031 mm	0.062 mm	0.125 mm	0.250 mm	0.500 mm	1.00 mm	2.00 mm
					Percent Finer Sediment Suspension										
18	1950		13700	21600						42					
18	2000		13700	25800						38					
18	2030		13800	22400						49					
18	2040		13800	22600						53					
18	2200	7.0	13500	29500	7	10	18	31	45	62	75	93	98	100	
18	2310		12800	31600						62					
19	0730	8.0	11800	18900						50					
19	0940		11000	15100						56					
19	0950	8.0	11000	15600						55					
19	1015	8.0	10700	21000	6	6	11	19	29	39	58	85	96	99	100
19	1040	8.0	10900	18400						47					
20	1020		24000	261000						52					
20	1022		23500	222000						38					
20	1030		21000	253000						46					
20	1200		19000	182000						48					
20	1205		18700	188000						55					
20	1230		18600	146000						44					
20	1245		19500	133000						59					
20	1250		19900	136000						51					
20	1300		20700	133000						55					
20	1310		21000	104000						68					
20	1315		21500	103000						67					
20	1355		27000	109000						60					
20	1400		27400	103000						64					
20	1435		33500	98400						62					
20	1445	11.0	35200	94400						65					
20	1450	10.5	33500	97700						64					
20	1500	10.5	32000	99100						62					
20	1505		31500	105000						62					
20	1530		30400	100000						62					
20	1540		30300	105000						57					
20	1815	9.0	25000	62600						55					
20	1905		26400	61100						53					
20	1930		24600	55800						56					
20	2000		25200	55200						58					
20	2040		27300	61700	8	10	18	29	42	54	69	93	99	100	
20	2150	7.0	27900	72000						60					
20	2240	6.0	25300	93800						57					
20	2250	6.0	24300	94600						55					
20	2300	6.5	23500	100000						50					
20	2310	6.5	23300	85700						52					
21	0015		22800	63400						52					

(Continued)

(Sheet 14 of 26)

APPENDIX B (Continued)

Date	Time	Temp °C	Flow cfs	Sed. Susp mg/ℓ	0.002 mm	0.004 mm	0.008 mm	0.016 mm	0.031 mm	0.062 mm	0.125 mm	0.250 mm	0.500 mm	1.00 mm	2.00 mm
					Percent Finer Sediment Suspension										
21	0145	5.5	21700	56000						46					
21	0920		15500	33600						49					
21	0955		15800	35200						47					
21	1035		16000	32800						50					
21	1245		14300	31800						47					
21	1305		14400	30800	6	7	15	25	37	49	67	91	99	100	
21	1335		14200	31400						46					
21	1440		13500	29400						42					
21	1505		13300	26100						48					
21	1525		12500	26300						47					
22	1300		8480	21900						38					
22	1610		8480	20600						36					
25	1340	7.0	4100	9460						32					
March															
02	1115	6.5	4020	6430						53					
02	1135	6.5	4020	9580						39					
02	1210	6.5	4020	6390						52					
05	1310	7.5	3770	8940						27					
05	1400	7.5	3770	4060						53					
09	1210	9.0	3830	6740						52					
09	1250	9.0	3830	8920						42					
09	1310	9.0	3830	6720						54					
16	1155	5.5	3460	6070						26					
16	1325	5.5	3460	6180						22					
20	0245		7100	918000						33	45	65	88	98	99
20	0315		6000	864000						34	45	64	88	97	99
20	0330		5500	790000						37	50	70	92	98	99
20	0405	11.0	4600	724000						38	53	75	94	98	100
20	0445		3800	596000						44	59	83	97	99	100
20	0520	11.0	3300	460000						58	78	94	99	100	
20	0600	10.0	2800	373000						65	81	97	100		
20	0720		2050	267000						73	89	98	100		
20	0930		2550	150000						79	94	98	100		
20	1430		2450	75900						69	88	96	99	100	
20	1648		2330	66600						67	87	96	99	100	
20	1700		2330	68300						65	84	95	99	100	
21	0840	6.0	2130	44600						52					
24	1250		1660	14900						64					
30	1130	7.5	1830	12000						51					
April															
07	1300	9.5	2190	6220						46	71	90	99	100	
13	1300	7.0	6220	14000						76					
13	1330	7.0	6220	24600						45	63	83	96	99	100

(Continued)

APPENDIX B (Continued)

Date	Time	Temp °C	Flow cfs	Sed. Susp mg/ℓ	Percent Finer Sediment Suspension 0.002 mm	0.004 mm	0.008 mm	0.016 mm	0.031 mm	0.062 mm	0.125 mm	0.250 mm	0.500 mm	1.00 mm	2.00 mm
20	1115	7.0	2470	6300						35	53	79	96	100	
20	1125	7.0	2470	4540						46					
27	1240	11.0	2280	5850						50	70	91	99	100	
May															
03	1005	10.5	2270	3820						63					
03	1255	10.5	2270	6820						43					
10	1225	10.0	1620	3760						42					
17	1150	13.5	2340	3440						67					
17	1210	13.5	2340	5480						45					
June															
02	0750	12.0	1350	1800						66					
02	1110	12.0	1350	4220						37					
10	1220	17.0	1470	3260						47					
18	1245	21.0	1470	4370						64					
18	1305	21.5	1470	3630						74					
22	1100	14.5	1150	4250						46					
29	1120		724	3100						43					
July															
08	1400	21.5	5584	1570						41					
08	1440	21.5	584	1870						36					
20	1125	19.5	518	1630						47					
28	1100		431	1350						47					
28	1220	19.0	431	1860						41					
August															
13	1125	17.0	381	791						32					
13	1140	17.0	381	2050						13					
September															
08	1155	21.0	293	1340						17					
20	1400		978	9280						58					
21	1535	16.0	789	4860						28	39	55	81	97	100
								Tower Road - Toutle River Gage							
October															
06	1200	13.0	8080	18000						72					
06	1245	13.0	7610	21200	10	19	32	49	64	73					
06	1400	13.0	7880	30900						73					
06	1530	13.0	6950	29600	13	24	40	60	75	82					
06	1640	13.0	7550	33000						85					
07	1005	11.0	4520	26600						75					
07	1120		4480	25800						78					
07	1200	11.0	4350	20900	16	28	44	62	74	73					
07	1205	11.0	4350	22400						83					
13	1330		1300	1100						8					
19	0950	10.5	723	997						29					

(Continued)

APPENDIX B (Continued)

Date	Time	Temp °C	Flow cfs	Sed. Susp mg/ℓ	Percent Finer Sediment Suspension 0.002 mm	0.004 mm	0.008 mm	0.016 mm	0.031 mm	0.062 mm	0.125 mm	0.250 mm	0.500 mm	1.00 mm	2.00 mm
19	1215	10.5	709	831						32					
19	1230	10.5	709	730						45					
19	1240	10.5	709	898						31					
27	1235	12.0	1010	2500						46					
27	1445	12.0	1000	2450						48					
27	1555	12.0	1080	2880						38					
28	1020	11.0	2720	36900						92					
28	1145	11.0	2460	31400		21	38	59	80	91	93	96	99	100	
28	1205	11.0	2380	28700						88					
28	1330	11.0	2140	16300						90					
November															
04	1210	7.0	1160	1790		10	16	24	35	52	71	86	98	100	
11	1930	11.5	1170	4040						39					
11	2010	11.5	1290	4500						46					
12	0955	9.5	2320	13200						70					
12	1150	9.5	2040	9710						67					
12	1220	9.5	2040	9180		12	21	34	50	67	82	93	98	100	
12	1335	9.5	1920	8160						62					
13	0950	8.5	1570	3830						54					
14	1355	9.5	7040	65200						78					
14	1515	9.5	7640	55500						78					
14	1530	9.5	7610	54600		16	26	41	59	74	85	95	98	100	
14	1625	9.0	8260	53800						72					
14	1710	9.0	8050	50600						73					
14	1840	8.5	6980	47400						74					
14	2015	7.5	6260	41300						68					
14	2045	7.5	6260	41200		13	21	34	49	67	78	88	95	99	100
14	2100	7.5	6290	38000						72					
15	0925	8.0	4300	12500						64					
16	0930	7.0	3660	15800						60					
16	1225	7.0	3440	14600						57					
16	1300	7.5	3420	13400		11	18	29	44	62	74	92	99	100	
16	1335	8.0	3380	13100						58					
16	1405	7.5	3360	12800						69					
16	1555	7.0	3360	13700						55					
17	1120	8.0	3020	11600						60					
18	0945	7.0	5120	11800						60					
18	1140	7.5	5030	14000		10	17	28	39	49	71	89	98	100	
18	1235		4760	11200						64					
24	1145	5.5	5700	5700		9	14	23	33	43	61	84	96	99	100
24	1230		3640	5220						30					

(Continued)

APPENDIX B (Continued)

Date	Time	Temp °C	Flow cfs	Sed. Susp mg/ℓ	Percent Finer Sediment Suspension 0.002 mm	0.004 mm	0.008 mm	0.016 mm	0.031 mm	0.062 mm	0.125 mm	0.250 mm	0.500 mm	1.00 mm	2.00 mm
December															
01	1130	6.0	2500	4690		13	19	29	38	51	67	88	98	100	
02	1115	8.0	10900	38300		11	22	34	49	67	82	94	98	99	100
02	1255	8.0	9880	34000		14	21	34	49	65	79	91	97	100	
02	1500	8.0	7520	23000		11	20	31	43	56	69	88	95	99	100
05	1150	9.0	17800	88300						54					
05	1410	9.0	19600	75200						58					
05	1600	9.0	16400	61900		11	17	27	38	53	60	87	95	99	100
05	1715	9.0	14500	71600						44					
05	2130	9.0	10900	53000						46					
05	2245	9.0	10900	40800		10	14	23	34	47	66	87	97	100	
06	0200	8.5	12700	31800						50					
06	0320		12200	30800		9	14	25	35	49	67	86	95	99	100
06	0915	7.5	10500	29800						40					
06	1005	7.5	10800	23300		9	14	24	34	50	63	86	95	99	100
06	1330	9.0	9960	21000		9	14	23	34	47	61	86	96	100	
06	1710	9.0	8610	16200						56					
07	1205		9080	11600						48					
08	1400	7.0	5780	10200		7	13	21	30	42	58	83	97	100	
10	1240	6.5	4790	8830		9	13	21	31	42	57	84	97	100	
11	0940	5.0	4060	5550						53					
11	1430	5.5	3920	5030						54					
15	0910	8.0	5340	7540						53					
15	1135	8.0	6340	9350						48					
15	1210	8.0	7560	13100		8	10	17	27	40	63	86	97	99	100
15	1310	8.0	8250	13200						50					
15	1500	8.0	10200	15600						52					
18	1210	8.0	4060	3590						51					
18	1230	8.0	4120	5940						34					
21	1145	6.0	3640	4850						52					
21	1230	6.0	3650	6620		8	12	19	28	39	57	82	97	100	
21	1310	6.0	3650	4400						50					
29	0930	3.0	2370	2040						41					
29	1150	2.5	2340	3220						27					
29	1230	2.5	2330	1730						46					
January															
08	1320		1200	883						67					
08	1505	3.0	1220	2080	4	5	10	15	20	31					
08	1535	3.0	1200	1300						58					
12	1255	5.0	1670	3280						28					
16	1240	7.5	6140	6440						45					
16	1325	7.5	6160	9920	2	5	8	13	20	28					
16	1630	7.5	9040	13400		4	4	6	13	21	34				

(Continued)

APPENDIX B (Continued)

Date	Time	Temp °C	Flow cfs	Sed. Susp mg/ℓ	Percent Finer Sediment Suspension 0.002 mm	0.004 mm	0.008 mm	0.016 mm	0.031 mm	0.062 mm	0.125 mm	0.250 mm	0.500 mm	1.00 mm	2.00 mm
16	1715	7.5	10500	12800						41					
17	1250	5.0	9540	7420						46					
17	1410	5.0	9950	11500		5	8	13	20	32	41	68	90	99	100
17	1435	5.0	9840	8520						41					
17	1640	5.0	9580	8140						40					
19	0925	6.0	5150	3030						38					
19	1315	6.0	4780	4120		6	9	14	20	28	42	68	93	99	100
19	1410	6.0	4780	3020						34					
23	1100	8.5	19100	22800						46					
23	1140	8.5	21900	26400						46					
23	1250	8.5	20900	21400						62					
23	1520	8.5	20200	17800		13	19	32	45	61	79	95	100		
23	1615		20300	18000						60					
23	1725	8.5	20400	20000						60					
23	1925	8.5	19900	18600		13	19	31	46	63	80	96	100		
23	2035		20100	17100						64					
23	2115	8.0	20300	15400						64					
23	2145	8.0	20800	17000						58					
24	0300	8.0	31500	29400		12	16	28	41	58	79	96	99	100	
24	0545	6.6	34800	43800		12	19	30	45	63	83	98	100		
24	0625	8.0	33400	42800						58					
24	0715	7.0	31600	37200						56					
24	0910	6.5	28100	32400		13	18	28	41	59	81	97	100		
24	0945	6.5	27300	39600						56					
24	1355	7.5	23100	22800		11	15	25	37	51	74	95	100		
24	1510		22000	20800						52					
26	1305		11200	11000						50					
26	1515		9950	11900		9	13	21	31	43	62	86	98	100	
26	1605		10200	9760						47					
27	1310		7580	5770						46					
29	1005	6.0	4360	3100						46					
29	1140	6.0	4360	4460			8	11	18	25	35	49	80	97	100
29	1225	6.0	4290	2900						45					
February															
02	0915	6.5	4000	3400						50					
02	1200	6.5	4090	4880	4	6	9	15	21	29					
02	1240	6.5	4120	3370						44					
04	1035	4.0	3380	2280						44					
04	1245	4.0	3350	3250						29					
04	1315	4.0	3140	2180						42					
09	1010	2.5	1910	980						58					
09	1205	2.5	1810	2010	4	8	13	20	26	29					

(Continued)

APPENDIX B (Continued)

Date	Time	Temp °C	Flow cfs	Sed. Susp mg/ℓ	Percent Finer Sediment Suspension 0.002 mm	0.004 mm	0.008 mm	0.016 mm	0.031 mm	0.062 mm	0.125 mm	0.250 mm	0.500 mm	1.00 mm	2.00 mm
12	1000	5.5	1810	732						73					
12	1140	5.5	1840	2230						30					
12	1245	5.5	1820	946						66					
14	0810	7.5	11000	41600						48					
14	1105	7.5	12100	30300						57					
14	1140	7.5	12600	40500						52					
14	1215	7.5	12500	36400						45					
15	1155	8.0	10500	25600						46					
16	0855	8.0	16300	38600						38					
16	1000	8.0	16500	33400						42					
16	1135	8.0	17400	33200						42					
16	1220	8.0	17900	32900	5	8	15	24	27	50	68	92	99	100	
16	1235	8.0	17700	34000						47					
16	1435	8.0	16700	37600						41					
17	0920	9.0	15800	78800						58					
17	1140	9.0	14800	44200	6	13	14	24	35	48	71	93	99	100	
17	1330	9.0	15300	37000						41					
19	0640		9750	29800						34					
19	0920	7.5	9000	24400	6	7	11	18	27	37	53	80	98	100	
20	1230		28400	104000						74					
20	1320		28600	88000						82					
20	1905	9.0	28700	57600						58					
20	1945	9.0	29500	51200						64					
20	2025	9.0	29800	51500						68					
20	2055	9.0	28500	68000						66					
20	2130	9.0	27200	80800						70					
20	2200		25700	89000						66					
20	2215		24900	71400						60					
20	2220		24900	81700						62					
20	2245	8.0	24900	65100						60					
20	2300		24300	72800						53					
20	2315		24300	61300						59					
20	2330		23100	54500						65					
20	2350	8.0	22600	54100						62					
21	0005		22500	50000						63					
21	0010		22000	44600						61					
21	0015		22000	51700						57					
21	0035		22300	47500						58					
21	0050	6.5	22800	51200						52					
21	0100		22800	51700						52					
21	0115	6.5	22700	45200						57					

(Continued)

APPENDIX B (Continued)

Date	Time	Temp °C	Flow cfs	Sed. Susp mg/l	Percent Finer Sediment Suspension 0.002 mm	0.004 mm	0.008 mm	0.016 mm	0.031 mm	0.062 mm	0.125 mm	0.250 mm	0.500 mm	1.00 mm	2.00 mm
21	0145		20800	44800						60					
21	0200		21100	50600						53					
21	1800	7.0	12000	23200	8	11	14	24	35	49					
21	1850	7.0	11800	25700						43					
24	1325	5.0	5480	9810	5	7	9	15	22	27					
24	1416	5.0	5540	6400						42					
01	0935	7.5	3550	6320						55					
01	1125	8.0	3900	9060						51					
01	1220	8.0	4020	9120						57					
05	1410	8.0	3320	5640						40					
09	1155	8.5	3540	7860						45					
15	1230	6.0	4130	5220						29					
19	1130	6.0	3320	2930						36					
19	2235	6.5	2500	1840						52	69	90	98	100	
19	2330		2500	2760						34	49	76	94	97	100
19	2352		2700	9740						11	17	37	87	100	
19	2359		8500	49400						45	69	89	98	99	100
20	0004	6.5	14000	98300						70	90	98	100		
20	0014	7.0	23000	158000						74	90	98	99	100	
20	0048		16000	1160000						23	31	47	67	85	96
20	0111		12400	1140000						24	34	50	72	89	96
20	0145		8500	1040000						29	37	58	78	92	95
20	0215		6100	935000						32	44	63	84	95	98
20	0238	10.5	5100	737000						43	57	76	95	98	99
20	0348		3600	606000						46	58	77	94	99	100
20	0625	9.0	2900	281000						61	80	95	99	100	
20	0817	8.5	2600	158000						72	89	97	100		
21	1035	6.0	1940	32400						57					
21	1220	7.0	2000	33400						64					
21	1345	10.0	2000	31000						55					
22	1020	6.0	1780	18400						69					
22	1345	9.0	1820	18400						69					
22	1435	10.0	1810	16500						70					
29	0930	6.0	1820	13800						48					
29	1120	6.5	1670	11400						55	80	96	100		
29	1225	6.5	1630	12600						47					
April															
05	0910	6.5	1950	10400						37					
06	0945		2360	6660						63					
06	1230	8.0	2260	9110						48	63	87	98	100	
06	1325	8.0	2230	10200						40					
12	0955	7.0	7020	41600						49					

(Continued)

APPENDIX B (Continued)

				Sed.	Percent Finer Sediment Suspension										
Date	Time	Temp °C	Flow cfs	Susp mg/ℓ	0.002 mm	0.004 mm	0.008 mm	0.016 mm	0.031 mm	0.062 mm	0.125 mm	0.250 mm	0.500 mm	1.00 mm	2.00 mm
12	1220	7.0	6070	32400						50	74	85	96	99	100
12	1315	7.0	6010	35800						41					
14	1250	7.0	3580	13700						46	66	89	98	100	
16	0900	5.5	2300	9700						44					
16	0940	5.5	2310	8870						49	65	88	99	100	
16	0955	5.5	2120	9280						45					
19	0920	6.5	2430	6300						36					
19	1255	9.0	2490	5960						36	53	79	97	100	
19	1345	10.5	2440	5410						37					
26	0910	8.5	2230	5890						45					
26	1230	10.5	2240	5410						54	66	85	97	99	100
26	1315	10.5	2260	5040						54					
May															
03	0910	8.0	2250	6180						42					
03	1150	9.0	2290	6290						40	64	88	99	100	
03	1300	10.5	2270	6680						37					
10	0915	9.0	1600	4460						32					
10	1135	9.0	1510	4060						39	55	85	99	100	
10	1230	10.0	1640	4530						32					
17	0905	11.5	2270	6620						37					
17	1200	12.0	2290	6010						45	63	85	97	100	
17	1345	12.5	2330	7440						35					
24	0920	12.5	1890	6600						28					
24	1230	14.5	1880	4430						40					
24	1310	16.0	1910	4380						35					
June															
01	0910	12.0	1460	3720						43					
01	1245	12.0	1550	4050						41					
08	1125	13.0	1350	2880						39					
08	1550	17.0	1340	2830						44					
14	1130	12.0	1240	3420						51					
21	1440	16.0	1400	5030						63	77	91	98	99	100
28	1105	15.0	836	2980						60					
July															
06	1045	14.5	740	1740						44					
12	1245	20.0	611	3060						45					
13	1340	17.5	604	1970						62					
13	1420	18.0	625	2600						62					
19	1035	16.5	537	1460						64					
19	1100	17.0	551	2180						44					
August															
04	0930	15.0	452	1750						27					
04	1115	16.0	432	1500						29					

(Continued)

APPENDIX B (Continued)

Date	Time	Temp °C	Flow cfs	Sed. Susp mg/ℓ	Percent Finer Sediment Suspension 0.002 mm	0.004 mm	0.008 mm	0.016 mm	0.031 mm	0.062 mm	0.125 mm	0.250 mm	0.500 mm	1.00 mm	2.00 mm
04	1145	16.0	465	973						44					
04	1235	17.0	452	1460						29					
13	1005	15.5	446	686						37					
24	1200	16.5	296	323						50					
September															
15	1305	14.5	530	2340						25	30	42	64	84	92
21	1040	12.0	835	2830						46	58	78	83	85	93
28	1240	12.5	705	1760						52					
					Kidd Valley-North Toutle River Gage										
October															
05	1150	10.0	400	104						64	84	91	98	100	
06	1440		4210	53200		28	45	70	82	86	90	96	99	100	
06	1705		4140	69600		25	46	69	81	86	89	97	99	100	
07	1320	12.5	2300	19400						78					
13	1600	10.5	1200	1550						45					
19	1045	9.5	482	670	11	16	25	36	45	54	60	69	88	99	100
26	1500	12.0	330	459						68	80	86	95	99	100
28	1040	9.5	1440	25200						82					
28	1120	9.5	1370	17600	18	19	27	43	67	85					
30	1350		790	4490						71					
November															
02	1100	9.0	648	4940	11	11	14	23	40	63					
09	1130	7.5	460	2280		9	13	21	33	46	68	88	92	95	97
12	0945	9.5	1260	11200						73					
12	1145	9.5	1130	10400		14	24	37	53	66	81	93	98	100	
13	1055	9.0	818	9900						48					
14	1415	8.0	4020	116000						62					
14	1520	8.0	4120	93800						62					
14	1525	8.0	4120	94700						62					
14	1555	8.0	3930	82800		12	21	34	49	61	78	95	99	100	
14	1640	8.0	3740	61600						53					
14	1720	8.0	3530	74100						60					
14	1745	8.0	3400	70700						62					
14	1825	8.0	3270	66600						60					
14	1935	8.0	2840	50200						63					
15	1340		2030	27400						45					
16	1045	7.0	1980	28200						49					
16	1205		1990	27600						50					
16	1250		1950	26800						46					
16	1315		1950	22400	10	11	14	22	34	51					
16	1335		1950	25800						42					

(Continued)

APPENDIX B (Continued)

Date	Time	Temp °C	Flow cfs	Sed. Susp mg/ℓ	Percent Finer Sediment Suspension 0.002 mm	0.004 mm	0.008 mm	0.016 mm	0.031 mm	0.062 mm	0.125 mm	0.250 mm	0.500 mm	1.00 mm	2.00 mm
16	1420		1950	21600						48					
16	1425		1950	24400						43					
18	1430		2820	18200						49					
23	1115	6.5	2130	12000	10	12	14	25	36	52					
30	1115	4.5	881	3560						35					
December															
02	1020	6.0	5500	53400						62					
02	1055	6.0	5150	46500						60					
02	1255	6.0	4380	26600	14	17	19	33	47	60	76	93	98	100	
02	1345	6.0	3760	27200						52					
02	1430	6.0	3640	25600						48					
02	1500	6.0	3590	22200						51					
02	1605		3240	22800						46					
02	1635	6.0	3190	21500						44					
03	1130	5.0	2370	12400	6	8	15	23	35	51					
05	1130	7.0	10800	46400						54					
05	1240	8.0	12200	100000						60					
05	1350	8.0	10800	95500						54					
05	1440	8.0	9700	91500	10	12	16	28	39	55	72	93	99	100	
24	1150		12100	31600	8	9	11	19	29	41	56	80	94	99	100
24	1255		11700	30000							42				
24	1350		11400	36400							34				
24	1450		11000	32000							34				
24	1720		10200	26400							36				
25	1600	6.5	5610	18000	9	10	11	21	31	45	62	81	94	99	100
26	1150		4370	17000	8	8	11	20	30	43	61	85	97	100	
29	1250	5.5	2440	7530						31	49	94	95	100	
February															
02	1120	6.0	2590	5440						35	53	78	96	100	
04	1240	3.0	1980	3860						31	47	77	96	99	100
08	1320	3.0	1210	3350						33	46	64	92	99	100
14	0950	6.5	6630	47000	8	9	18	28	41	55	75	91	98	99	100
15	0820	6.5	7200	37600						53					
15	1000	6.5	7030	34400	9	10	12	23	34	46	62	85	97	99	100
16	1125	7.0	10500	46800						52					
16	1[illegible]40	7.0	10200	47400	9	10	14	24	34	47	66	87	96	99	100
16	1450		9200	43200						50					
17	1220	7.0	7150	44300	7	9	12	21	31	44	59	82	95	99	100
18	1335	6.5	8040	28200						31					
18	2155		6750	44800						56					
19	1200	7.0	5760	29800	6	8	12	19	28	40	57	78	94	99	100
20	1010		13000	182000						58					
20	1315		20000	114000						69					

(Continued)

APPENDIX B (Continued)

Date	Time	Temp °C	Flow cfs	Sed. Susp mg/ℓ	Percent Finer Sediment Suspension 0.002 mm	0.004 mm	0.008 mm	0.016 mm	0.031 mm	0.062 mm	0.125 mm	0.250 mm	0.500 mm	1.00 mm	2.00 mm
20	1330		19600	106000	9	14	24	38	53	66	81	96	99	100	
20	1550		17100	65000						66					
20	1605		17200	66000	13	15	21	38	54	67	79	94	99	100	
20	1715		17300	76600						58					
20	1750		17000	69100						58					
20	1751		17000	70700						57					
20	1810		16500	71800						60					
20	1820		16400	88600						54					
20	1830		16100	94100						62					
20	1850		15700	136000						60					
20	1900		15500	146000						56					
20	1915		15000	134000						65					
20	1920		14900	173000						53					
20	1930		14500	182000						55					
20	1935		14400	197000						48					
20	1950		13900	136000						56					
20	2030		13700	90800						58					
20	2105		13800	82400						56					
20	2130		13100	72400						57					
20	2205		12300	69400						54					
20	2230		12600	60900						56					
20	2240		12400	66800						53					
20	2330		12600	60600						60					
20	2400	5.5	11900	63200						55					
21	0020		11700	61000						55					
21	1115		8950	54700						38					
21	1200		9240	34900						49					
21	1210		9160	48500						39					
21	1315		8680	37900						51					
21	1425		8230	36800						47					
22	1215	4.5	4720	20200						46	65	87	97	100	
March															
01	1225	7.0	3320	25500	13	15	20	34	48	62	78	93	99	100	
04	1325	7.0	2080	11700						43	60	74	97	100	
09	1135	8.5	2290	13800						70	80	91	96	99	100
15	1235	5.5	2290	5440						38	55	71	94	99	100
21	1250	9.5	1420	29300	5	18	22	37	54	72	88	97	99	100	
23	1420	7.0	1280	23000						68					
31	1230	5.5	960	17800						54					
April															
05	0220	4.5	1370	11400						51	71	94	99	100	
08	1325	11.0	1310	7620						50					
16	1245	8.0	1830	10300						51	74	92	99	100	
19	1125	6.5	1250	8000						44					
29	1155	6.0	1500	7040						49					

(Continued)

(Sheet 25 of 26)

APPENDIX B (Concluded)

Date	Time	Temp °C	Flow cfs	Sed. Susp mg/ℓ	Percent Finer Sediment Suspension 0.002 mm	0.004 mm	0.008 mm	0.016 mm	0.031 mm	0.062 mm	0.125 mm	0.250 mm	0.500 mm	1.00 mm	2.00 mm
May															
07	1305	11.0	1320	5860						48					
12	1305	11.0	1100	4580						47	70	91	98	100	
17	1200	10.0	1600	6580						40	61	84	96	99	100
24	1255	14.5	1310	3940						46					
June															
04	1125	11.0	813	4000						38	57	83	94	96	99
07	1140	10.0	834	3560						33	52	77	94	98	100
14	1305	12.5	969	4200						53	69	88	97	99	100
23	1300	18.0	798	4440						47	67	81	98	100	
July															
01	1300	15.0	532	4390						36	47	95	96	99	100
06	1130	15.5	498	2230						64					
13	1030	17.0	421	2600						49	70	93	100		
22	1615		306	1980						51					
29	1200	17.5	293	2040						50	66	91	99	100	
August															
06	1400	22.5	246	1040						50					
17	1110	17.0	219	906						29	45	76	93	96	97
31	1150	17.0	207	964						42					
September															
07	1155	19.0	200	800						52					
13	1505	17.5	515	2320						58					
20	1110		825	9700						60	74	90	98	99	100

(Sheet 26 of 26)

APPENDIX C
BED MATERIAL DATA

Percent Finer Than					
2.00 mm	1.00 mm	0.50 mm	0.25 mm	0.125 mm	0.0625 mm
		Castle Rock (USGS)			
100.0	100.0	99.0	61.0	5.0	0.0
100.0	100.0	100.0	90.0	9.0	0.0
99.0	98.0	87.0	19.0	1.0	0.0
100.0	100.0	97.0	75.0	16.0	1.0
100.0	100.0	93.0	38.0	3.0	0.0
88.0	84.0	55.0	14.0	1.0	0.0
100.0	100.0	96.0	13.0	0.0	0.0
100.0	100.0	99.0	76.0	11.0	1.0
100.0	100.0	85.0	28.0	5.0	1.0
100.0	100.0	94.0	22.0	4.0	0.0
99.0	97.0	50.0	8.0	3.0	1.0
100.0	100.0	92.0	21.0	2.0	0.0
100.0	100.0	94.0	26.0	3.0	0.0
100.0	100.0	92.0	21.0	2.0	0.0
95.0	85.0	46.0	14.0	3.0	1.0
100.0	100.0	100.0	75.0	14.0	1.0
100.0	100.0	100.0	81.0	11.0	1.0
86.0	82.0	73.0	35.0	5.0	0.0
98.0	87.0	14.0	2.0	1.0	0.0
98.0	94.0	88.0	48.0	18.0	4.0
100.0	99.0	96.0	35.0	3.0	1.0
100.0	100.0	98.0	38.0	2.0	0.0
100.0	100.0	100.0	64.0	6.0	0.0
100.0	99.0	87.0	40.0	6.0	1.0
97.0	96.0	78.0	24.0	1.0	0.0
100.0	100.0	98.0	38.0	4.0	0.0
100.0	100.0	95.0	18.0	1.0	0.0
100.0	100.0	98.0	34.0	2.0	0.0
97.0	91.0	72.0	20.0	2.0	0.0
100.0	100.0	88.0	17.0	2.0	0.0
95.0	91.0	62.0	8.0	1.0	0.0
100.0	100.0	89.0	15.0	1.0	0.0
100.0	100.0	99.0	85.0	37.0	6.0
100.0	100.0	100.0	84.0	25.0	4.0
100.0	100.0	89.0	28.0	8.0	1.0

(Continued)

APPENDIX C (Continued)

Percent Finer Than					
2.00 mm	1.00 mm	0.50 mm	0.25 mm	0.125 mm	0.0625 mm
100.0	100.0	97.0	32.0	11.0	2.0
100.0	100.0	97.0	46.0	8.0	1.0
100.0	100.0	100.0	94.0	20.0	1.0
96.0	95.0	89.0	45.0	9.0	2.0
100.0	100.0	98.0	62.0	12.0	1.0
100.0	100.0	98.0	49.0	11.0	2.0
99.0	97.0	60.0	9.0	2.0	0.0
100.0	100.0	88.0	29.0	4.0	0.0
100.0	100.0	98.0	45.0	11.0	2.0
98.0	94.0	78.0	25.0	4.0	1.0
100.0	100.0	92.0	21.0	8.0	2.0
100.0	100.0	67.0	8.0	2.0	1.0
97.0	87.0	34.0	6.0	2.0	1.0
99.0	98.0	83.0	40.0	6.0	1.0
100.0	100.0	99.0	44.0	2.0	1.0
100.0	100.0	95.0	40.0	4.0	0.0
100.0	100.0	98.0	28.0	3.0	0.0
100.0	97.0	52.0	15.0	2.0	0.0
98.0	96.0	79.0	17.0	1.0	1.0
98.0	88.0	50.0	10.0	1.0	0.0
100.0	100.0	94.0	20.0	1.0	0.0
100.0	100.0	89.0	18.0	1.0	0.0
96.0	90.0	56.0	15.0	2.0	0.0
94.0	85.0	46.0	14.0	2.0	0.0
96.0	92.0	63.0	8.0	0.0	0.0
99.0	96.0	69.0	12.0	1.0	0.0
100.0	100.0	95.0	23.0	1.0	0.0
91.0	78.0	47.0	20.0	2.0	1.0
93.0	84.0	42.0	5.0	0.0	0.0
99.0	97.0	71.0	6.0	0.0	0.0
96.0	90.0	55.0	5.0	0.0	0.0
100.0	99.0	67.0	6.0	0.0	0.0
95.0	82.0	36.0	11.0	2.0	0.0
100.0	100.0	95.0	10.0	0.0	0.0
95.0	76.0	27.0	5.0	1.0	0.0
98.0	92.0	42.0	3.0	0.0	0.0
100.0	97.0	61.0	6.0	0.0	0.0
94.0	85.0	52.0	6.0	0.0	0.0
99.0	94.0	27.0	4.0	0.0	0.0

(Continued)

APPENDIX C (Continued)

Percent Finer Than					
2.00 mm	1.00 mm	0.50 mm	0.25 mm	0.125 mm	0.0625 mm
97.0	91.0	48.0	3.0	2.0	0.0
100.0	98.0	61.0	7.0	0.0	0.0
98.0	96.0	65.0	8.0	0.0	0.0
96.0	86.0	41.0	4.0	1.0	0.0
99.0	96.0	52.0	4.0	0.0	0.0
100.0	94.0	39.0	3.0	0.0	0.0
100.0	99.0	63.0	4.0	0.0	0.0
96.0	85.0	34.0	12.0	6.0	1.0
99.0	95.0	54.0	6.0	0.0	0.0
97.0	96.0	40.0	1.0	0.0	0.0
98.0	92.0	32.0	2.0	0.0	0.0
99.0	96.0	39.0	2.0	0.0	0.0
97.0	76.0	11.0	0.0	0.0	0.0
97.0	89.0	34.0	2.0	0.0	0.0
98.0	89.0	49.0	5.0	0.0	0.0
95.0	85.0	62.0	15.0	1.0	0.0
99.0	97.0	75.0	15.0	1.0	0.0
97.0	94.0	71.0	15.0	1.0	0.0
98.0	90.0	48.0	6.0	1.0	0.0
Highway 99 Bridge					
88.0	57.0	12.0	1.0	0.0	0.0
96.0	72.0	20.0	2.0	0.0	0.0
97.0	85.0	37.0	3.0	0.0	0.0
99.0	97.0	85.0	14.0	1.0	0.0
99.0	89.0	24.0	2.0	0.0	0.0
100.0	95.0	47.0	5.0	0.0	0.0
93.0	61.0	16.0	1.0	0.0	0.0
99.0	95.0	45.0	10.0	2.0	0.0
98.0	86.0	41.0	10.0	2.0	0.0
100.0	96.0	70.0	23.0	6.0	1.0
96.0	90.0	54.0	11.0	2.0	0.0
93.0	64.0	15.0	3.0	1.0	0.0
94.0	75.0	34.0	11.0	2.0	0.0
100.0	99.0	75.0	20.0	2.0	0.0
100.0	97.0	64.0	16.0	2.0	0.0

(Continued)

APPENDIX C (Continued)

Percent Finer Than					
2.00 mm	1.00 mm	0.50 mm	0.25 mm	0.125 mm	0.0625 mm
100.0	96.0	57.0	10.0	2.0	0.0
99.0	96.0	74.0	15.0	2.0	0.0
92.0	76.0	38.0	8.0	1.0	0.0
99.0	89.0	45.0	7.0	1.0	0.0
92.0	74.0	34.0	6.0	1.0	0.0
100.0	97.0	62.0	18.0	3.0	0.0
95.0	86.0	45.0	11.0	2.0	0.0
100.0	97.0	63.0	12.0	1.0	0.0
98.0	84.0	32.0	6.0	1.0	0.0
100.0	100.0	90.0	20.0	3.0	0.0
100.0	100.0	99.0	34.0	2.0	0.0
100.0	88.0	33.0	6.0	1.0	0.0
100.0	100.0	88.0	16.0	2.0	0.0
100.0	100.0	95.0	26.0	2.0	0.0
100.0	98.0	60.0	10.0	1.0	0.0
100.0	96.0	81.0	37.0	9.0	2.0
100.0	96.0	70.0	19.0	5.0	1.0
98.0	89.0	51.0	6.0	1.0	0.0
97.0	83.0	52.0	12.0	1.0	1.0
99.0	98.0	91.0	30.0	4.0	0.0
100.0	98.0	78.0	22.0	3.0	1.0
99.0	94.0	67.0	20.0	4.0	1.0
91.0	63.0	12.0	1.0	0.0	0.0
95.0	86.0	40.0	6.0	2.0	0.0
100.0	100.0	86.0	18.0	2.0	0.0
100.0	100.0	99.0	39.0	6.0	0.0
100.0	99.0	78.0	10.0	1.0	0.0
97.0	88.0	55.0	16.0	3.0	0.0
94.0	78.0	25.0	6.0	2.0	0.0
100.0	95.0	62.0	11.0	2.0	0.0
95.0	76.0	42.0	9.0	2.0	0.0
100.0	98.0	80.0	18.0	2.0	0.0
100.0	100.0	91.0	26.0	4.0	0.0
97.0	90.0	65.0	14.0	2.0	0.0
100.0	97.0	78.0	23.0	2.0	0.0
100.0	98.0	80.0	20.0	2.0	0.0
99.0	92.0	58.0	10.0	1.0	0.0
99.0	95.0	60.0	11.0	2.0	0.0
100.0	98.0	58.0	7.0	1.0	0.0

(Continued)

APPENDIX C (Continued)

Percent Finer Than					
2.00 mm	1.00 mm	0.50 mm	0.25 mm	0.125 mm	0.0625 mm
96.0	91.0	65.0	18.0	3.0	0.0
97.0	92.0	68.0	16.0	1.0	0.0
99.0	92.0	53.0	9.0	1.0	0.0
100.0	92.0	42.0	5.0	0.0	0.0
98.0	83.0	32.0	3.0	0.0	0.0
90.0	70.0	29.0	4.0	0.0	0.0
91.0	70.0	34.0	6.0	0.0	0.0
86.0	60.0	24.0	4.0	0.0	0.0
89.0	66.0	24.0	4.0	0.0	0.0
		Tower Road			
99.0	91.0	45.0	10.0	2.0	1.0
93.0	83.0	52.0	14.0	2.0	1.0
95.0	86.0	80.0	42.0	5.0	1.0
99.0	96.0	63.0	12.0	2.0	0.0
88.0	96.0	17.0	6.0	1.0	0.0
97.0	61.0	15.0	4.0	1.0	0.0
81.0	62.0	28.0	8.0	2.0	1.0
97.0	75.0	30.0	3.0	0.0	0.0
99.0	92.0	42.0	6.0	0.0	0.0
90.0	68.0	21.0	2.0	0.0	0.0
98.0	96.0	90.0	51.0	9.0	1.0
89.0	79.0	51.0	12.0	3.0	1.0
88.0	75.0	25.0	7.0	2.0	0.0
92.0	83.0	63.0	17.0	2.0	0.0
90.0	76.0	25.0	3.0	0.0	0.0
94.0	73.0	24.0	6.0	1.0	0.0
91.0	61.0	13.0	2.0	1.0	0.0
87.0	67.0	43.0	20.0	7.0	1.0
92.0	77.0	47.0	13.0	2.0	0.0
89.0	84.0	65.0	18.0	3.0	0.0
88.0	76.0	30.0	8.0	2.0	0.0
94.0	54.0	18.0	6.0	2.0	0.0
90.0	68.0	18.0	3.0	1.0	0.0
99.0	98.0	92.0	40.0	4.0	0.0
100.0	100.0	86.0	17.0	2.0	0.0

(Continued)

APPENDIX C (Continued)

Percent Finer Than					
2.00 mm	1.00 mm	0.50 mm	0.25 mm	0.125 mm	0.0625 mm
100.0	98.0	69.0	11.0	1.0	0.0
92.0	69.0	21.0	3.0	0.0	0.0
87.0	74.0	33.0	6.0	0.0	0.0
97.0	88.0	46.0	8.0	1.0	0.0
98.0	90.0	43.0	6.0	1.0	0.0
99.0	96.0	87.0	53.0	24.0	5.0
100.0	100.0	78.0	21.0	4.0	1.0
99.0	71.0	19.0	5.0	1.0	0.0
100.0	100.0	95.0	27.0	4.0	1.0
100.0	100.0	84.0	18.0	3.0	1.0
97.0	89.0	33.0	9.0	3.0	1.0
100.0	100.0	95.0	40.0	8.0	2.0
100.0	100.0	91.0	29.0	5.0	1.0
99.0	91.0	27.0	6.0	2.0	1.0
100.0	100.0	99.0	30.0	4.0	0.0
100.0	100.0	88.0	18.0	2.0	0.0
94.0	72.0	28.0	7.0	1.0	0.0
86.0	63.0	31.0	8.0	1.0	0.0
95.0	75.0	33.0	6.0	1.0	0.0
99.0	96.0	70.0	14.0	2.0	0.0
100.0	100.0	96.0	23.0	2.0	0.0
86.0	74.0	44.0	12.0	2.0	0.0
95.0	87.0	58.0	15.0	2.0	0.0
99.0	98.0	93.0	51.0	10.0	2.0
91.0	85.0	61.0	14.0	2.0	0.0
99.0	95.0	60.0	14.0	2.0	0.0
95.0	82.0	48.0	12.0	2.0	0.0
100.0	100.0	88.0	17.0	1.0	0.0
99.0	93.0	62.0	14.0	2.0	0.0
100.0	92.0	43.0	7.0	1.0	0.0
90.0	69.0	31.0	4.0	0.0	0.0
98.0	95.0	82.0	52.0	20.0	8.0
97.0	91.0	76.0	38.0	20.0	8.0
97.0	90.0	77.0	48.0	24.0	11.0
88.0	74.0	52.0	26.0	14.0	7.0
99.0	97.0	84.0	29.0	4.0	1.0
99.0	94.0	67.0	18.0	3.0	1.0
100.0	97.0	76.0	30.0	8.0	1.0
97.0	89.0	53.0	17.0	4.0	1.0

(Continued)

APPENDIX C (Continued)

Percent Finer Than					
2.00 mm	1.00 mm	0.50 mm	0.25 mm	0.125 mm	0.0625 mm
98.0	86.0	59.0	23.0	7.0	2.0
94.0	78.0	45.0	14.0	4.0	0.0
91.0	75.0	42.0	12.0	3.0	0.0
100.0	100.0	97.0	49.0	11.0	2.0
92.0	82.0	47.0	11.0	3.0	1.0
92.0	78.0	40.0	10.0	3.0	1.0
91.0	76.0	46.0	16.0	3.0	0.0
92.0	76.0	39.0	8.0	1.0	0.0
81.0	45.0	23.0	13.0	2.0	0.0
96.0	87.0	56.0	14.0	2.0	0.0
94.0	77.0	29.0	3.0	0.0	0.0
83.0	44.0	10.0	4.0	2.0	0.0
86.0	68.0	39.0	10.0	1.0	0.0
91.0	77.0	50.0	16.0	3.0	0.0
86.0	69.0	40.0	8.0	1.0	0.0
98.0	87.0	37.0	6.0	1.0	0.0
95.0	76.0	36.0	11.0	3.0	0.0
84.0	36.0	10.0	4.0	1.0	0.0
97.0	92.0	59.0	10.0	1.0	0.0
82.0	76.0	54.0	14.0	1.0	0.0
91.0	54.0	12.0	1.0	0.0	0.0
		Kidd Valley			
100.0	97.0	78.0	18.0	2.0	0.0
97.0	82.0	41.0	9.0	1.0	0.0
85.0	67.0	35.0	8.0	1.0	0.0
97.0	90.0	51.0	24.0	8.0	0.0
88.0	62.0	26.0	9.0	3.0	1.0
100.0	99.0	83.0	24.0	4.0	1.0
100.0	98.0	76.0	22.0	4.0	1.0
100.0	97.0	58.0	14.0	3.0	1.0
99.0	95.0	73.0	16.0	2.0	0.0
100.0	97.0	71.0	18.0	3.0	0.0
92.0	69.0	25.0	5.0	1.0	0.0
87.0	72.0	54.0	21.0	9.0	3.0
93.0	84.0	72.0	52.0	30.0	11.0
90.0	79.0	51.0	16.0	3.0	0.0
95.0	75.0	42.0	10.0	1.0	0.0

(Continued)

APPENDIX C (Concluded)

Percent Finer Than					
2.00 mm	1.00 mm	0.50 mm	0.25 mm	0.125 mm	0.0625 mm
83.0	52.0	18.0	5.0	1.0	0.0
90.0	68.0	32.0	10.0	2.0	0.0
95.0	63.0	24.0	6.0	2.0	0.0
94.0	65.0	31.0	9.0	1.0	0.0
98.0	72.0	26.0	4.0	1.0	0.0
92.0	90.0	88.0	71.0	22.0	3.0
85.0	73.0	48.0	20.0	7.0	1.0
82.0	48.0	21.0	10.0	4.0	1.0
96.0	93.0	84.0	40.0	10.0	1.0
80.0	66.0	36.0	9.0	2.0	0.0
91.0	83.0	57.0	17.0	3.0	0.0
95.0	66.0	18.0	3.0	1.0	0.0
98.0	82.0	32.0	6.0	1.0	0.0

(Sheet 8 of 8)

APPENDIX D

LIST OF SYMBOLS

Symbol	Definition
a	constant in Equation 2.3
a'	distance from the streambed to the sampler inlet tube
A	constant in Equation 2.11; parameter related to flow regimes in Equation 2.35; cross-section area
A_s	aspect ratio equal to width/depth
B	$f/8(1 - y_o/d)R$, Bingham number; stream width; constant in Equation 2.11
C	coefficient that equals 24 for Newtonian fluids and for a non-Newtonian Bingham fluid
C_a	concentration of a particle size at a reference elevation a above the bed
C_D	drag coefficient
C_E	correction factor for relative plastic viscosity
C_f	fine sediment concentration, parts per million
C_s	concentration of suspended sediment by weight
C'_s	measured suspended sediment concentration
C_T	correction factor for relative yield stress
C_v	sediment concentration by volume
C_w	sediment concentration by weight
C_y	concentration of a grain size at a distance y above the bed
C_{vf}	concentration of fines by volume
C_{vi}	volume fraction of the ith phase
C_{vs}	concentration of volume by sand

LIST OF SYMBOLS (Continued)

Symbol	Definition
C_{wf}	concentration of fines by weight
C_{ws}	concentration of sand by weight
C_1	quantity defined by Equation 2.20
C_2	quantity defined by Equation 2.21
d	flow depth; particle size
d_i	geometric mean particle size
d_v	mean value of depths at verticals where suspended sediment samples were taken
E'	a'/d_v
f	friction factor
g	acceleration of gravity
H_e	Hedstrom number
i_b	size distribution of the bed material at the cross section
i_s	size distribution of the measured suspended sediment
k_b	empirical constant equal to 4.4
k_s	roughness height
K	$7\pi/24$, a constant in Equation 2.32; 0.0027, conversion factor in Equation 4.1
K_1	constant defined by Equation 2.12
K_2	constant defined by Equation 2.13
K_1	adjustment coefficient for water temperature different from 60°F
K_2	adjustment coefficient for concentration of fine sediment
K_3	adjustment coefficient for median bed material particle size; reference size is 0.02-0.03 mm, i.e., $K_3 = 100$ expressed as percentage

LIST OF SYMBOLS (Continued)

Symbol	Definition
n_1	n_2+1 , coefficient in the power-law velocity equation
n_2	$u_*/k\bar{u}$, exponent in the power-law velocity equation
N_r	Reynolds number defined by $N_r = \rho V(4d)/\mu$
P_m	constant in Equation 2.55
q	unit stream discharge; stream discharge per unit width
q'_{si}	sediment discharge through the unit width of the sampled zone
q_s	adjusted bed material discharge per unit width
q'_s	suspended sediment discharge of the various size fractions per unit width of the sampled zone
q_{s1}	Colby's empirical bed material discharge per unit width
Q	measured stream discharge in cubic feet per second
Q'	stream discharge in the sampled zone
Q_{sm}	measured suspended sediment discharge
Q_{Ti}	total sediment discharge through the cross section for a size fraction
R	hydraulic radius
R'	hydraulic radius as defined by Einstein
R_b	Bingham Reynolds number
R_n	quantity defined as $R_b f^{1/2}$
R_{bc}	critical Bingham Reynolds number
R_{bw}	the ratio of the volume bound water to that of the sediment particles
Re^*_p	particle Reynolds number in Equation 2.30
s	yield stress
S_e	slope of the energy grade line

LIST OF SYMBOLS (Continued)

Symbol	Definition
S_o	surface area per unit volume of a sphere of equivalent dimension
S_p	surface area per unit volume of the actual particle
SG	specific gravity
$(SR)_m$	quantity obtained by solving Equation 2.58 for SR for a known value of $\bar{u}$
T	fluid temperature, degrees Kelvin
T_1	quantity defined by Equation 2.22
T_2	quantity defined by Equation 2.23
u	velocity at a distance y from the bottom
u_*	shear velocity
u_m	shear velocity
u_{max}	maximum point velocity
$\bar{u}$	mean flow velocity
v	flow velocity at a distance y above the bed
V	mean flow velocity
W_i	fall velocity of a sediment grain of size d_i
W_o	settling rate of a single particle in the same suspending medium in the Maude and Whitmore equation (2.33)
W_s	fall velocity of sand particles
x	indirectly a function of the shear velocity and is a trial value with the aid of Figure 4 (Einstein 1950)
y	depth of point velocity
y_o	vertical distance from the bed corresponding to the yield stress
z	exponent in the theoretical equation for vertical distribution of sediment of a particular size range

LIST OF SYMBOLS (Continued)

Symbol	Definition
z'_i	exponent of the concentration distribution curves computed by trial and error in modified Einstein method.
α	exponent in Equation 2.33 and a function of particle Reynolds number, particle shape, and size distribution
α_c	critical value of the ratio of the Bingham yield stress and the boundary shear stress
β	numerical constant related to the diffusion (1.0)
γ	specific weight of fluid
γ_c	specific weight of fine sediment
γ_i	specific weight of the ith phase
γ_f	specific weight of water-fine sediment mixture
γ_m	specific weight of water-sediment mixture
γ_s	specific weight of sand particles
γ_w	specific weight of pure water
ΔP_i	the volume of fraction of particles of diameter d_i
δ	thickness of the laminar sublayer
δ_i	the bound water film thickness usually taken as 1 micron
η	plastic viscosity
η_D	plastic viscosity of the dispersion
η_r	relative plastic viscosity
κ	von Karman constant
μ	viscosity of water
μ_D	viscosity of dispersion
μ_e	effective viscosity of a Bingham fluid in Equation 2.31
μ_m	viscosity of mixture

LIST OF SYMBOLS (Concluded)

Symbol	Definition
μ_o	Newtonian viscosity of the suspending medium
$\mu_{r1}-\mu_{r3}$	relative viscosities of discrete sizes
ν	fluid kinematic viscosity
ρ	mass density of water
ρ_f	density of water-fine sediment mixture
τ_b	Bingham yield stress
τ_r	relative Bingham yield stress
τ_w	boundary shear stress
τ_y	yield stress of Bingham fluid
τ_{bD}	Bingham yield stress of the dispersion
ϕ	solid volume fraction
ϕ_m	maximum possible volume fraction
ϕ_*	Einstein's transport rate function
ψ	cross-section shape factor equal to $A_s + 2$ for a rectangular channel
ψ_m	intensity of shear on the particles
ψ_1	shape factor in the calculation of Bingham yield stress
ψ_2	shape factor in the calculation of plastic viscosity
ψ_*	shear intensity factor